Master Thesis in Geosciences

Late Mesozoic – Early Cenozoic structural evolution of Sørvestsnaget Basin

Wibi Aulia Harsum

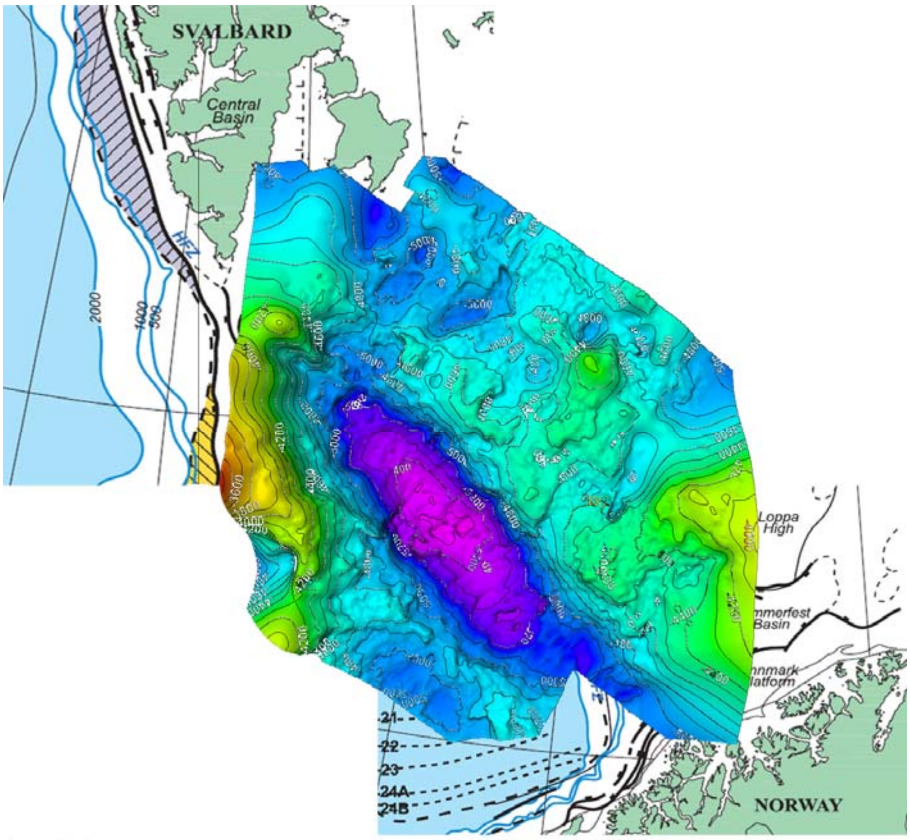

UNIVERSITY OF OSLO

FACULTY OF MATHEMATICS AND NATURAL SCIENCES

Late Mesozoic – Early Cenozoic structural evolution of Sørvestsnaget Basin

Wibi Aulia Harsum

Master Thesis in Geosciences

Discipline: Petroleum Geology and Petroleum Geophysics

Department of Geosciences

Faculty of Mathematics and Natural Sciences

UNIVERSITY OF OSLO

June 2009

Tutor(s): Prof. Jan Inge Faleide and Prof. Roy Helge Gabrielsen

This work is published digitally through DUO – Digitale Utgivelser ved UiO

http://www.duo.uio.no

It is also catalogued in BIBSYS (http://www.bibsys.no/english)

Preface

This master thesis completes the two year master thesis program in Petroleum Geology and Petroleum Geophysics undertaken at the Department of Geosciences, University of Oslo. The topic of this master thesis is associated with PETROBAR project at the University of Oslo. The 2D and 3D seismic data have been interpreted by the use of Geoframe and Petrel softwares respectively. Prof. Jan Inge Faleide and Prof. Roy Helge Gabrielsen supervised the thesis work.

<u>Acknowledgements</u>

I would like to thank my tutors, Jan Inge Faleide and Roy Helge Gabrielsen, for their supervision in completing this thesis. Both of them and I had lot of discussions, encouragement, and constructive comments that have been truly inspiring. I would also like to thank Michael Heeremans who has helped me prepare all of the data I needed to accomplish my thesis. Karen Agneta Leever and Olav Antonio Blaich also helped with many interesting discussions. Eventually, I would like to thank to Petrobar (Petroleum-related regional studies of the Barents Sea region) that has provided several interesting thesis topics to select.

June 2009

Wibi Aulia Harsum

Contents

Chapter 1

Introduction

Exploration for hydrocarbons in western Barents Sea started in 1979. Recent drilling in Sørvestsnaget Basin which is located in the southwestern Barents Sea (figure 1.1) was conducted by Norsk Hydro in summer 2000 and well 7216/11-1S tested the Cenozoic hydrocarbon play of the Sørvestsnaget Basin (Ryseth et al. 2003).

The southwestern Barents Sea has undergone a complex tectonic history since Late Devonian time including Carboniferous, Late Middle Jurassic - Early Cretaceous, and Late Cretaceous - Early Cenozoic rifting. This strongly influences the structural geology and stratigraphy of Sørvestsnaget Basin which is unparalleled by other basins in Barents Sea. Thus, the most prominent Upper Cretaceous succession in the Barents Sea is mainly confined to the Sørvestsnaget Basin, confirming the Late Cretaceous-Cenozoic separation of the Sørvestsnaget Basin from the remaining deep basins in the area (see also Faleide et al. 1993a,b; Breivik et al. 1998).

The objective of this thesis is to reconstruct the basin evolution in the Sørvestnaget Basin from Late Cretaceous to Paleogene times including details of its structural development.

Both computer and paper-based seismic interpretation work have been performed to complete this thesis. Understanding of regional geology is more easily extracted by interpreting several long 2D seismic lines crossing Sørvestsnaget Basin. 3D seismic was used to produce more detailed interpretation of several horizons needed to map the structural evolution.

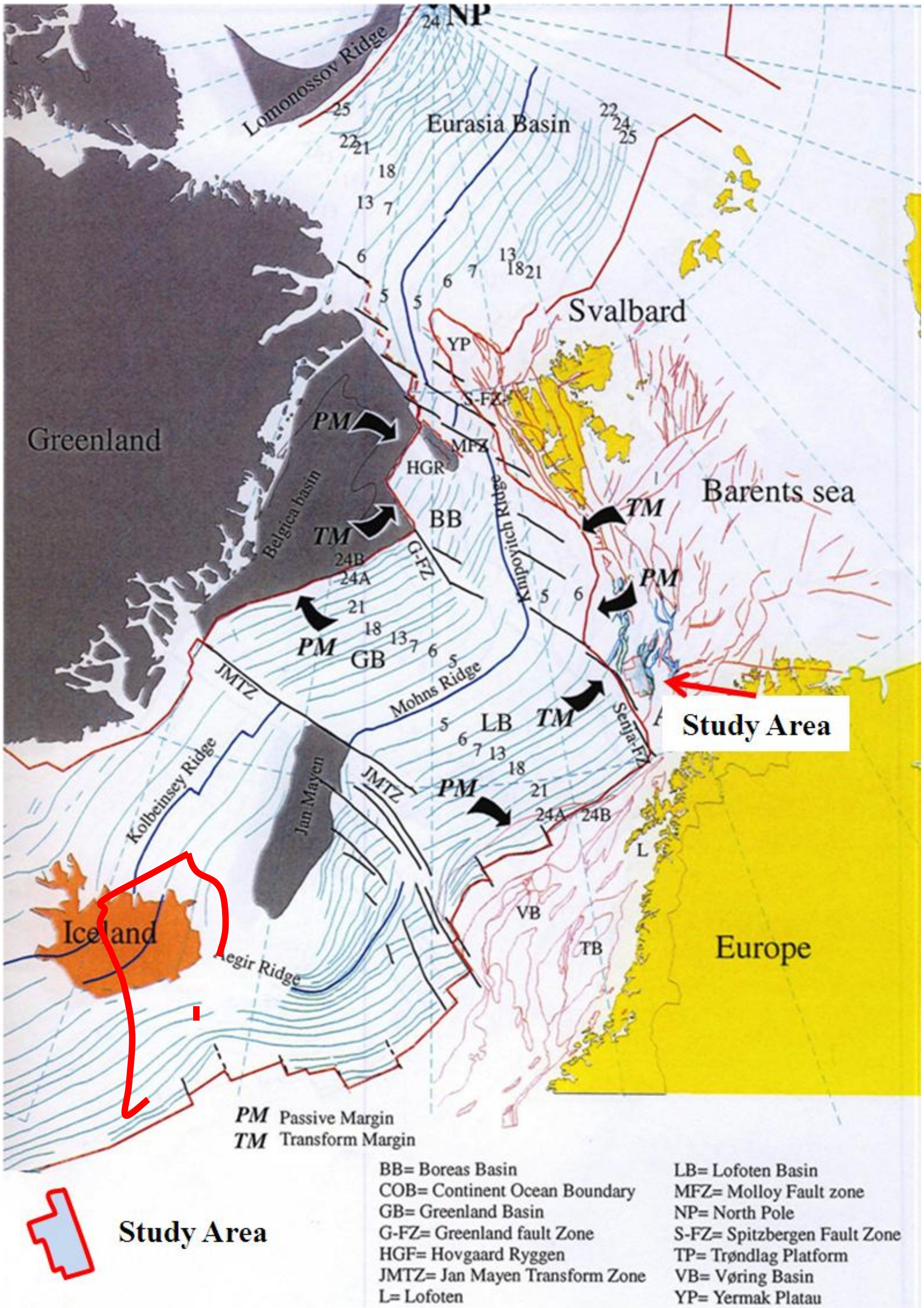

Figure 1.1. Location of Sørvestsnaget Basin in Southwestern Barents Sea (red box) (modified from Mosar, 1990)

Chapter 2

Geological Framework

The Sørvestsnaget Basin is situated between 71^0 and 73^0 N (figure 1.1), and between the oceanic crust and 18^0E (Gabrielsen et al., 1990). Figure 2.1 shows some main structural features framing Sørvestsnaget Basin such as Senja Ridge, Veslemøy High and Vestbakken volcanic province.

Faleide et al. (1993a) summarized the tectonic evolution of the North Atlantic-Artic (table 2.1). Furthermore, Faleide et al. (1991) suggested that the Cenozoic margin including the Sørvestsnaget Basin has experienced oblique shear transtension in the south and oblique extension in the north during latest Paleocene to earliest Eocene break up (table 2.2). Faleide et al. (1993a) also found that in the southwestern Barents Sea, the late Cretaceous development was complex with extension still dominating west of the Senja Ridge and the Veslemøy High.

There are quite a few publications discussing this area within Mesozoic era. However, some such as Gabrielsen et al. (1990) and Ryseth et al. (2003) noted that Sørvestsnaget Basin has a very thick succession of Cretaceous and Cenozoic sediments.

2.1. Regional Tectonic evolution

Pre break up

The pre-opening, structural margin framework is dominated by the NE Atlantic-Arctic Late Jurassic–Early Cretaceous rift episode responsible for the development of major Cretaceous basins such as the Møre and Vøring basins off mid-Norway, and the deep basins in the SW Barents Sea (Faleide et al., 2008). It has been suggested that the main Late Paleozoic–early Mesozoic rift episodes took place in mid-Carboniferous, Carboniferous–Permian and Permian–Early Triassic times (Doré, 1991). Faleide et al. (2008) furthermore noted that the later Triassic basin evolution was characterized by regi-

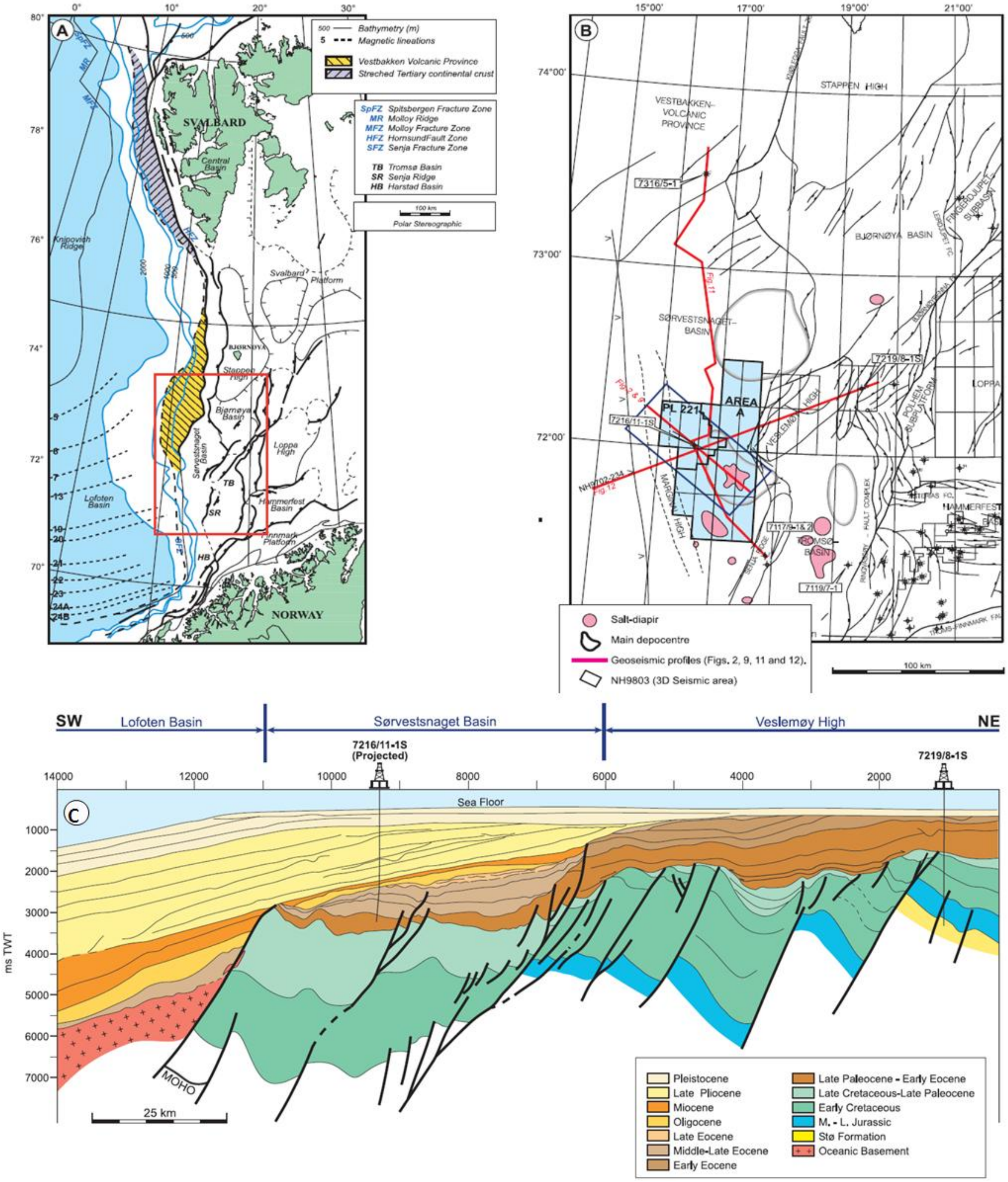

Figure 2.1 Regional overview of the study area; A. Main structural features; B. Close-up to the study area; C. Regional 2D interpretation of line 234 covering Lofoten Basin, Sørvestsnaget Basin, and Veslemøy High.

Megasequences	Plate tectonic events
Oligocene–Present	
	Plate reorganization (3 → 2 plates)[9]
	End spreading Labrador Sea[8]
Eocene	(Eurekan and Spitsbergen orogenies)
	Breakup Norwegian–Greenland Sea and Eurasia Basin[7]
	New spreading direction Labrador Sea[6]
Late Cretaceous–Palaeocene	(Eurekan Orogeny)
	End spreading Amerasia Basin[5]
	Breakup Labrador Sea[4]
Early Cretaceous	
	Breakup southern North Atlantic[3]
	Breakup Amerasia Basin[2]
Middle–Late Jurassic	
	Breakup Central Atlantic[1]

[1] Middle Jurassic; Ziegler (1988)
[2] Valanginian–Hauterivian; McWhae (1986); Ziegler (1988); Rowley and Lottes (1988)
[3] Pre-AM0; Hauterivian; Srivastava and Tapscott (1986); Keen and de Voogd (1988)
[4] Pre-A34; Latest Cenomanian; Roest and Srivastava (1989)
[5] Santonian; McWhae (1986)
[6] Earliest Eocene (A25–A24); Roest and Srivastava (1989)
[7] Earliest Eocene (A25–A24); Talwani and Eldholm (1977); Eldholm *et al.* (1989)
[8] Pre-earliest Oligocene (A13); Roest and Srivastava (1989)
[9] Earliest Oligocene (A13); Talwani and Eldholm (1977)

Table 2.1 Tectonic Evolution of the North Atlantic-Arctic (from Faleide, 1993a)

onal subsidence and deposition of large sediment volumes. The Lower-Middle Jurassic strata (mainly sandstones) reflect shallow marine deposition prior to the onset of the next major rift phase (Faleide et al., 2008).

A shift in the extensional stress field vector to NW-SE is recorded by the prominent NE Atlantic-Arctic late Middle Jurassic–earliest Cretaceous rift episode, an event associated with northward propagation of Atlantic rifting (Faleide et al. 1993). Considerable crustal

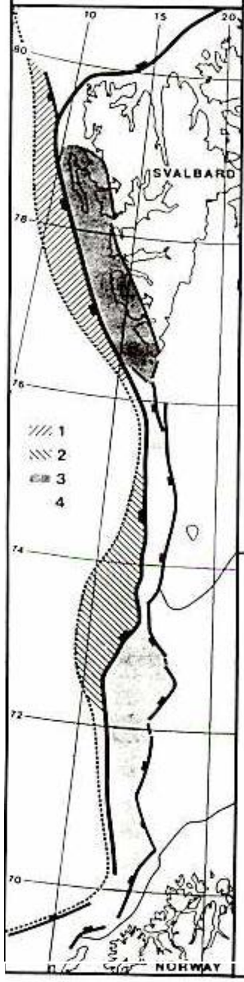

CENOZOIC MARGIN GEOLOGY	PRE-BREAKUP GEOLOGIC SETTING	CENOZOIC MARGIN EVOLUTION				STRUCTURE ACROSS THE MARGIN		
			A24 - A13		A13 - PRESENT	OCEANIC	TRANSITION	CONTINENTAL
	STABLE PLATFORM BOUNDED BY A CONTINENTAL TRANSFORM ZONE TO THE WEST ACTIVE IN LATE MESOZOIC TIMES	LATEST PALEOCENE - EARLIEST EOCENE BREAKUP	OBLIQUE? SHEAR TRANSTENSION?	EARLIEST OLIGOCENE PLATE TECTONIC REORGANIZATION	OBLIQUE EXTENSION	NORMAL OCEANIC CRUST	STRETCHED CONTINENTAL CRUST	
			OBLIQUE SHEAR TRANSPRESSION WEST SPITSBERGEN OROGENY					SPITSBERGEN FOLD AND THRUST BELT TERTIARY GRABENS DOWNFAULTED BLOCKS WEST OF HORNSUND FZ
			OBLIQUE SHEAR TRANSTENSION		PASSIVE	HIGH VELOCITY-DENSITY OCEANIC CRUST	NARROW STEEP MARGINAL FAULTS	DOWNFAULTED TERRACE BOUNDING THE SVALBARD PLATFORM
	BASINAL PROVINCE FORMED IN RESPONSE TO SEVERAL PHASES OF LATE PALEOZOIC AND MESOZOIC EXTENSION		OBLIQUE EXTENSION EARLY EOCENE VOLCANISM		OBLIQUE EXTENSION OLIGOCENE VOLCANISM PASSIVE SINCE MID OLIGOCENE	VOLCANIC COMPLEX AT MARGINAL HIGH NORMAL OCEANIC CRUST FURTHER WEST	TERTIARY VOLCANICS MASKING THE COT COT MODIFIED BY MID TERTIARY TECTONISM	
			OBLIQUE SHEAR TRANSTENSION		PASSIVE	HIGH VELOCITY-DENSITY OCEANIC CRUST	NARROW STEEP MARGINAL FAULTS	TERTIARY MARGINAL BASIN
			EXTENSION EARLY EOCENE VOLCANISM		PASSIVE	NORMAL OCEANIC CRUST	NARROW STEEP MARGINAL FAULTS	DOWNFAULTED BLOCKS COVERED BY VOLCANICS

Table 2.2 Cenozoic margin evolution and structure across the western Barents Sea-Svalbard margin. COT=continent-ocean transition (from Faleide et al., 1991)

extension and thinning led to the development of major Cretaceous basins off mid-Norway (Møre and Vøring basins) and East Greenland, and in the SW Barents Sea (Harstad, Tromsø, Bjørnøya and Sørvestsnaget basins) (Faleide et al., 2008). These basins underwent rapid differential subsidence and segmentation into sub-basins and highs.

In the North Atlantic realm, there is evidence for modest mid- Cretaceous extension in the Vøring Basin (Doré et al., 1999), Lofoten-Vesterålen margin (Tsikalas et al., 2001), onshore East Greenland (Whitham et al., 1999), and SW Barents Sea (Faleide et al., 1993). However, Skogseid et al. (2000) and Færseth and Lien (2002) argued that no distinct structures of this age are identified within the Vøring Basin. Biostratigraphic data from the Vøring margin reveal a change from neritic to bathyal conditions and an increase in sediment accommodation space in the Aptian-Albian, attributed to eustatic sea-level rise and regional tectonism (Gradstein et al., 1999).

Aptian rifting is well constrained in the SW Barents Sea (Faleide et al., 1993). Farther north, there are few signs of Cretaceous extensional deformation, but magmatism of Barremian-Aptian age is widespread within an Arctic large igneous province (LIP) (Grogan et al., 1998; Maher, 2001). Regional uplift in the north gave rise to southward sediment progradation in the Barents Sea. By mid-Cretaceous time, most of the structural relief within the Møre and Vøring basins had been filled in and thick Upper Cretaceous strata, mainly fine-grained clastics were deposited in wide basins (Faleide et al., 2008). Pulses of coarse clastic input with an East Greenland provenance appeared in the Vøring Basin from Early Cenomanian to at least Early Campanian times (Færseth and Lien, 2002).

Break up

Breakup in the NE Atlantic was preceded by prominent Late Cretaceous–Paleocene rifting (Faleide et al., 2008). Furthermore, Faleide et al. (2008) noted that at the onset of this rifting, the area between NW Europe and Greenland was an epicontinental sea covering a region in which the crust had been extensively weakened by previous rift episodes. Ren et al. (2003) suggested onset of rifting at about 81 Ma and that the main period of brittle faulting occurred in Campanian time followed by smaller-scale activity towards break up. The Campanian rifting resulted in low-angle detachment structures that updome thick Cretaceous sequences and sole out at medium-to deep intra-crustal levels on the Vøring and Lofoten-Vesterålen margins (Tsikalas et al., 2001; Gernigon et al., 2003; Ren et al., 2003).

The Late Cretaceous–Paleocene extension between Norway and Greenland was taken up by strike-slip movements/deformation within the De Geer Zone (figure 2.2). Pull-apart basins formed in the SW Barents Sea (e.g., Faleide et al., 1993; Breivik et al., 1998; Ryseth et al., 2003) and in the Wandel Sea Basin in NE Greenland (Håkansson and Pedersen, 2001). A relatively complete Paleocene succession was deposited under deep marine conditions in the Sørvestsnaget Basin and Vestbakken Volcanic Province (Ryseth et al., 2003).

Faleide et al. (2008) suggested that final lithospheric break up at the Norwegian margin occurred near the Paleocene–Eocene transition at ~55–54 Ma (Chron 24r). It culminated in a 3–6 m.y. period of massive magmatic activity during break up and onset of early sea-floor spreading. During the main igneous episode at the Paleocene– Eocene transition, sills intruded into the thick Cretaceous successions throughout the NE Atlantic margin, including the Vøring and Møre basins (Faleide et al., 2008).

The SW Barents Sea margin, along the Senja Fracture Zone (figure 2.1), developed during the Eocene opening of the Norwegian-Greenland Sea, first by continent-continent shear followed by continent-ocean shear, and has been passive since earliest Oligocene time (Faleide et al., 2008). Deep marine conditions persisted in the SW Barents Sea (Sørvestsnaget Basin) throughout Eocene time, with deposition of significant sandy submarine fans during the Middle Eocene (Ryseth et al., 2003). Breakup-related magmatism in the Vestbakken Volcanic Province was followed by down-faulting and deposition of thick Eocene strata (Faleide et al., 2008). The Bjørnøya-Spitsbergen margin segment experienced oblique continent-continent and partly continent-ocean shear with

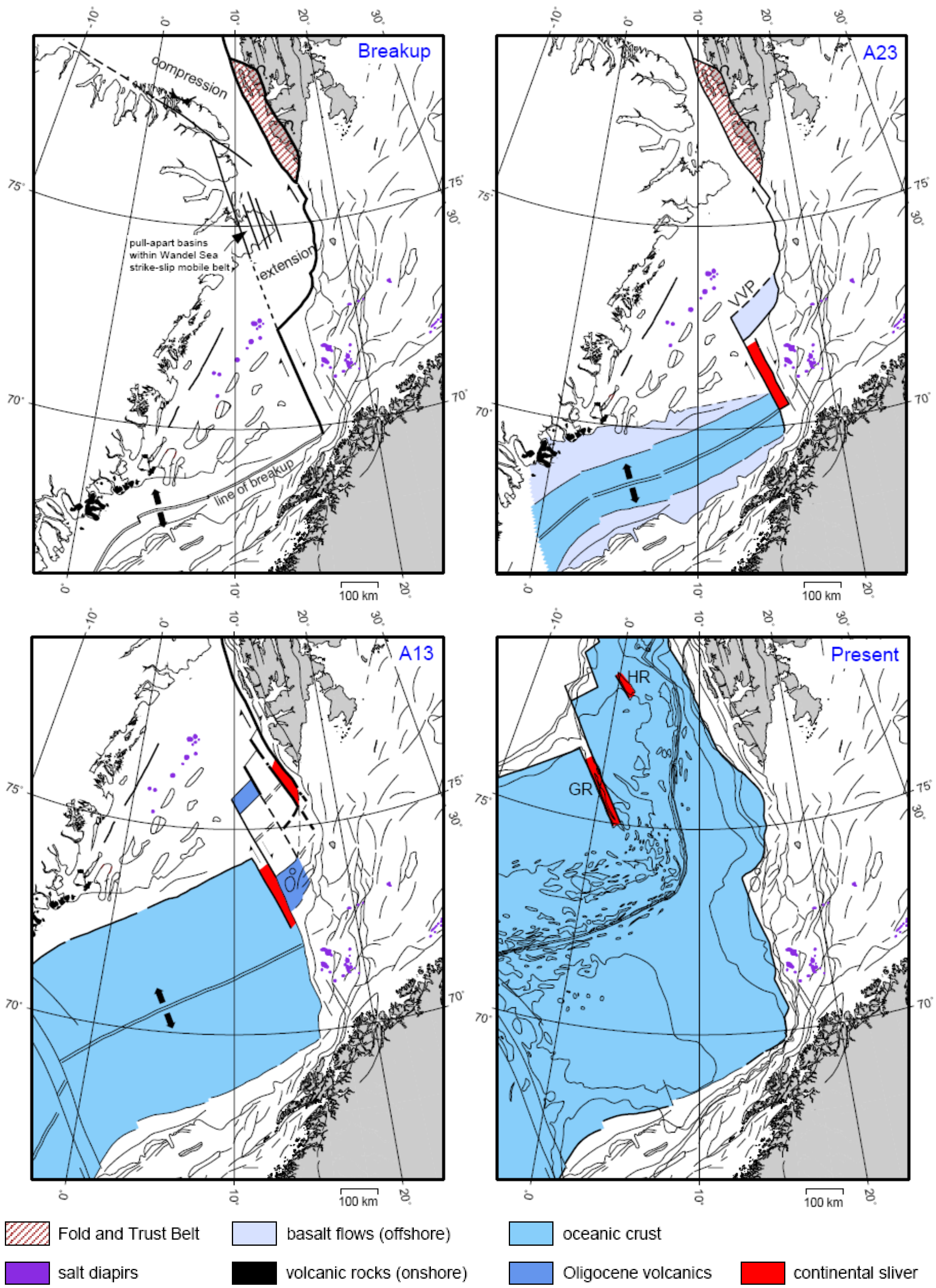

Figure 2.2 Cenozoic plate tectonic evolution of the Norwegian-Greenland Sea. GR: Greenland Ridge, HR: Hovgård Ridge, VVP: Vestbakken Volcanic Basin (Faleide et al., 2008)

both transtensional and transpressional components during Eocene time (Grogan et al., 1999; Bergh and Grogan, 2003).

At the end of Eocene, sea floor spreading had reached the margin off southern Spitsbergen and a narrow oceanic basin existed between the western Barents Sea and NE Greenland continental margins (figure 2.2) (Faleide et al., 2008). After a plate tectonic reorganization in earliest Oligocene time, Greenland (and North America) moved in a more westerly direction with respect to Eurasia (figure 2.2). Significant marine shallowing took place at the Eocene–Oligocene transition in the Sørvestsnaget Basin (Ryseth et al., 2003). Early Oligocene rifting, related to the change in relative plate motion, reactivated faults in the Vestbakken Volcanic Province, in particular those with a NE-SW trend (Faleide et al., 2008). This phase was also associated with renewed volcanism partly overprinting the break up structures (Jebsen and Faleide, 1998).

Post break up

Mid-Cenozoic compressional deformation (including domes/ anticlines, reverse faults, and broad-scale inversion) is well documented on the Vøring margin, but its timing and significance are highly debated (Doré and Lundin, 1996; Vågnes et al., 1998; Lundin and Doré, 2002; Løseth and Henriksen, 2005; Stoker et al., 2005a). The main phase of deformation is clearly Miocene in age but some of the structures were probably initiated earlier in Late Eocene– Oligocene times.

There is increasing evidence on the Norwegian margin for Late Miocene outbuilding on the inner shelf (Molo Formation; Eidvin et al., 2007) indicating a regional, moderate uplift of Fennoscandia (Faleide et al., 2008). At the western Barents Sea margin, a Late Miocene uplift event increases in amplitude eastwards within the Vestbakken Volcanic Province and may be related to pre-glacial tectonic uplift of the Barents Shelf (Jebsen and Faleide, 1998).

Over the entire shelf there is a distinct unconformity, which changes on the slope to a downlap surface for huge prograding wedges of sandy/silty muds sourced on the mainland areas around the NE Atlantic and the shelf (e.g., Barents Sea) (Faleide et al., 2008). Furthermore, Faleide et al. (2008) suggested that this horizon mark the transition to glacial sediment deposition during the Northern Hemisphere Glaciation since about 2.6 Ma. Large Plio-Pleistocene depocenters formed fans in front of bathymetric throughs scoured by ice streams eroding the shelf (Faleide et al., 1996; Laberg and Vorren, 1996; Dahlgren et al., 2005; Nygård et al., 2005; Rise et al., 2005). Plio-Pleistocene uplift and glacial erosion of the Barents Shelf and deposition of large volumes of glacial deposits in submarine fans along the margin resulted in a regional tilt of the margin (Dimakis et al., 1998). In terms of post-opening sediments, the glacial component constitutes more than half of the total volume deposited on the mid-Norwegian and western Barents Sea margins (Faleide et al., 2008). The greatly enhanced Plio-Pleistocene deposition rates within the fans induced excess pore pressure and sediment instability resulting in a series of submarine slides of various sizes and timing (Bryn et al., 2005; Evans et al., 2005; Solheim et al., 2005; Hjelstuen et al., 2007).

2.2. Structural features in the SW Barents Sea

The regional geology of Sørvestsnaget Basin comprises some complex structural features (see figure 2.1). It is because the Barents Sea area has undergone several phases of tectonism and sedimentation since the Devonian, eventually leading to crustal break up and sea floor spreading in the north Atlantic rift.

2.2.1. Sørvestsnaget Basin

The Sørvestsnaget Basin is situated between 71^0 and 73^0, and between the oceanic crust and 18^0E (Gabrielsen et al., 1990). Furthermore, Gabrielsen et al. (1990) suggested that this basin has a very thick succession of Cretaceous and Tertiary sediments. In deep seismic lines, the base of the Cretaceous is interpreted as dropping to more than 9 seconds TWT.

At Cretaceous levels, the Sørvestsnaget Basin represents a structural continuation of the Bjørnøya Basin (Gabrielsen et al., 1990). However, at the Jurassic level there is a deeply buried high between two basins, as pointed out by Rønnevik and Jacobsen (1984). It has therefore been closely linked to the Bjørnøya Basin for some of its history and been a separate structure at other times.

The Sørvestsnaget Basin is separated from Bjørnøya Basin by a system of normal faults of Tertiary age, referred to as a Tertiary hinge line by Faleide et al. (1988). Faults of the same age are found within the basin, too (Gabrielsen et al., 1990). Thick basin contains a thick sequence of Tertiary rocks and is covered by a thick wedge of Pliocene to Pleistocene sediments (Spencer et al., 1984

The northern limit of the basin is defined by the lavas in the Vestbakken volcanic province and by the NE-SW trending fault complexes on the southern part of Stappen High (Gabrielsen et al., 1990). To the southeast, the basin is bounded by the Senja Ridge (Brekke and Riis., 1987) and the Veslemøy High.

2.2.2. Senja Ridge

The Senja Ridge runs subparallel to the continental margin and defines the western limit of the Tromsø Basin (Gabrielsen et al., 1990). Furthermore, Gabrielsen et al., (1990) suggested that it is a complex ridge possibly containing different types of intrusion, some of which may be interpreted as carrying salt and/or shale. It is characterized by N-S trending, positive gravity anomaly which has been taken as an indication that the ridge is underlain by a basement high (Syrstad et al., 1976) that may be overlain by a thin upper Paleozoic, Triassic, and Jurassic sequence (Brekke & Riis, 1987). An intra Cretaceous unconformity cuts nearly down to the estimated basement surface at the highest point of the ridge, and thick Paleocene to Pleistocene sequences drape the structure (Spencer et al., 1984)

Gabrielsen et al. (1990) noted that to the east and west, the southern segment of the Senja Ridge is limited by step-like normal faults trending NNW-SSE and NNE-SSW, identified at Cretaceous level. The structure is cross-cut by NW-SE trending fault, and along its northwestern shoulder and at its southern termination the Tertiary and Cretaceous sequences are locally folded (Gabrielsen et al., 1990).

Furthermore, Gabrielsen et al. (1990) estimated that the difference in elevation between the Senja Ridge and Trømso Basin defined at the level of the base of the Cretaceous to is around 8000m.

The activation of the Senja Ridge has been viewed in connection with Tertiary dextral shear along the continental margin (e.g. Hinz & Weber, 1975; Rønnevik et al., 1975), although opposing views have been put forward (Spencer et al., 1984). Riis et al. (1986) argued that the development of the ridge may be linked to dextral shear along the continental margin in Late Cretaceous resulting in conjugate sinistral shear along the ridge, the system being reactivated in Oligocene times.

2.2.3. Veslemøy High

The Veslemøy High is separated from Senja Ridge by a narrow depression probably caused by faulting at depth and bounded by the deep Bjørnøya Basin and the Sørvestsnaget Basin to the north and northwest and the Tromsø Basin to the south (Gabrielsen et al., 1990).

It can be mapped as a structurally isolated high at the Cretaceous and Tertiary levels, and is also a pronounced gravimetric high (Norsk Polarinstitut 1985). Large rotated fault blocks and gentle domes may be defined at the intra Jurassic level, but the Cretaceous sediments are deformed by formation of elongated domes (Gabrielsen et al., 1990).

Furthermore, Gabrielsen et al. (1990) related the formation of the Veslemøy High to the development of the Bjørnøyrenna Fault Complex, and the timing of normal and lateral faulting is probably the same.

2.2.4. Vestbakken Volcanic Province

To the north, the Vestbakken Volcanic Province with Early Eocene and Pliocene magmatism (see Faleide et al. 1988; Mørk & Duncan 1993; Sættem et al. 1994; Rasmussen et al. 1995) is separated from the Sørvestsnaget Basin by a zone of NE-trending normal faults.

Faleide et al. (1993a) suggested that the Vestbakken Volcanic Province consists of an igneous complex, which is elevated with respect to the adjacent oceanic crust and which masks the continent-ocean boundary at the rifted margin segment. It is characterized by a smooth acoustic basement surface and some subbasement reflections, particularly below its inner part (Faleide et al. 1988; Myhre and Eldholm 1988).

The province includes an outer oceanic part and a stretched continental part, both covered by lava flows and interbedded sediments (Faleide et al. 1993a). Renewed extensional faulting and volcanism related to the earliest Oligocene change in relative plate motion have partly overprinted the break up structures (Faleide et al. 1988; 1991). The Vestbakken Volcanic Province is bounded landwards by a listric fault complex formed in Early Tertiary times. Locally, flows are recognized within the fault complex, revealing large scale vertical movements in Eocene- Oligocene times (Faleide et al. 1988).

2.2.5. Senja Fracture Zone

The Cenozoic evolution of the Senja Fracture Zone (SFZ) at the southern sheared margin is closely linked to the opening of the Norwegian - Greenland Sea (e.g. Talwani & Eldholm 1977; Myhre et al. 1982; Eldholm et al. 1987; Faleide et al. 1991, 1993a, 1996, 2008; Vågnes 1997; Skogseid et al. 2000). Landward of the SFZ, the margin bounds a basinal province in which as much as 18–20 km of sedimentary strata cover a highly attenuated crystalline crust (Tsikalas et al. 2002).

The Senja Fracture Zone separates the Lofoten Basin, which contains ca. 5 - 7 km of mainly Neogene sediments (Faleide et al., 1993b) above the oceanic crust, from the

Sørvestsnaget Basin. The transition from oceanic to continental crust occurs over a ca. 20 km wide zone (Faleide et al., 1993b; Breivik et al., 1998), and encompasses a marginal high along the western margin of the Sørvestsnaget Basin

This marginal high is characterized by truncation of Paleogene strata, as inferred from seismic data (Brekke & Riis 1987; Faleide et al. 1993a,b; Knutsen & Larsen 1997; Vågnes 1997; Brevik et al. 1998). Geophysical modelling of ocean bottom seismic data (OBS) and potential field data (Mjelde et al. 2002) indicate that igneous intrusions are present at about 9,5 km along the marginal high, suggesting that the initial uplift was related to magmatism during break up. It is reported not to have been tectonically active since the mid-Oligocene (Knutsen and Larsen 1997; Ryseth et al. 2003).

2.3. Stratigraphy

The first regional surveys in the Barents Sea showed that the area was underlain by thick sedimentary sequences (Eldholm and Ewing 1971; Sundvor 1974; Renard and Malod 1974; Eldholm and Talwani 1977; Hinz and Schlüter 1978; Rønnevik 1981). Only a few wells that have penetrated the Mesozoic sequence and the first wells were drilled on Tromsøflaket in 1980 (Dalland et al., 1988).

The definitions of lithostratigraphical units herein (figure 2.3) are based mainly on well data from the Hammerfest Basin, but also taking into account data from other structural provinces drilled to date (Dalland et al., 1988).

2.3.1. Late Cretaceous Stratigraphy

Gabrielsen et al. (1990) suggested that Sørvestsnaget Basin has experienced significant subsidence since the Early Cretaceous, providing accommodation space for a substantial thickness of Cretaceous and Cenozoic sediments. Breivik et al. (1998) noted that the Sørvestsnaget, Bjørnøya, and Tromsø basins show equal rates of Early Cretaceous subsidence, with the Sørvestsnaget Basin subsequently showing more pronounced Late

Cretaceous and Cenozoic subsidence as compared to that of the Tromsø and Bjørnøya basins, indicating a temporal, westward migration of the tectonic activity, towards the transform margin.

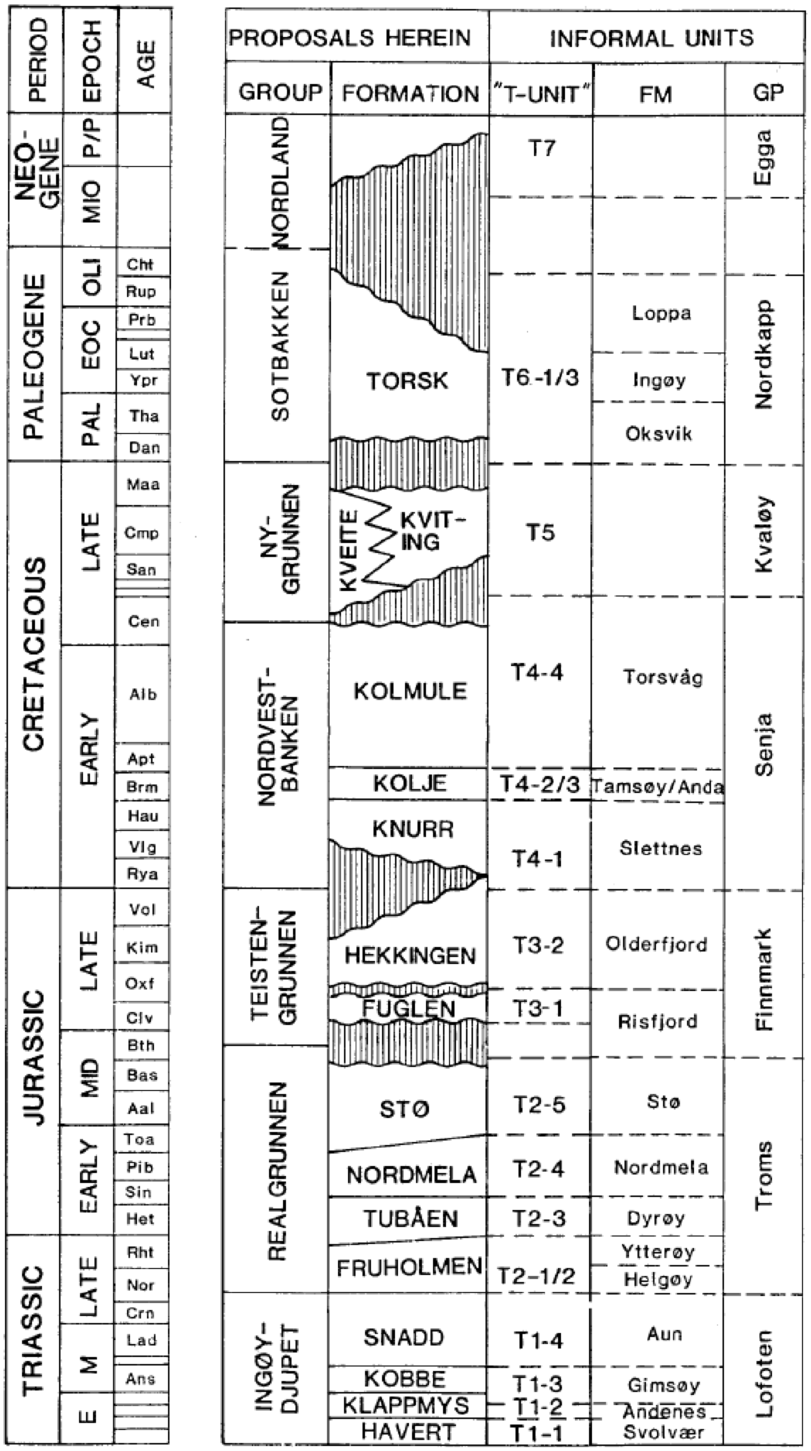

Figure 2.3. Lithostratigraphical column of Tromsøflaket (Dalland et al., 1988)

2.3.2. Paleocene to Early Eocene Stratigraphy

According to Ryseth et al. (2003), it is clear that, there is a complete Upper Paleocene – Lower Eocene succession dated by biostratigraphic methods. Furthermore, a thin unit of Danian is found. The Paleocene - Lower Eocene section comprises deposits of Late Paleocene and Early Eocene age where most of the deposits are dominated by greyish mudrocks, with traces of very fine- to fine-grained sandstone, stringers of limestone and dolomite, grey, greenish to blackish mudrocks (see Ryseth et al. 2003).

In addition, Ryseth et al. (2003) suggested that the completely fine-grained nature of the Paleocene - Lower Eocene succession is indicative of deposition in a generally low-energy marine environment.

2.3.3. Middle Eocene to Miocene Stratigraphy

The Middle Eocene (Lutetian-Bartonian) is dominated by grey to dark grey mudstones with limestone/dolomite stringers and scattered traces of very fine- to fine grained sandstones except for a significant Lutetian sandstone unit. The Lutetian interval (2546 - 3166 mMSL) is the only significant potential reservoir rock penetrated by well 7216/11-1S that was deposited as submarine fans (see Ryseth et al 2003).

The Late Eocene (fig 2.4) sequence consists of a thin and condensed Priabonian unit with varicoloured grey, green, and brown to blackish mudrocks associated with minor limestones (Ryseth et al. 2003).

The Oligocene and Miocene succesion (fig 2.4) probably represents deposits in shallow marine environment (Ryseth et al., 2003). Onlap of these strata towards the western marginal high is a clear indication that the high formed a positive topographic element during deposition showing that this marginal was re-activated at the Eocene - Oligocene. Subsequently, Oligocene - Miocene deposits filled in a more shallow marine basin confined to the west, and separated from age-equivalent deposits in the Lofoten Basin, by the marginal high. This aspect is further discussed below.

2.3.4. Late Pliocene – Pleistocene Stratigraphy

The entire section down to 2246 mMSL contains calcareous benthonic foraminifera and reworked Cenozoic and Mesozoic palynomorphs and microfossils (e.g. *Inoceramus* prisms) (Ryseth et al., 2003). The lithology is dominated by grey clays and claystones with minor beds of fine- to very coarse sand. Deep incisions occur within the clinoforms (figure. 4.3), apparently truncating deposits of Eocene - Paleocene age in the vicinity of the marginal high.

A glacio-marine depositional environment can be inferred from the available micropaleontological data, in good agreement with previous studies of the clastic wedge (e.g. Sættem et al. 1994; Faleide et al. 1996). The clinoforms are related to progradation of glacial deltas supplied from the uplifted shelf to the east, whereas the incisions probably represent feeder channels cut during glacio-eustatic sea level falls (Ryseth et al., 2003).

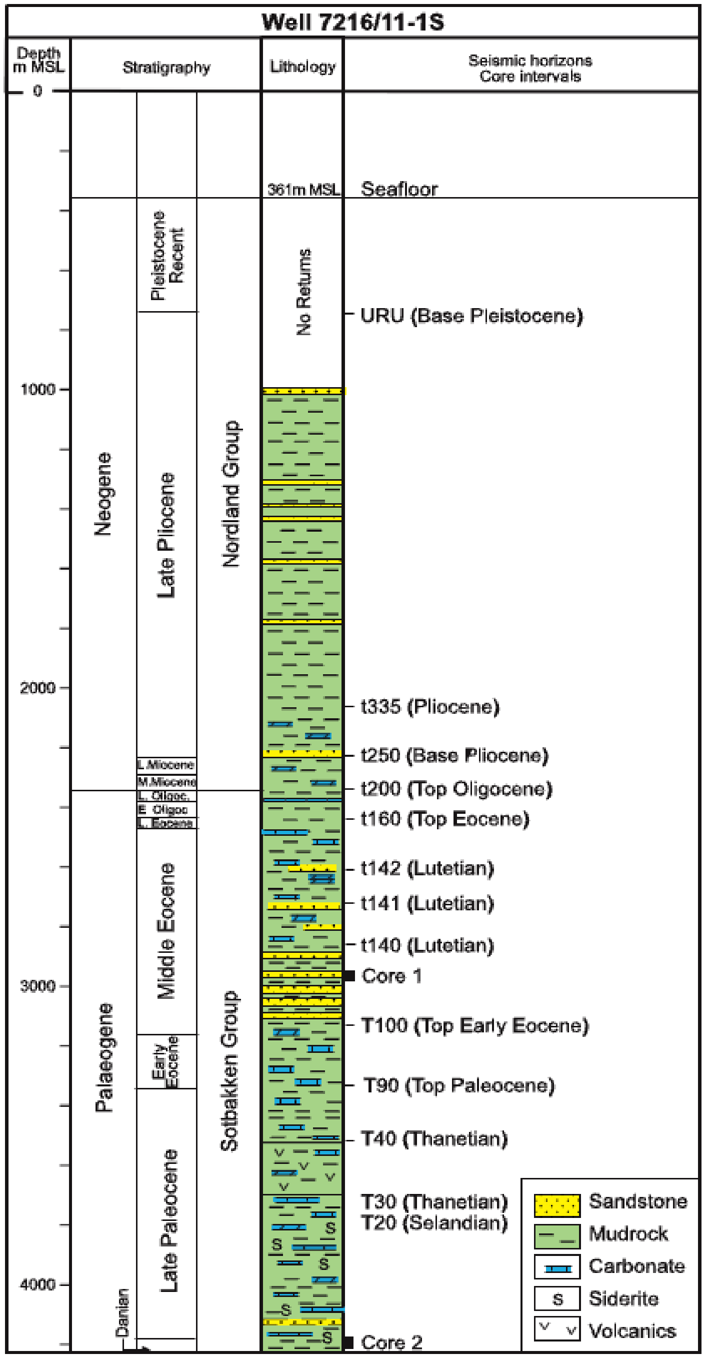

Fig 2.4 Cenozoic Stratigraphy from well 7216/11-1S in Sørvestnaget Basin Ryseth et al. (2003)

Chapter 3

Data and methods

3.1. Data

The southwest Barents Sea continental margin is covered by a relatively dense grid 2D reflection seismic data. Figure 3.1 shows all of the data used in this study that includes 2D and 3D seismic data. The primary seismic database for the present study has been the NH9702 and NPD-TR-82 surveys. The 2D survey NH9702 comprises 5752 km of reflection seismic data, including four deep seismic lines, and covers the seismic area in a line spacing of 1 x 2 km (Ryseth et al. 2003). Most of the 2D lines are recorded to 8 seconds two way time (TWT). However, a few long 2D lines for example NH9702-234 have images down to 17 s TWT. The 3D seismic data which is used in this study is NH9803. It trends NW-SE and displays 7.5 s TWT seismic data. This 3D seismic survey covers 2000 km^2 area in central Sørvestsnaget Basin (figure 3.1). 2D seismic data are used to show the regional geology structural interpretation over the study area whereas the 3D seismic data are for more detailed seismic structural interpretation.

In general, the 3D seismic data quality is good. The 2D seismic quality varies from poor to good. A comparison of an arbitrary 3D seismic data along a 2D seismic line will also be shown in the next chapter.

3.2. Methods

The strategy applied in this study is firstly to perform regional seismic interpretation on paper-based 2D seismic sections. Several seismic sections were selected to see the main structural features and to understand the regional geology over the study area where the 3D seismic data do not cover (for instance NH9702-234, NH9702-101, NH9702-102, NH9702-103, and 441).

After interpreting several 2D lines, Geoframe (Charisma) software was used to map out the four seismic reflectors selected for this study. Faults, anticlines, synclines, and salt diapirs were also noted and plotted on a paper basemap.

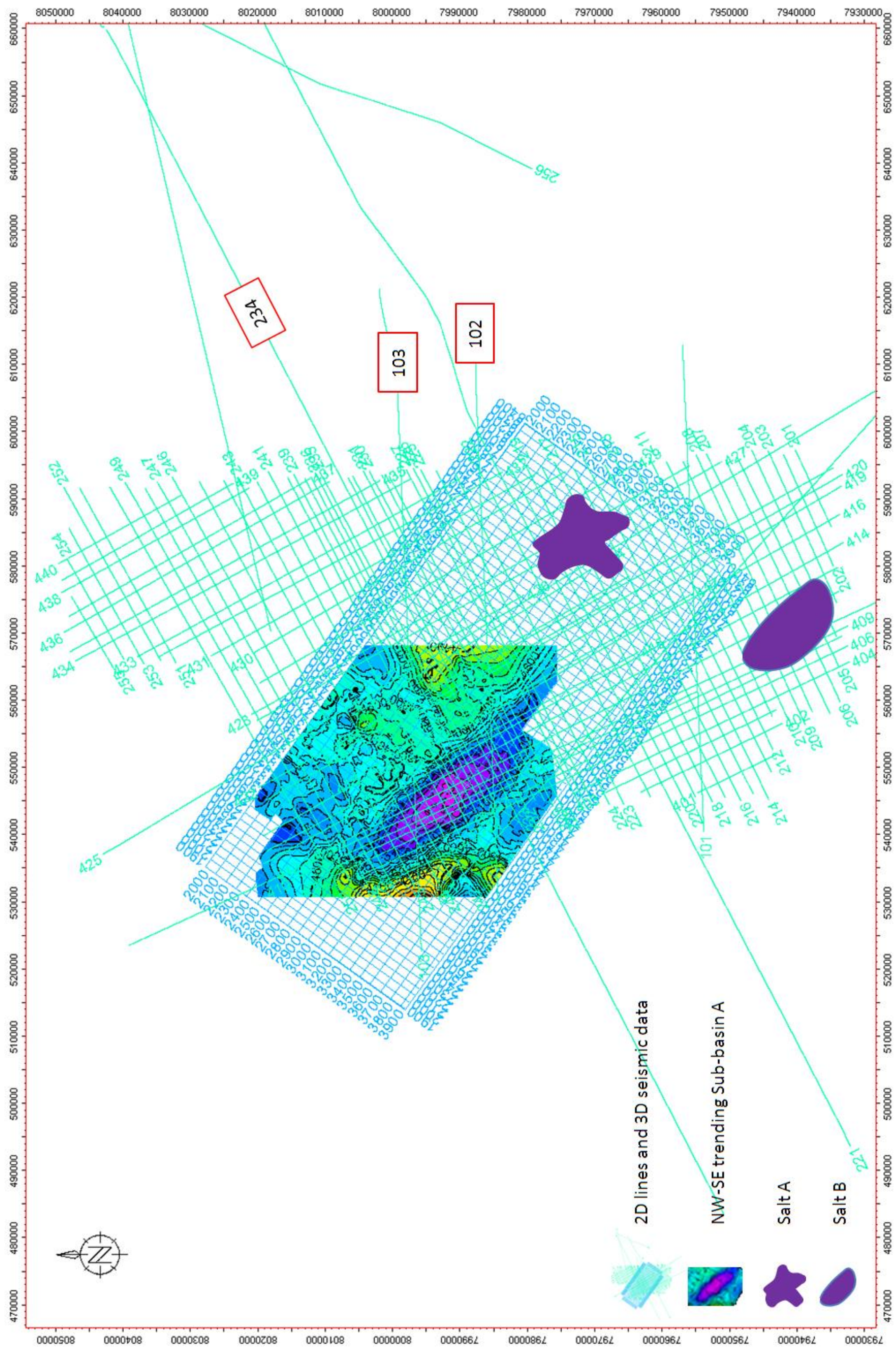

Figure 3.1. Location of study area showing 2D lines and 3D grid. This figure also includes identified salt A and B and the NW-SE trending Sub-basin A.

Furthermore, Petrel software was used to interpret the 3D seismic data. In this phase, a more detailed structural interpretation was carried out. The reflectors selected which are Base Oligocene, Top Early Eocene, Intra Late Paleocene, and Mid Cretaceous were generated by using this software. The two shallowest reflectors show the most continuous reflection on the 3D seismic data. They have strong amplitude, relatively high frequency, and good continuity as well. Therefore, the seismic interpretation was performed in every 250 inlines and 500 crosslines. The Intra Late Paleocene and Mid-Cretaceous reflectors show more complexities. Therefore, they were interpreted every 200 inlines and 300 crosslines. However, in some cases very complex areas cannot be solved by such increment so that the interpretation needs to be interpreted every 10 inlines and 10 crosslines.

The interpretation used a “loop” technique (figure 3.2). This technique simply shows the interpretation of inlines and crosslines in one display. It means that both inline and crossline interpretations are always controlled to match each other. Therefore, any shift between the reflections tracked can be minimized. Seismic volume attribute in Petrel called structural smoothing was performed to display the seismic section more clearly (figure 3.2). In addition to that, a surface attribute was also created to see fault or fold indicators on the seismic surface.

The challenge of interpreting the seismic data in this study is at first the 2D regional seismic data resolution (horizontal resolution) which is relatively poor in some areas. When it comes to 3D seismic data, the interpretation can be more detail as the data have better horizontal resolution. However, in several areas which are seismically obscured due to massive deformation, more closely interpretation is needed to resolve the interpretation. Showing the time slice was also performed to see the coverage of the 3D seismic data and quickly see through the salt diapirs and Sub-basin A extents.

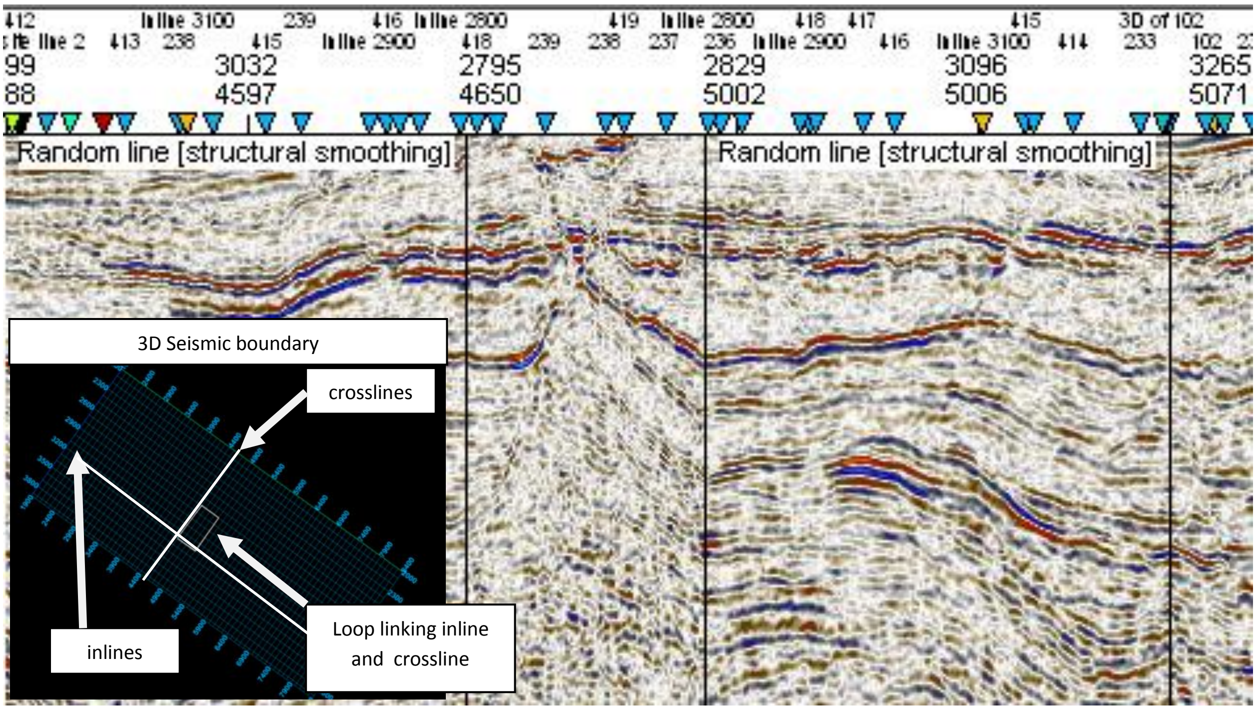

Figure 3.2. Inline and crossline section combined in one display to minimize shifting in reflection interpretation

Chapter 4

Seismic Interpretation

4.1. Interpretation procedure

In this study, the main focus is the Sørvestsnaget Basin. Therefore, detailed major interpretation is only performed in the Sørvestsnaget Basin. There is an illustration (figure 2.1) showing the regional interpretation of NH-9703-234 covering Sørvestsnaget Basin, Lofoten Basin, and also Veslemøy High. The other illustration (figure 4.1) covers only Sørvestsnaget Basin with the seismic stratigraphy markers. The seismic stratigraphy is correlated to the projected well and used in this study as guidance. In addition, one of the seismic sections that is shown with the interpreted reflections is inline 2800 (figure 4.2).

This line was interpreted with a complete series of reflections in Cenozoic which are Base Pliocene, Base Late Miocene, Base Miocene, Base Oligocene, Intra Lutetian, Top Early Eocene, and Intra Late Paleocene. Well 7216/11-S is projected and shown penetrating through Paleocene. Figure 4.3 also shows that Oligocene - Miocene strata onlap the Eocene - Oligocene boundary towards the western marginal high of the Sørvestsnaget Basin, testifying to the unconformable nature of the basal Oligocene surface (Ryseth et al. 2003). This line is then used as a calibrated seismic section. Eventually, there are 4 reflections interpreted for this study which are Base Oligocene, Top Early Eocene, Intra Late Paleocene, and Mid-Cretaceous (see figure 4.3).

4.2. Structural feature identification

A map showing structural features (figure 3.1) was firstly studied to identify what structural features frame Sørvestsnaget Basin (study area) and also some major faults. This identification process quickly helped understanding what exist in the coverage area of the 2D data.

In the southern part of the study area, there are two major salt diapirs observed (figure 4.4). These diapirs leave a structural low in their surroundings that is rimmed structure. In the eastern part, there are some ridges bounding Sørvestsnaget Basin which are Senja Ridge in the southern part of the basin and Veslemøy High in the northern part (figure 3.1).

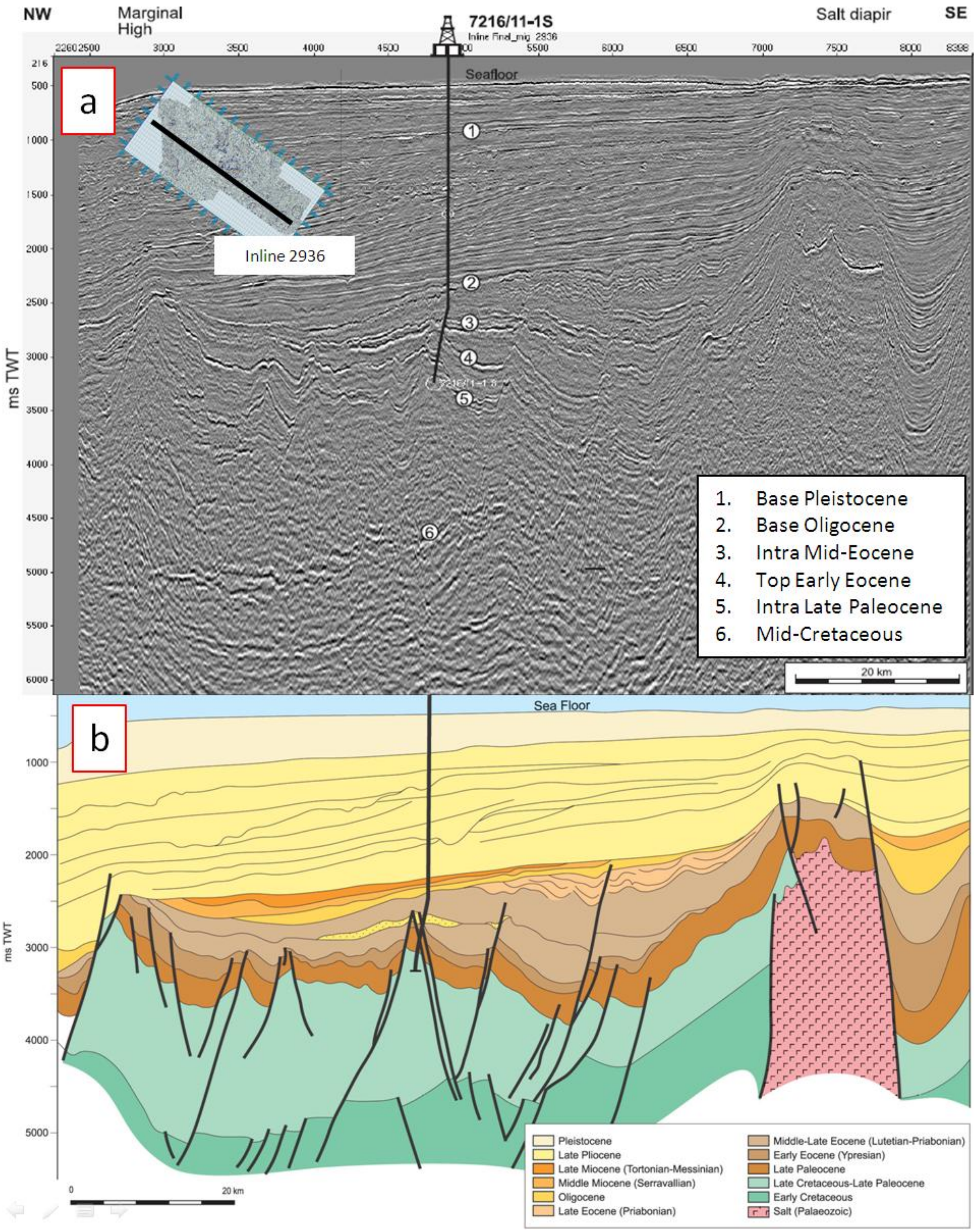

Figure 4.1. Illustration of interpreted 3D seismic section NH-9803-2936 correlated to well 7216/11-S (modified from Ryseth et al., 2003).

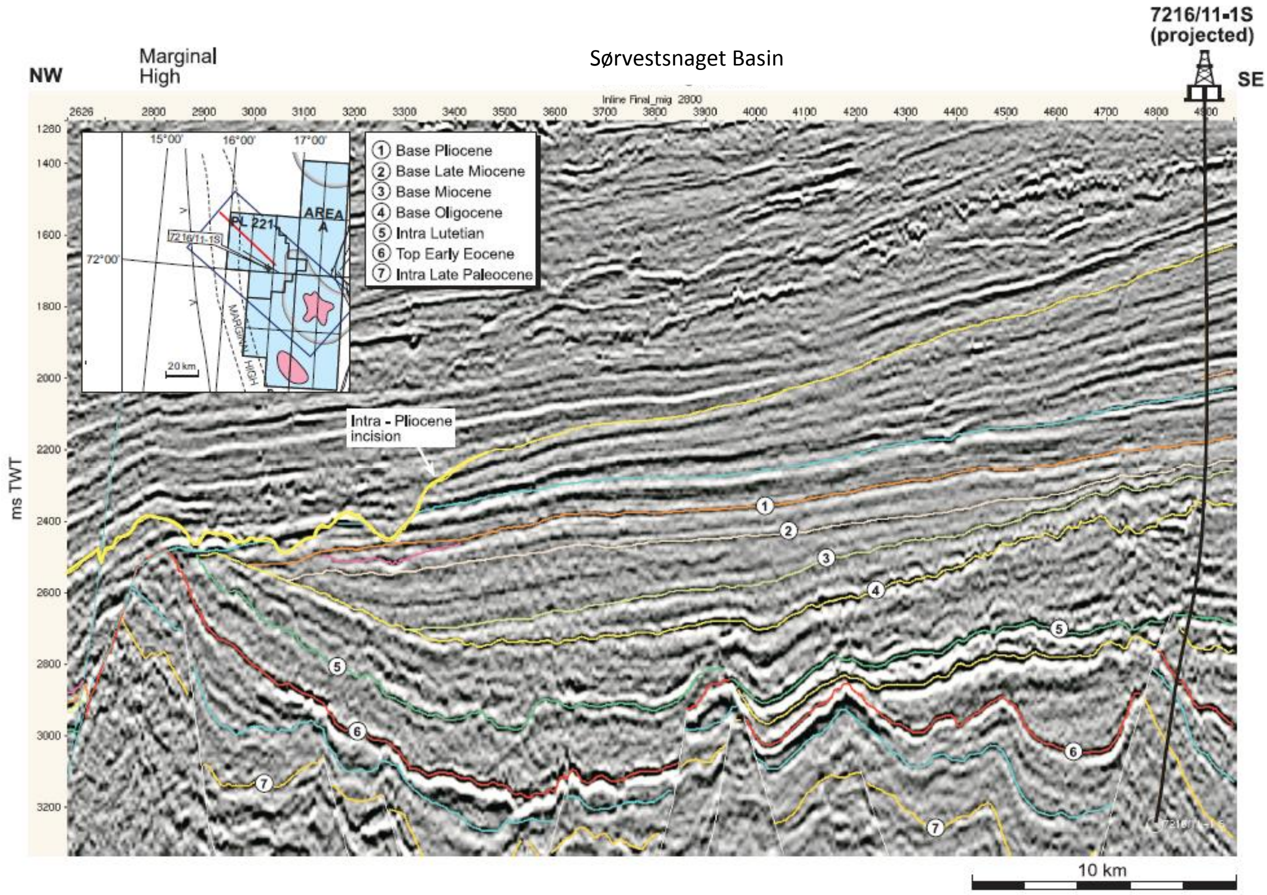

Figure 4.2. Seismic section with calibrated reflections by well 7216/11-1S (from Ryseth et al. 2003).

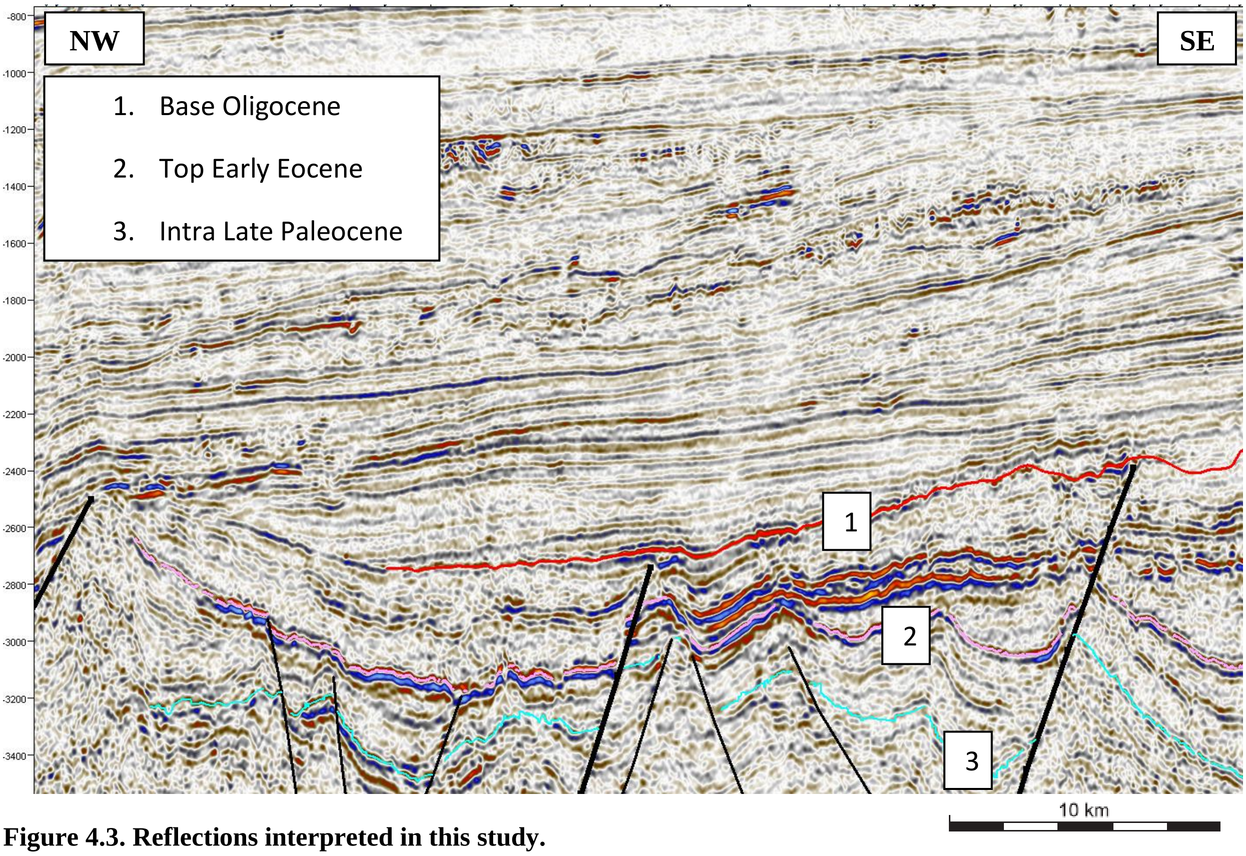

Figure 4.3. Reflections interpreted in this study.

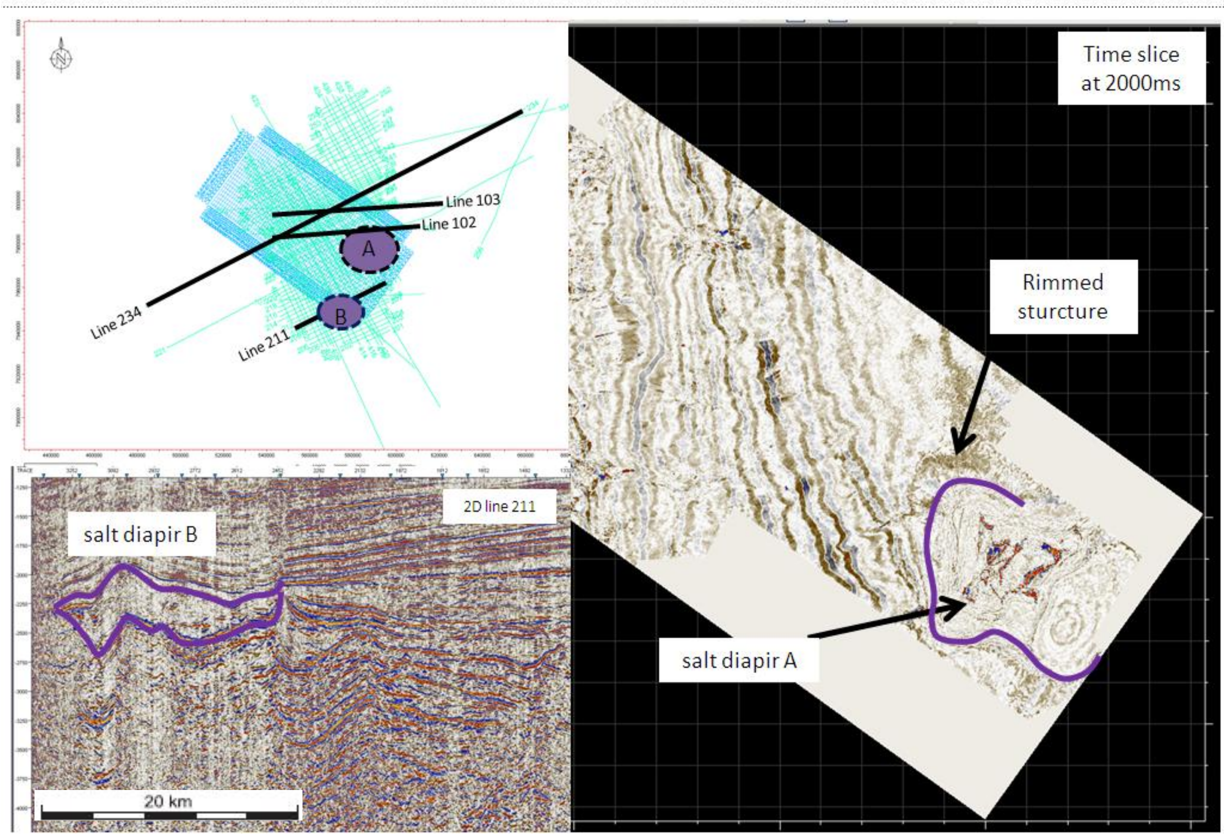

Figure 4.4. Major salt diapirs observed in the southern part of study area. There are also several 2D lines shown (102, 103, and 234) that will mainly be observed in this study.

4.3. Main Reflections

Several reflections were chosen for this study based on the interpretation of 3D seismic data and its correlation to the well from Ryseth et al. (2003). These reflections are Mid-Cretaceous, Intra Late Paleocene, Top Early Eocene, and Base Oligocene. A correlation was performed to show how the well (lithology and stratigrapy) correlates with a seismic section (figure 4.5).

Mid-Cretaceous

This reflection remains undrilled as it was not penetrated by well 7216/11-1S which is the only well in Sørvestsnaget Basin. However, long distance correlation to the Tromsø Basin supports this dating and is consistent with interpretation of Faleide et al. (1993a). Mid-Cretaceous reflection is characterized by medium to strong amplitude, low frequency, and high continuity. Mid-Cretaceous in Sørvestsnaget Basin can be found at 3500 – 5500 ms two way travel time (TWT) (figure 4.1). It has been difficult to track this reflection to the southwestern part of the study area. It is also poorly defined towards the marginal high.

Intra Late Paleocene

Intra Late Paleocene reflection is situated at 2900 - 4100 ms TWT. It is the lowermost reflection which has medium to strong amplitude, medium to high frequency, and fair continuity that is penetrated by the well (figures 4.1 – 4.3). The limestone stringers (figure 4.5) overlain by volcanic tuffaceous fragments might create the medium to strong reflection. Intra Late Paleocene is either truncated or onlaps towards a local high between the marginal high and the main Late Cretaceous Basin.

Top Early Eocene

This reflection has a strong amplitude and medium to high frequency. It is located at 2200 – 3700 ms TWT (figures 4.1 – 4.3). Top Early Eocene is lithologically represented by dark mudrocks with carbonate cemented stringers overlain by several layers of sandstones (figure 4.5). Therefore this layer is fairly strong to be tracked in most of areas on the seismic section inside the 3D data (figure 4.3).

Base Oligocene

Base Oligocene represents the boundary between folded reflections and reflections dipping to west (figures 4.1 – 4.3). This reflection has medium to strong amplitude and high continuity. Its frequency is relatively high. It can be found at 1900 – 3000 ms TWT.

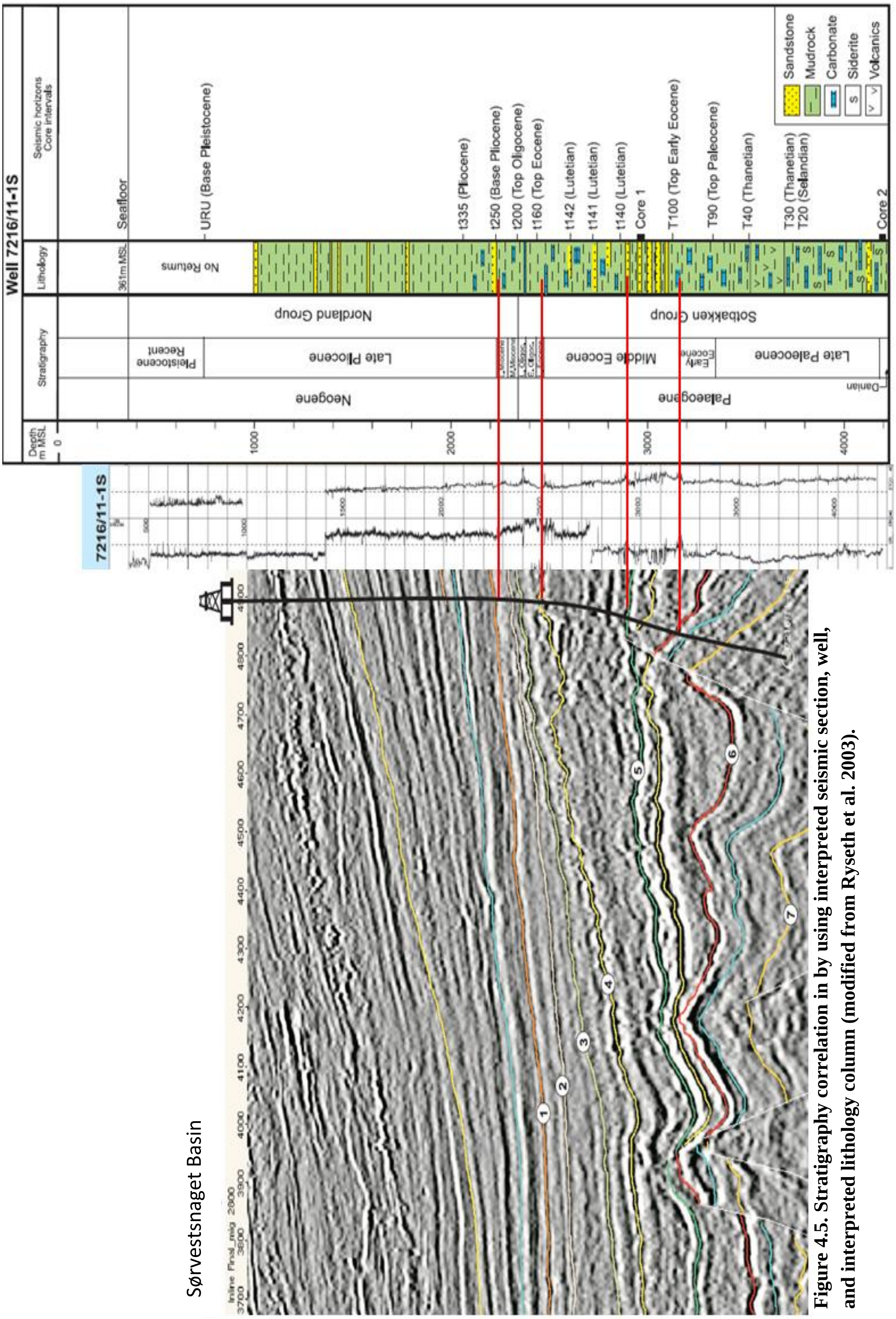

Figure 4.5. Stratigraphy correlation in by using interpreted seismic section, well, and interpreted lithology column (modified from Ryseth et al. 2003).

4.4. 2D Seismic Interpretation

Three regional lines were selected for illustrating the main structural and sedimentary units of the Sørvestsnaget Basin, namely NH-9709-102, NH-9709-103, and NH-9709-234 (figure 4.4). It is emphasized that NH-9709-102 particularly well illustrates the geology of the middle to southern part of the study area, NH-9709-103 is to see the center of the basin, and NH-9709-234 is to see the one of the best views of Mid-Cretaceous basin.

Line NH-9709-102

Figure 4.6 shows the interpretation of the E-W trending line NH-9709-102 (see figure 4.4 for location). The seismic quality is not very good but it covers salt diapir A (figure 4.4) in the eastern part and the internal basin as well. This regional interpretation tells that in the southeastern part of the study area, there is a salt diapir that penetrates through Mid-Cenozoic.

Base Oligocene reflection and its above sequences dip to the western part of the section. In the marginal high area, it is uplifted and creates a local syncline. Top Early Eocene to Intra Late Paleocene is one of the most interesting sequences to observe deformation that might have happened in this section. There are some thickness differences in this sequence in some areas which are noticeably seen in this section. However, the faults interpreted in the central part of the basin do not penetrate the Mid-Cretaceous. These faults have less displacement compared to Fault 1 and Fault 2 (figure 4.6).

There are two major folds observed on this section. The fold in the footwall part of Fault 1 figure 4.6) has symmetrical geometry. However, this section is almost parallel to its strike (refer to figures 4.22 and 4.23). The other fold trending NE-SW can be tracked up to 20 kilometers to the NE (refer to figures 4.22 and 4.23). It has a 10 kilometers wavelength (figure 4.6). The folds observed cover Paleocene – Eocene sequences. However, Late Cretaceous succession is not folded like Paleocene – Eocene sequence. It formed a significantly narrow and deep basin located between Fault 1 and Fault 2 (figure 4.6).

Line NH-9709-103

Line NH-9709-103 shows slightly better quality in terms of continuity of the reflections and is less chaotic compared to section 102 (figure 4.7). It trends E-W similar to line 102, but is

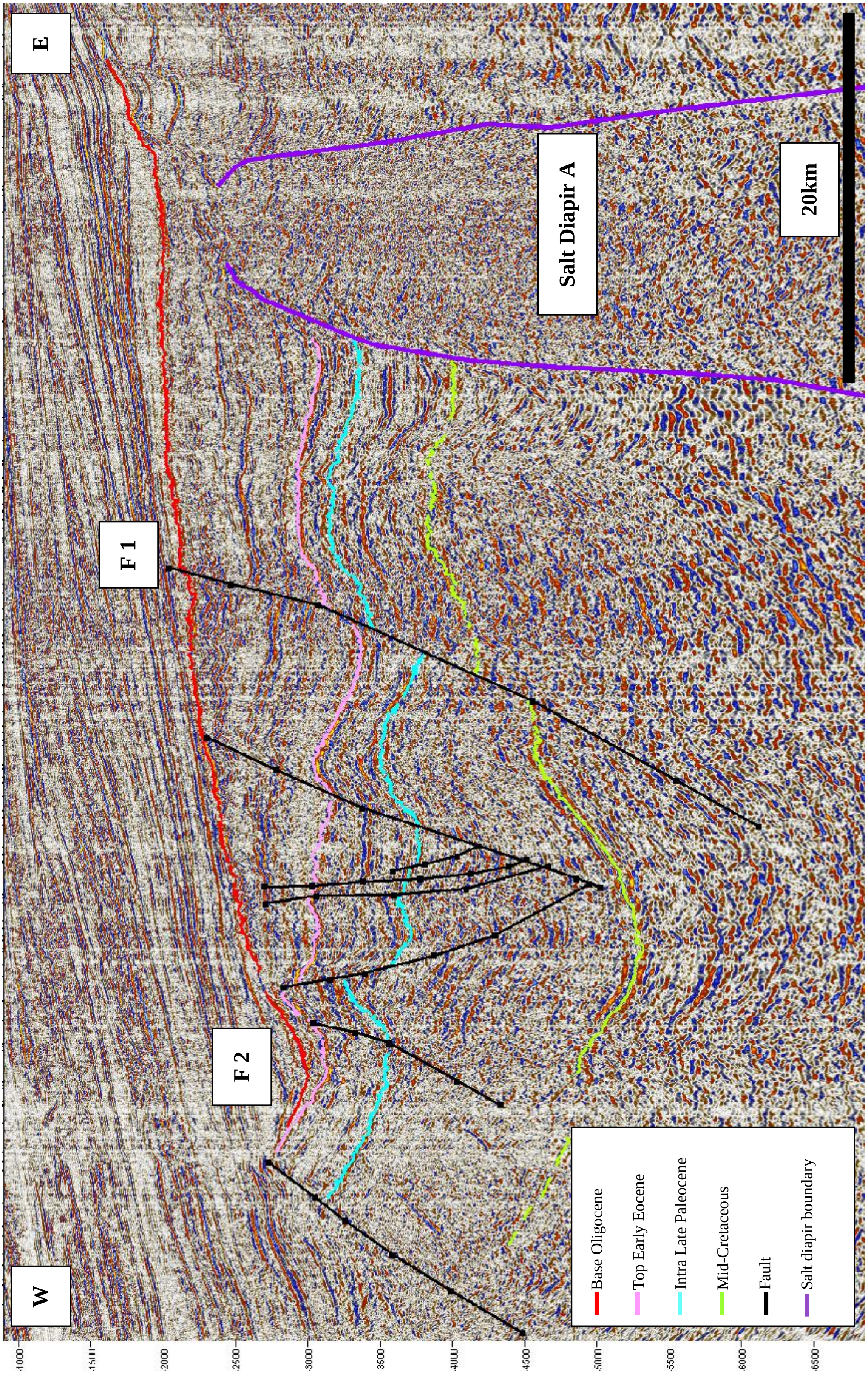

Figure 4.6. NH-9709-102 trending E-W across the study area from a salt diapir in the east to the marginal high in the west. See figure 4.4 for line location.

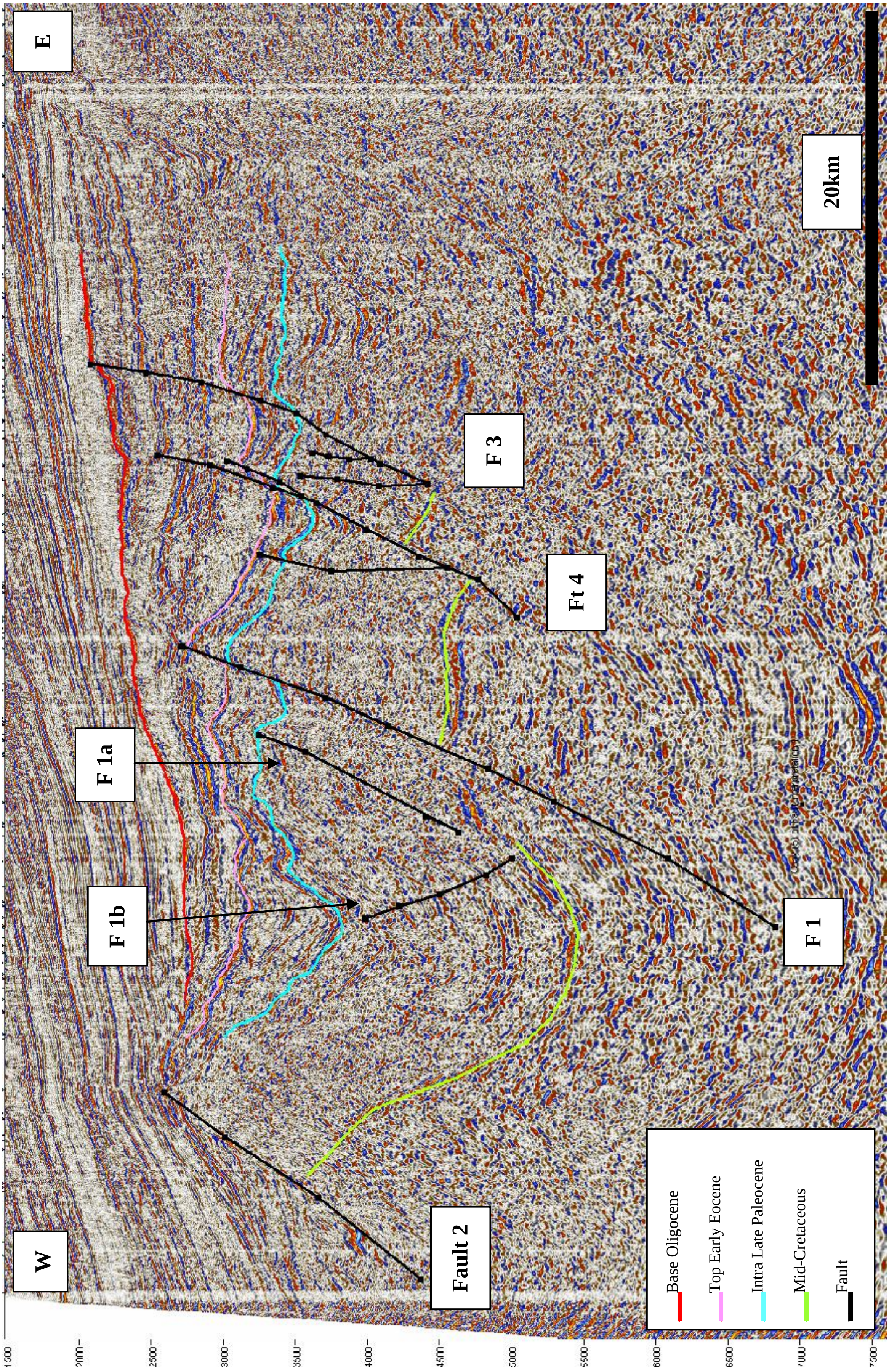

Figure 4.7. NH-9709-103 trending E-W across the study area slightly north of line 102 in figure 4.6. See figure 4.5 for line location.

located more to the north. This line is expected to not cover or have less influence of salt diapir compared to line 102.

This section shows more extensional faults towards the eastern part. Fault 3 and Fault 4 (figure 4.7) appear at the area where Salt diapir A exists (figure 4.6). There is a thickness difference in the Intra Late Paleocene – Top Early Eocene sequence. Furthermore, Mid-Late Eocene sequence shows this thickness difference as well.

Mid-Cretaceous was folded to become even narrower than in 102 section between Fault 1 and Fault 2 (figure 4.6). There is a small variation in thickness of the Mid-Cretaceous – Intra Late Paleocene sequence. However, it shows a thickening trend towards the east. Moreover, two faults interpreted Fault 1a and Fault 1b (figure 4.6) in the basin zone between Mid-Cretaceous and Intra Late Paleocene (Fault 1a and Fault 1b; figure 4.6) again do not show any significant displacement compared to the extensional faults that shows both displacement and thickness differences.

There are several folds observed in the Intra Late Paleocene reflection. Their amplitude and frequency then decrease towards the younger units. In addition to that, some very subtle folds exist in the Base Oligocene. These folds look subtler compared to the older ones. In Mid-Cretaceous interpretation, there is a little hesitation to pick the reflection towards Fault 1. This can be a concern to interpret this reflection later.

Line NH-9709-234

This line is one of the longest lines among the NH-9709 lines (figure 4.8). It is also one of the deepest that was shot among those lines. The interpretation does not cover the entire section from this line since the focus of the study is more into Sørvestsnaget Basin. The age unit interpreted does not cover the entire sequences as well since the focus of this study is Late Mesozoic to Early Cenozoic. Therefore the 17 seconds of 234 seismic section leaves a lot of information in the lower units.

The two prominent faults, Fault 1 and Fault 2, still exist in this section (figure 4.8). Fault 2 is the one located in the western part of the study area close to the continent - ocean boundary (COB) while Fault 1 is shown in the central to the eastern part of the study area. The extensional fault that separates Mid-Cretaceous reflection seems to show no displacement due to the fault.

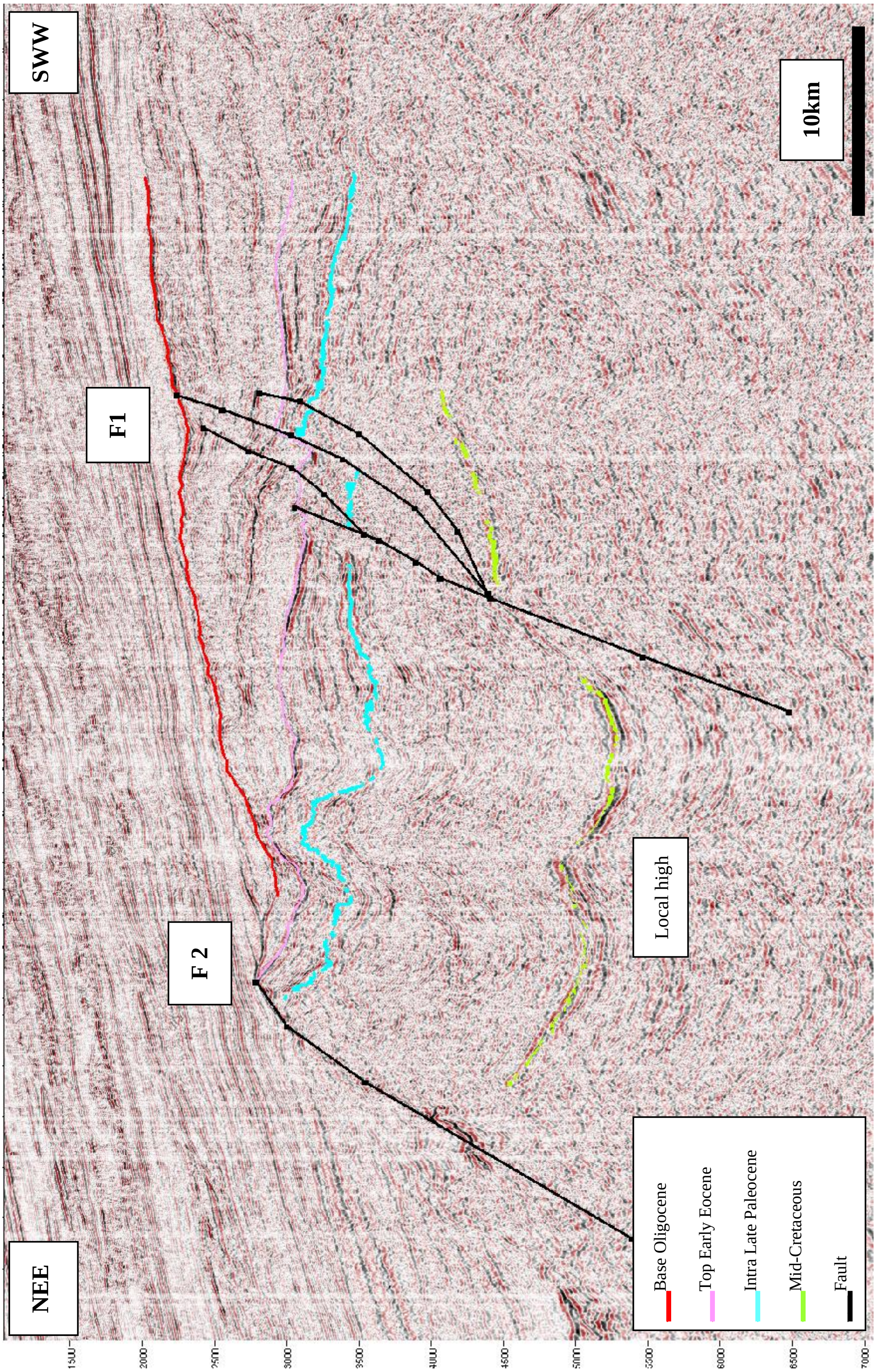

Figure 4.8. NH-9709-234 interpretation covering northeast to southwestern part of the study area.

Furthermore, consistency of Base Oligocene can still be shown in this section. It onlaps to the Base Oligocene. There is evidence of thickness difference in this section for Intra Late Paleocene – Top Early Eocene sequence which is shown by one extensional fault (Fault 1) in the central part of the section. The most interesting part of this section is to see a fold in Mid-Cretaceous reflection in the central part of the basin (figure 4.8). It shows a consistent fold through Intra Late Paleocene. A uniform thickness of Mid-Cretaceous - Intra Late Paleocene is clearly shown by this section. It is overlain by different thickness of in Intra Late Paleocene – Top Early Cretaceous sequence.

A 3D arbitrary line along NH-9709-234

An arbitrary line was generated from the 3D cube along the 2D line NH-9709-234 (figure 4.9). However, the extent of this arbitrary line is limited than the long 2D line. This, it has fewer features compared to NH-9709-234. It ends in marginal high and does not cover the Fault 2 (figures 4.6 – 4.8). Faults can also be more firmly interpreted since the displacement of the layers can more clearly be seen on this section.

There might also be some contractional faults that are possibly interpreted on this section in west of Fault 1 that might create the folds in the Intra Late Paleocene reflection. The interpretation of this section might tell a little bit more about the separation of the Mid-Cretaceous by the fault. The assumed Mid-Cretaceous reflection can be tracked along the section. However, part of it which is close to the fault goes vertically and reaches the fault and connects with the eastern part of the Mid-Cretaceous

A consistent fold is also clearly shown here (figure 4.9). The uniform thickness of the Mid-Cretaceous to Intra Late Paleocene sequence appears on this section as well. Thickness difference in the unit of Intra Late Paleocene – Top Early Eocene also exists and is obviously shown on this 3D arbitrary line. Top Early Eocene is cut by an extensional fault on the marginal high which is associated with the COB. Intra Late Paleocene undergoes the same situation on the edge of the two sections.

4.5. 3D Seismic Interpretation

After going through the 2D sections to see a wider picture of the study area, a smaller and more detailed 3D seismic interpretation is then performed. A more precise approach and method which is interpreting the 3D data is inevitably demanding to see more detailed pictures such as smaller folds, reflection interpretation towards faults which is very important for measuring a thickness difference for example, and high resolution basin infill reflection for stratigraphy observation. Therefore, the 3D seismic data NH9803 was then interpreted for a more precise observations.

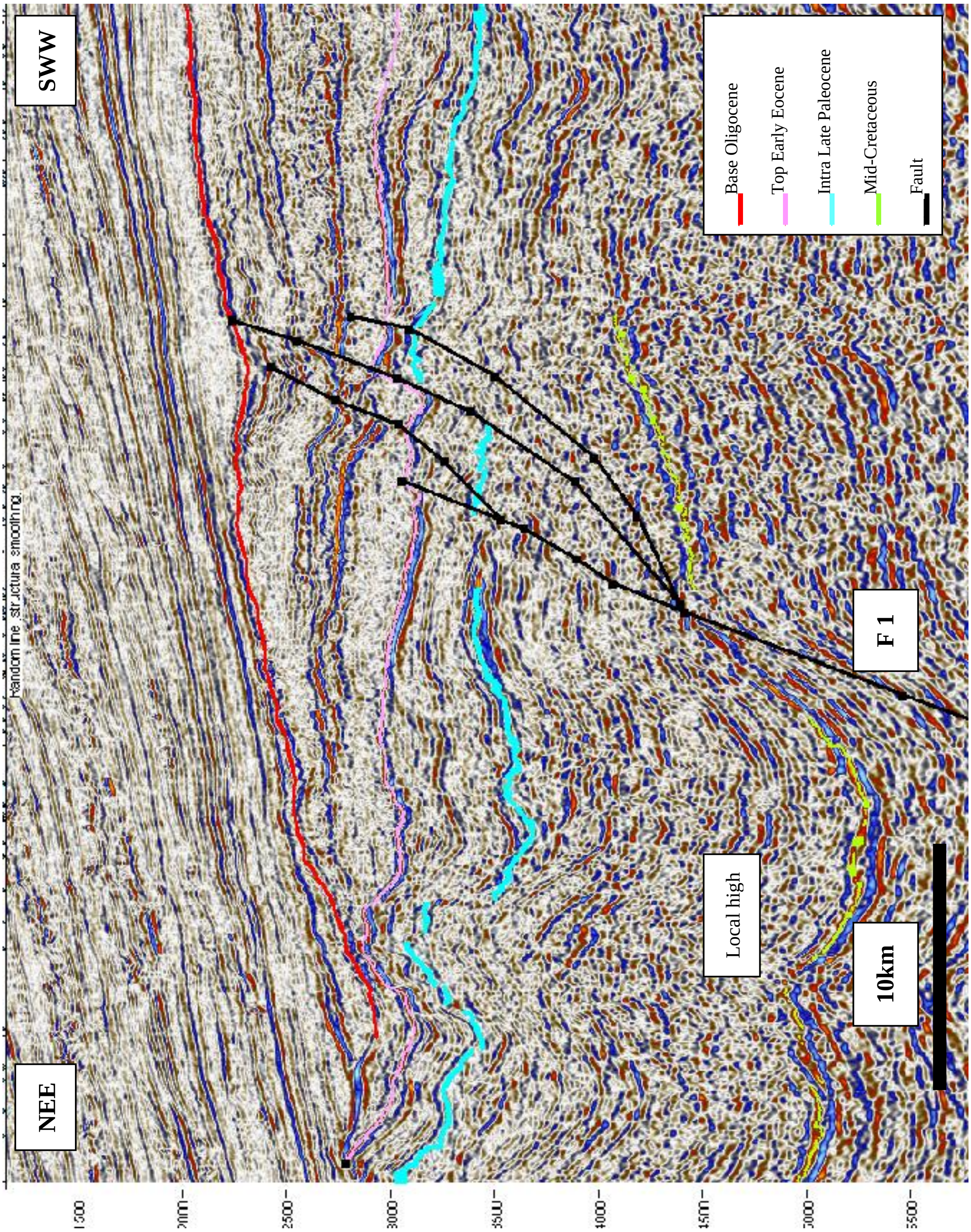

Figure 4.9. An arbitrary line from the 3D seismic data created along the NH-9709-234.

In the 3D seismic data used in this study, distribution of inlines and crosslines are from 2000-3900 and 1900-8400 respectively (figure 4.10). The seismic data do not cover the entire square. The time slice in figure 4.10 shows the coverage of the 3D data. Moreover, this thesis will show several 3D inline and crossline sections for the interpretation purpose.

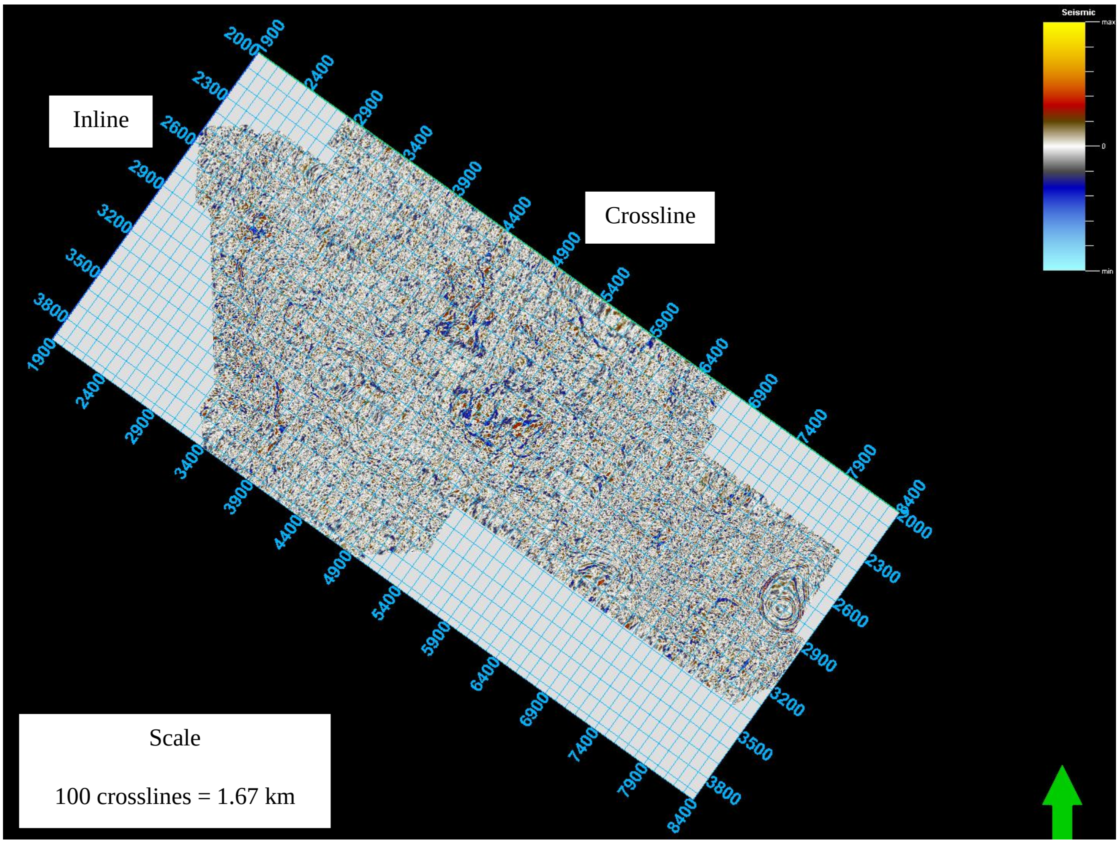

Figure 4.10. Extent of inlines and crosslines over the 3D data.

Inline Sections

A number of inlines were picked to represent the interpretation of the 3D seismic data. These lines which are inline 2500, 2900, 3100, and 3300 (figure 4.10) were selected because each of the line brings at least one different type of deformation from another.

Inline 2500

This section is located in the northeastern part of the 3D seismic data (figure 4.11). The extensional faults seen in the previous sections are essentially best-viewed from inline sections. There are a few major faults which are Fault 1, Fault 2, and Fault 4 observed on this section. It means that the faults dip along the inline direction (NW-SE) and trend along the

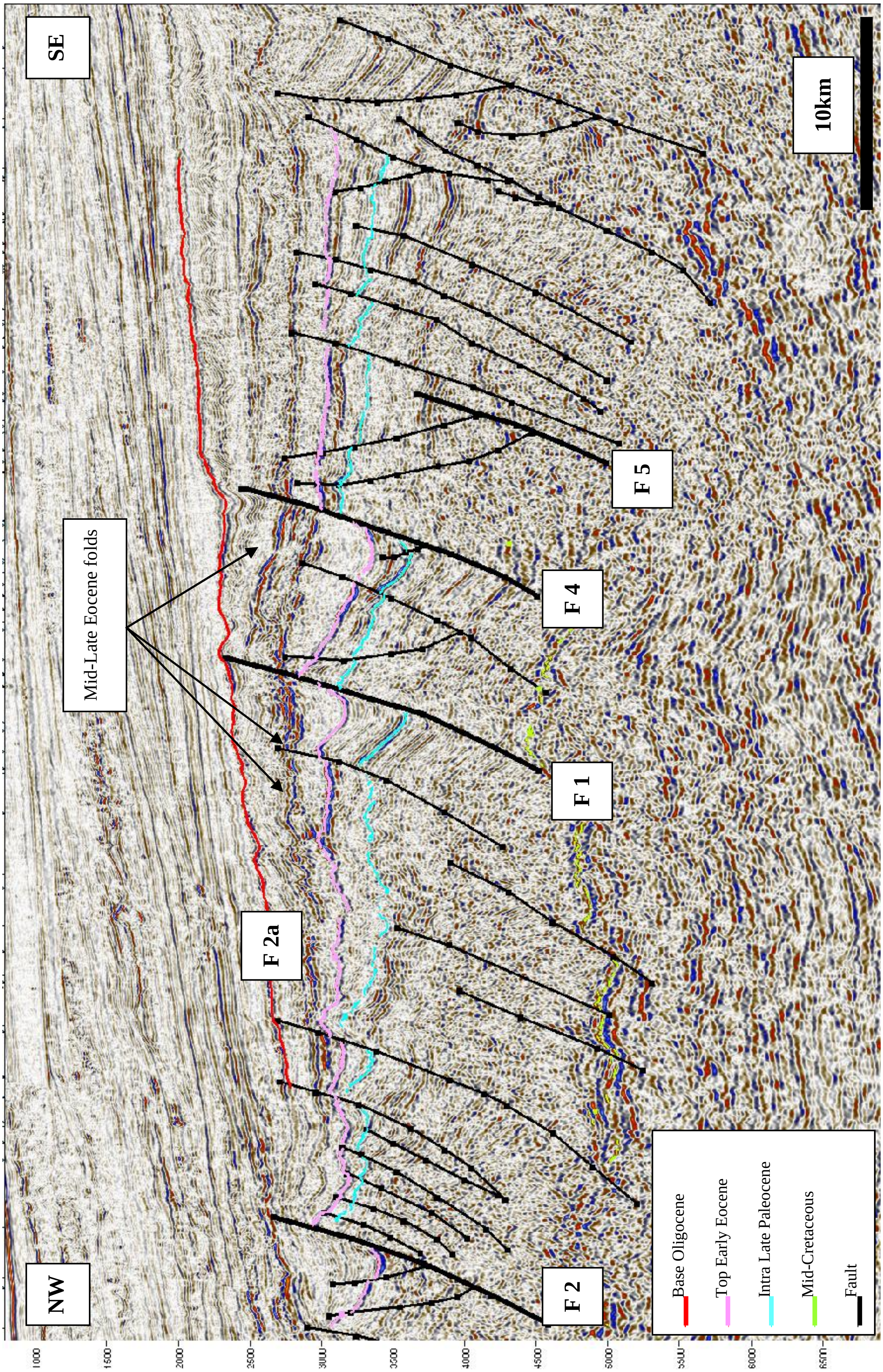

Figure 4.11. 3D Inline 2500 seismic interpretation. See figure 4.10 for line location.

crossline direction (NE-SW). In addition to that, the fault names are consistent from one section to another.

A detailed observation starts from the succession below the assumed Mid-Cretaceous. There are some discontinuous reflections which have strong amplitude and low frequency. In the northwestern part, the reflections are slightly uplifted. However, the reflections are less strong and even less continuous compared to the ones in the middle. In the southeastern part, the reflections are even more chaotic compared to the ones in the middle.

The Mid-Cretaceous reflection is interpreted rather firmly in the northwestern part of the section. This reflector generated a fairly strong reflection but again, towards the southwestern part, it starts to disappear. The amplitudes towards NE also get weaker to the marginal high.

The interpretation stops where the reflections start to be chaotic. Mid-Cretaceous reflection is faulted in the middle of the section. However, the interpretation of the fault penetrating this reflection is rather uncertain due to less obvious fault signature on the seismic section compared to the units above. Some of the extensional faults are interpreted to penetrate this reflection where obvious displacement or extensional faulting marks are seen. The thickness of the assumed Mid-Cretaceous to Intra Late Paleocene sequence increases towards the northwest. Most of the extensional faults penetrate up to this unit.

Intra Late Paleocene and Top Early Eocene are consistently interpreted almost through the entire section. The thickness of the sequence in between is generally thinner towards northwest. Some displacements due to extensional faulting are clearly shown this section. There are some thickness differences as well throughout the section related to the extensional faulting. Most of the faults also penetrate this unit. Some minor folds which are located between Fault 1 and Fault 2 can be observed in the Top Early Paleocene reflection. There is also one fold observed on this section which are located in the footwall and attached with associated Fault 2a.

The Top Early Eocene and Base Oligocene sequence is well displayed on this seismic section. In general, there is a trend of thinning of this sequence towards northwestern part of this section. In addition to that, some faults penetrate this unit as well such as Fault 1, Fault 2a, and Fault 4. There are very weak reflections within the Middle Eocene succession that fills this extensional basin. Above, there is a series of strong reflections. Observing more into the transparent layers, there is a thickness difference among this unit separated by the extensional faults. Some folds are also possible to observe in this unit (figure 4.11). However, these are minor folds that have around 1-3 kilometers of wavelength.

Within the unit of Base Oligocene – Pleistocene succession, there are not too much tectonic activity to be observed. However, in the northwestern part of the section there is significant deformation. Generally, the dip direction of this unit is NW on this 2D section. There is a clinoformal feature also observed on this section.

Some more interesting features that can be observed on this section are a general folding trend within the Mid-Cretaceous to Intra Late Paleocene sequence, some exaggerated synclinal features, a lens shaped feature, and a “Christmas tree” structural feature. The bold faults (Fault 1, Fault 2, Fault 4, and Fault 5) displayed are some of the major faults that were tracked in the 3D seismic data. In the middle of the section, the reflections are shallower compared to both sides part of the NW-SE section. In addition to that, there are two exaggerated synclinal features located on the hanging wall of Fault 1. Moreover, there is one lens shaped feature observed on this section which is located within the Intra Late Paleocene – Top Early Eocene sequence in the northwestern side of the section in the hanging wall of Fault 2a.

Inline 2900

Inline 2900 (figure 4.12) seismic section extends between crossline 2500 and crossline 6500 (figure 4.10). The extensional faults observed have consistent trends (NE-SW) and dip directions compared to Inline 2500. They can also be traced because they are continuous up to this section such as Fault 1, Fault 2, Fault 4, and Fault 5 (figure 4.12). Generally, this section still consistently shows the rotated fault blocks that are created by a series of extensional faults.

Below the Mid-Cretaceous reflection, there are some reflections that are partly discontinuous and have strong amplitude in some areas. These reflections have low frequency. A different trend is found in this part compared to Inline 2500 towards southeastern part. These reflection sequences get shallower to the southwestern part (figure 4.12). In the northwestern part, the reflections are uplifted not slightly but significantly. There is an obvious indication of uplift in the area of marginal high covering this unit as well.

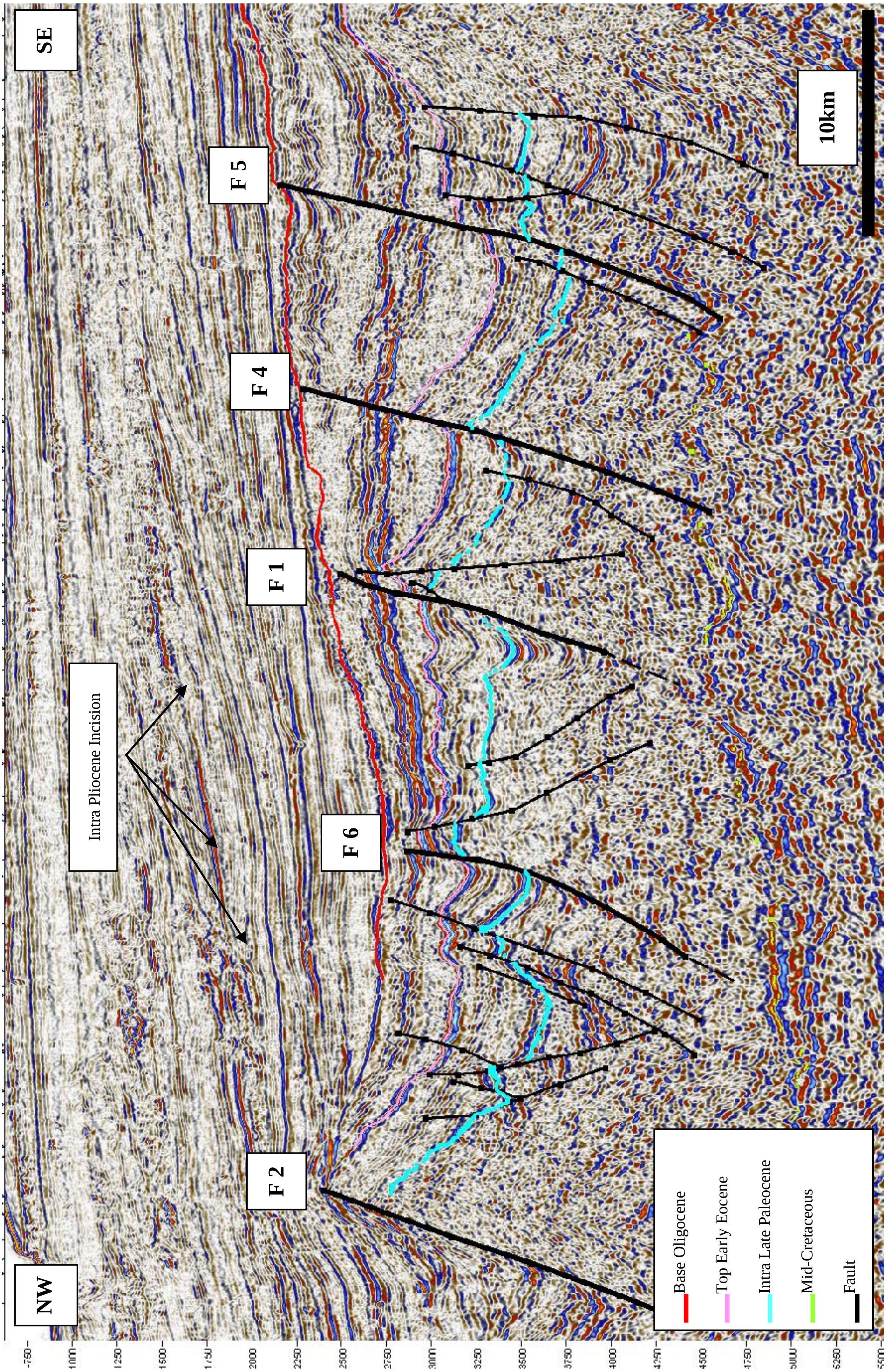

Figure 4.12. 3D Inline 2900 seismic interpretation. See figure 4.10 for line location.

Mid-Cretaceous reflection is continuous throughout the entire section. It slightly gets more chaotic towards the marginal high. Similar to the lower reflections of Mid-Cretaceous, there is a fold in the middle of the section with generally large wavelength. The extensional faults may also penetrate through this reflection and create displacement which is similar to the above layers. However, the displacement is not clearly shown within this sequence so that it is relatively difficult to draw a fault down to this sequence.

Interpretation of both Intra Late Paleocene and Top Early Eocene reflections are obvious and cover almost the entire section (figure 4.12). Thickness differences between Intra Late Paleocene and Top Early Eocene due to extensional faulting are observed at Fault 1 and Fault 6. It shows the difference within this unit by a thicker hanging wall and a thinner footwall at these two faults. Two minor folds with 3-4 kilometers of wavelength are found between Fault 1 and Fault 6. Folds having even smaller wavelength are found between Fault 2 and Fault 6. There is also an interesting observation about the footwall which is displaced by Fault 1. The top Early Eocene is folded in the footwall side of this extensional fault. This is also found on the previous section in a different rotated fault block.

The thickness differences of the Mid-Late Eocene sequence seen in Inline 2500 can also be found on this section especially in the transparent unit. This unit is significantly displaced by the faults and there is a thickness difference between the hanging wall and the footwall. This thickness difference occurs across Fault 1, Fault 4, Fault 5, and Fault 6. The strong reflections within this unit which are located above the transparent sequence have the fold axis in the middle of the section if it is seen in a small scale. However, in the Late Eocene succession there is another thickness difference between the footwall and hanging wall which is observed in Fault 5 (figure 4.12).

Some layers above the near top Oligocene reflection onlap to the Base Oligocene. Generally, the dip direction of this unit is towards the northwest on this 2D section. There is also a clinoformal feature observed on this section. Intra Pliocene incision also exists on this similar to figure 4.2 (figure 4.12).

One more interesting feature that can be observed on this section is the exaggerated synclinal feature. There are two narrow exaggerated depocenters which are both located in the hanging wall as a result of extension. One of them is located in the hanging wall of Fault 1 and the other is located in the hanging wall of Fault 2. Moreover, both of them are within Intra Late Paleocene – Top Early Eocene sequence.

Inline 3100

Inline 3100 extends from around crossline 2700 to 6700 (figure 4.10). Generally, it still follows the trend of the previous inlines that comprise extensional faults and rotated fault blocks. Some interesting features that can be observed on this section are a fold within Paleocene-Eocene sequence, and some displacements due to extensional faulting. What makes this section different from the previous lines is the displacements without any thickness difference in Intra Late Paleocene – Top Early Eocene sequence and also a fold on the footwall in Intra Late Paleocene reflection.

The assumed Mid-Cretaceous reflection was interpreted confidently almost everywhere on the section but the edges. This reflection has a very strong and continuous amplitude, towards the southeast and marginal high, it starts to disappear or gets discontinuous. The interpretation stopped when the reflection goes to the edges of the section. Some of the extensional faults are interpreted to penetrate this reflection where obvious displacement or extensional faulting marks are displayed. The thickness of the assumed Mid-Cretaceous to Intra Late Paleocene sequence increases towards the northwest. Another difference from the previous sections is the big synclinal Late Cretaceous basin is narrower. It is also deeper as it shows a value of 5200 ms TWT while in figure 4.12 the deepest part was around 5000 ms TWT.

In the Intra Late Paleocene and Top Early Eocene sequence, there are two different patterns of fault systems in the northwestern and southeastern part of the section. Therefore, this large basin is divided into three parts which are marginal high, Sub-basin A, and Sub-basin B to simplify the observation details (figure 4.13). In Sub-basin A, there is a complex fault system. Intra Late Paleocene is folded and created that complex system. The other pattern which is located in Sub-basin B has less complex faulting.

There is an absolute thickening towards the Sub-basin B within Intra Late Paleocene - Top Early Eocene sequence. In addition to that, at least two faults which are Fault 4 and Fault 5 penetrate this unit. Another obvious observation is the transparent unit throughout Eocene succession that fills the extensional basins and they have thickness difference again on

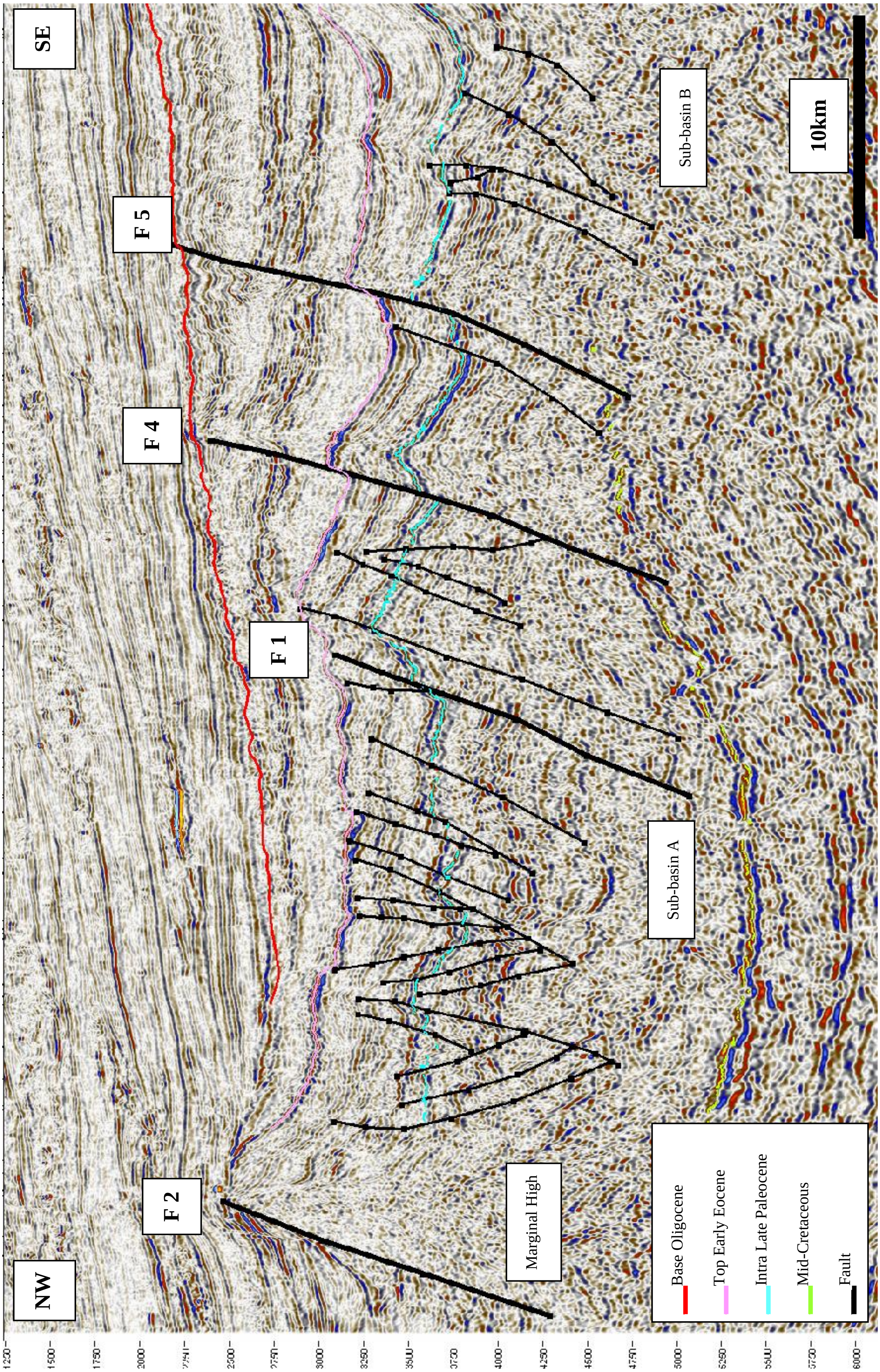

Figure 4.13. 3D Inline 3100 seismic Interpretation. See figure 4.10 for line location.

this section. One fold in the footwall can also be found at the same rotated fault block as the footwall fold that can be found in the Intra Late Paleocene reflection which is Fault 4 (figure 4.13).

Inline 3300

The last inline section is inline 3300 which is shown in figure 4.14 and it extends from crossline 2900 to crossline 6900 (figure 4.10). This section is located down to the southwestern part of the 3D seismic data. It has a very different pattern from the previous sections. Extensional faults do not dominate this section anymore especially in the Sub-basin A and marginal high (figure 4.14). However, there are several extensional faults that cause the displacements that are located in the Sub-basin B which relatively are not large. What appears throughout the section is a big fold above the Mid-Cretaceous through Top Early Eocene which is similar to a lens shaped feature in an immense version.

Mid-Cretaceous reflection is continuous throughout Sub-basin A. However, it gets more discontinuous towards the marginal high and Sub-basin B. Mid-Cretaceous reflection is located in the deepest on this section which reaches close to 5400 ms TWT compared to the previous inlines. The extensional faults penetrating this reflection are located only in the Sub-basin B.

Top Early Eocene reflection is confidently interpreted as it is a strong and continuous reflection. In addition to that, the Intra Late Paleocene also shows a strong amplitude even though there are a lot of fractures affecting this reflection in Sub-basin A. Thickness difference which is shown on the other sections does not exist on this section as a few extensional faults are found. A large wavelength Mid-Cretaceous - Top Early Eocene fold is followed by minor folds which have much shorter wavelength on this section. Therefore, parasitic folds related to this kind of feature are shown on the section (figure 4.14).

In the Top Early Eocene – Base Oligocene sequence, the extensional faults found in the Sub-basin B do not penetrate this unit. It means that the transparent unit is not faulted. The same thing happens to the strong reflections above the transparent layer which are not faulted.

Crossline Sections

By looking at inline sections in figures 4.11 – 4.14, the best view to observe the faults is from inlines. However, crossline section is good for other purposes such as to observe stratigraphy,

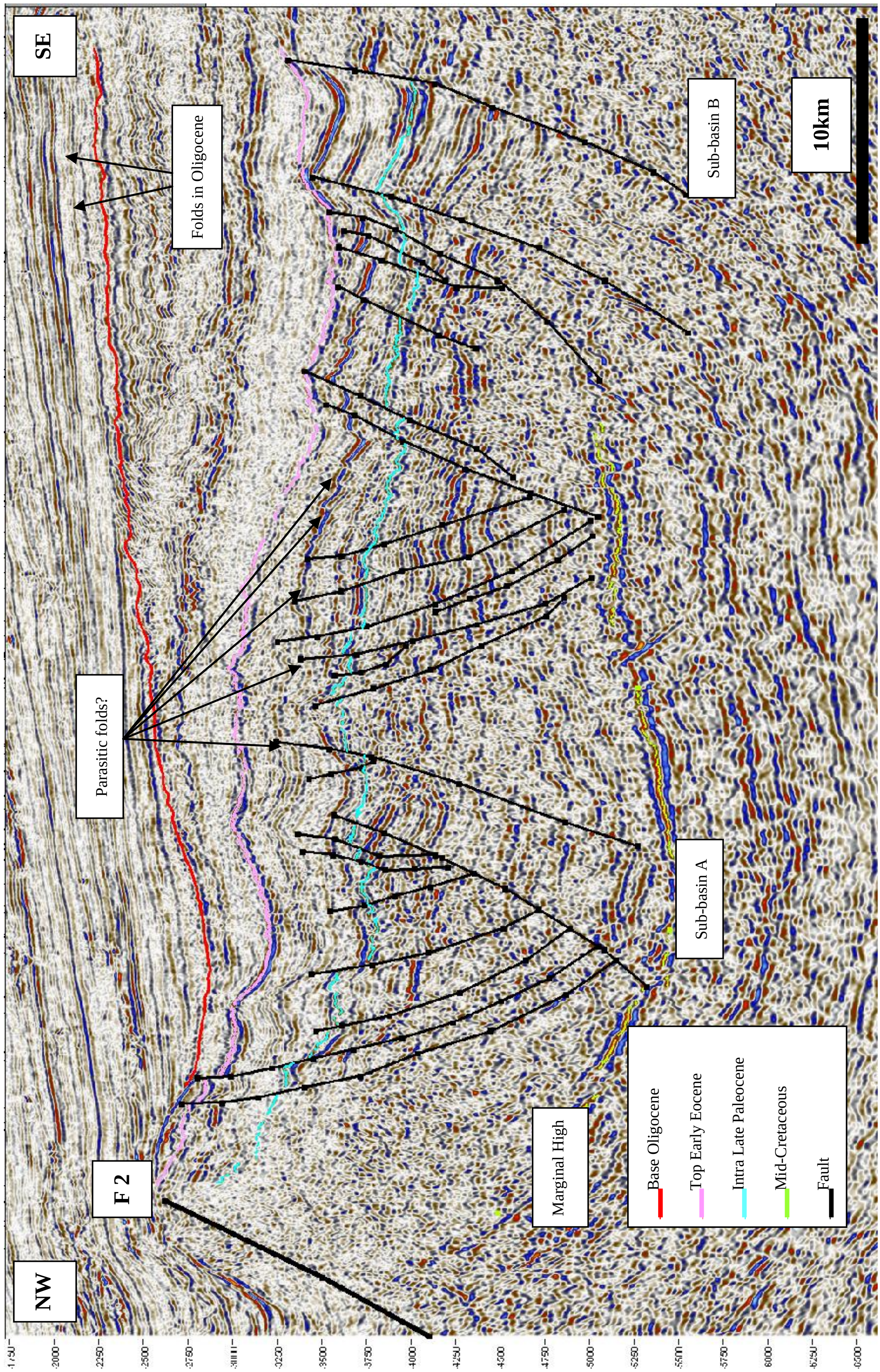

Figure 4.14. 3D Inline 3300 seismic Interpretation. See figure 4.10 for line location.

NW-SE trending Sub-basin A (see figure 4.24), and timing of the uplift in the marginal high. Due to the variety of the observation, there are several crosslines eventually selected for the observation which are crossline 3600, 3850, 4000, and 4600. There will be two zoomed section inside the Sub-basin A as well for both crosslines 3850 and 4000 to see how the detailed reflections are affected by the structure.

Crossline 3600

Crossline 3600 is located in the northwestern most part of the 3D seismic data are among the crosslines selected to be observed (figure 4.10). The section basically covers the entire inlines within the seismic data. Crossline 3600 shows that generally there is a fold which affects almost the entire section. In addition to that, some faults were also interpreted even though they do not have deep penetration shown in inline sections.

Below the Mid-Cretaceous, some reflections having strong amplitudes and partly continuity can be observed. They are uplifted in the marginal high. Sub-basin A is around 10 kilometer wide observed on this section. It flanks to marginal high and Sub-basin B. However, in Sub-basin B, the Mid-Cretaceous reflection is rather flat with one local syncline compared to the other part of the section.

The Mid-Cretaceous to Intra Late Paleocene sequence experienced the same structuring as the underlying sequence such as uplift in the area of marginal high and syncline in the Sub-basin A. In addition to that, Fault 2 and Fault 2b were also interpreted southwest of the marginal high associated with the continent-ocean boundary (figure 4.15). Fault 2 penetrates up into the succession of probably Miocene – Pliocene age. The reflections within Mid-Cretaceous – Intra Late Paleocene sequence are discontinuous, have weak amplitudes, and are rather subparallel. However, there are several reflections (in Sub-basin A) that onlap the assumed Mid-Cretaceous (figure 4.15). This unit is located between 4750-5000 ms. Moreover, the succession above the unit onlap to it. Starting from 3750ms, some folded strong reflections are found in Sub-basin A which may be the Early Paleocene (figure 4.15). The assumed Early Paleocene – Intra Late Paleocene sequence wedges towards both sides and has a maximum thickness inside the basin.

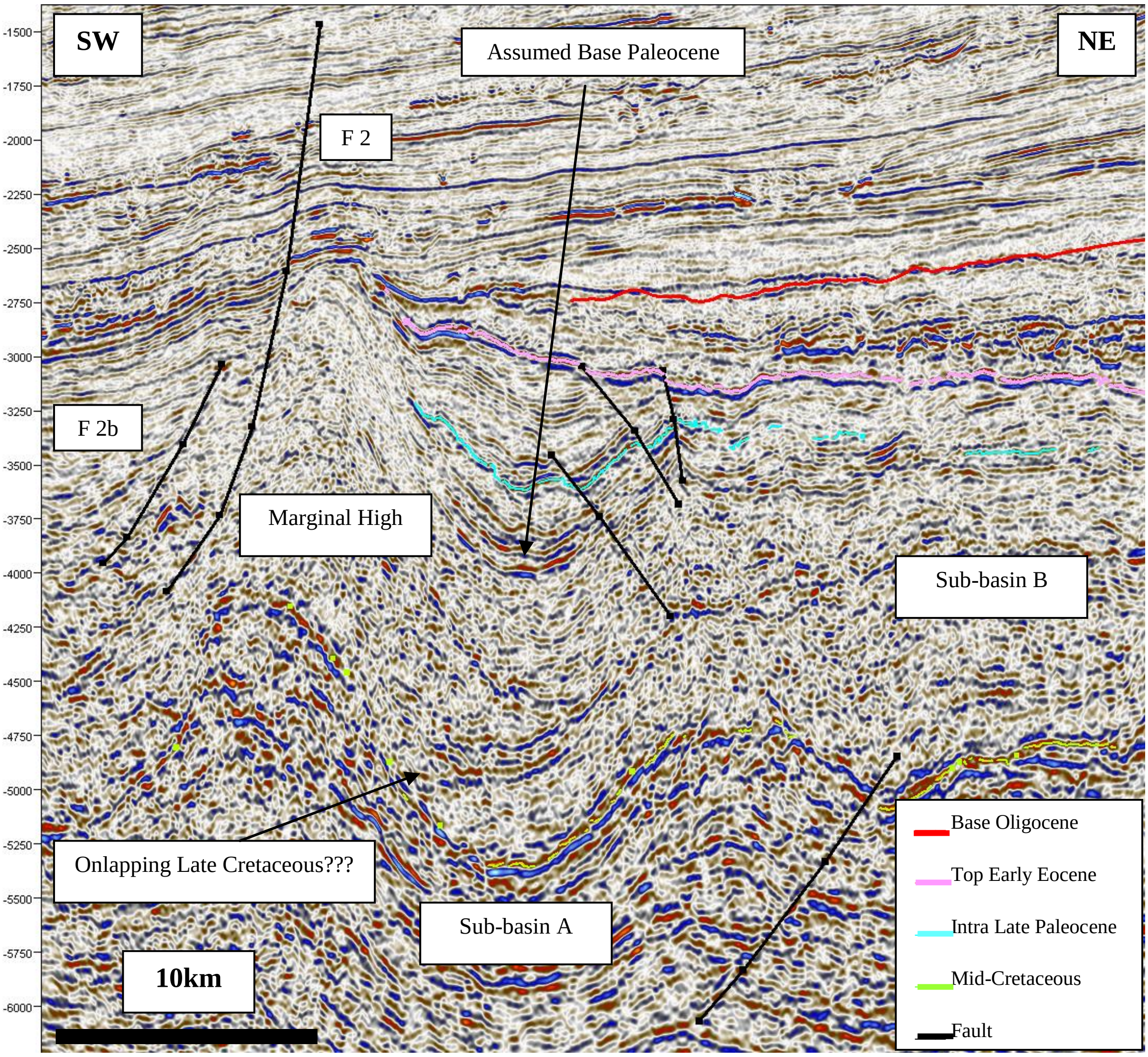

Figure 4.15. Crossline 3600 seismic interpretation. See figure 4.10 for line location.

Intra Late Paleocene – Top Early Eocene sequence wedges as well towards the marginal high and Sub-basin B. Intra Late Paleocene reflection is even interpreted to onlap the older reflection below it. There are three faults interpreted within this unit.

The Late – Mid Eocene sequence wedges towards the marginal high. Some strong reflections are found in this sequence. They were also described on the inline sections. However, these reflections look wiggly and discontinuous even though they have strong amplitudes (figure 4.15).

Reflectors above Base Oligocene have relatively strong amplitudes and are continuous, which dip to the SW (figure 4.15). However, the marginal high makes some Oligocene units onlap to it. The non-onlapping layers above it even are slightly affected by the high since there is an indication of folding. Fault 2 which is a normal fault also penetrates this sequence.

Crossline 3850

One of the most interesting lines that will be described is crossline 3850 (figure 4.16). Fault 2 and Fault 2b which are located in the southwestern part of the marginal high were also interpreted on this section. Fault 4 is located at the flank of Sub-basin A (figure 4.16). Mid-Cretaceous reflection and its underlying reflections are more when they are close to the marginal high while the ones on the previous section are not. This underlying unit is also folded and creates a syncline and followed by an anticline high towards the NE. Moreover, in the northeasternmost part of the section, the Mid-Cretaceous reflection is rather flat with a fold having wavelength around 8-10 kilometers.

The Mid-Cretaceous – Intra Late Paleocene sequence is faulted by Fault 4 (figure 4.16). However, since Fault 4 trends NE-SW which is almost parallel to crosslines, it is interpreted as a shorter fault (figure 4.16) compared to the fault on the inline section (figure 4.13). The reflections within this sequence are partly discontinuous, have weak to medium amplitudes, and are more conformably subparallel compared to crossline 3600.

Intra Late Paleocene reflection is interpreted to onlap to its underlying sequence towards the marginal high. This sequence is cut by fault which is definitely extensional (see figure 4.11-4.13). The Sub-basin A is located in the hanging wall of this extensional fault. In addition to that, Fault 4 created a thickness difference on the transparent layers (Eocene succession).

Base Oligocene and above lying reflections consist of layers have relatively strong amplitudes and continuity. However, Fault 4 does not penetrate all the way up to this sequence.

Details of the reflection in Sub-basin A can be clearly differentiated (figure 4.17). The lowermost reflections which have very strong amplitude are shown as orange and blue colors which mean peak and trough respectively. The orange reflection is assumed as Base Paleocene (see also figure 4.15) which can actually be tracked all the way to the marginal high at least on this section. Moreover, several more reflections above are able to be tracked to the marginal high. However, they were followed by more reflections onlapping. Intra Late Paleocene was also observed to onlap to a reflection below it. This kind of event keeps happening until Base Oligocene reflection. There is also a local high between Sub-basin A and marginal high that makes some reflections onlap (figure 4.17).

Crossline 4000

The Mid-Cretaceous – Intra Late Paleocene sequence has similar pattern to the underlying reflections (figure 4.18). However, the reflections within this unit are less strong than the reflections below the Mid-Cretaceous reflection. There are two faults that are interpreted in the upper part of this Mid-Cretaceous – Intra Late Paleocene unit. The reflections within this sequence are even more conformable compared to both crosslines 3600 (figure 4.15) and 3850 (figure 4.16). However, there are two reflections which do not appear to be conformable within this unit in Sub-basin A (see figure 4.18). Moreover, although Intra Late Paleocene reflection onlaps to the local high (see figure 4.17), it still exists on the southwestern part of the local high (figure 4.15).

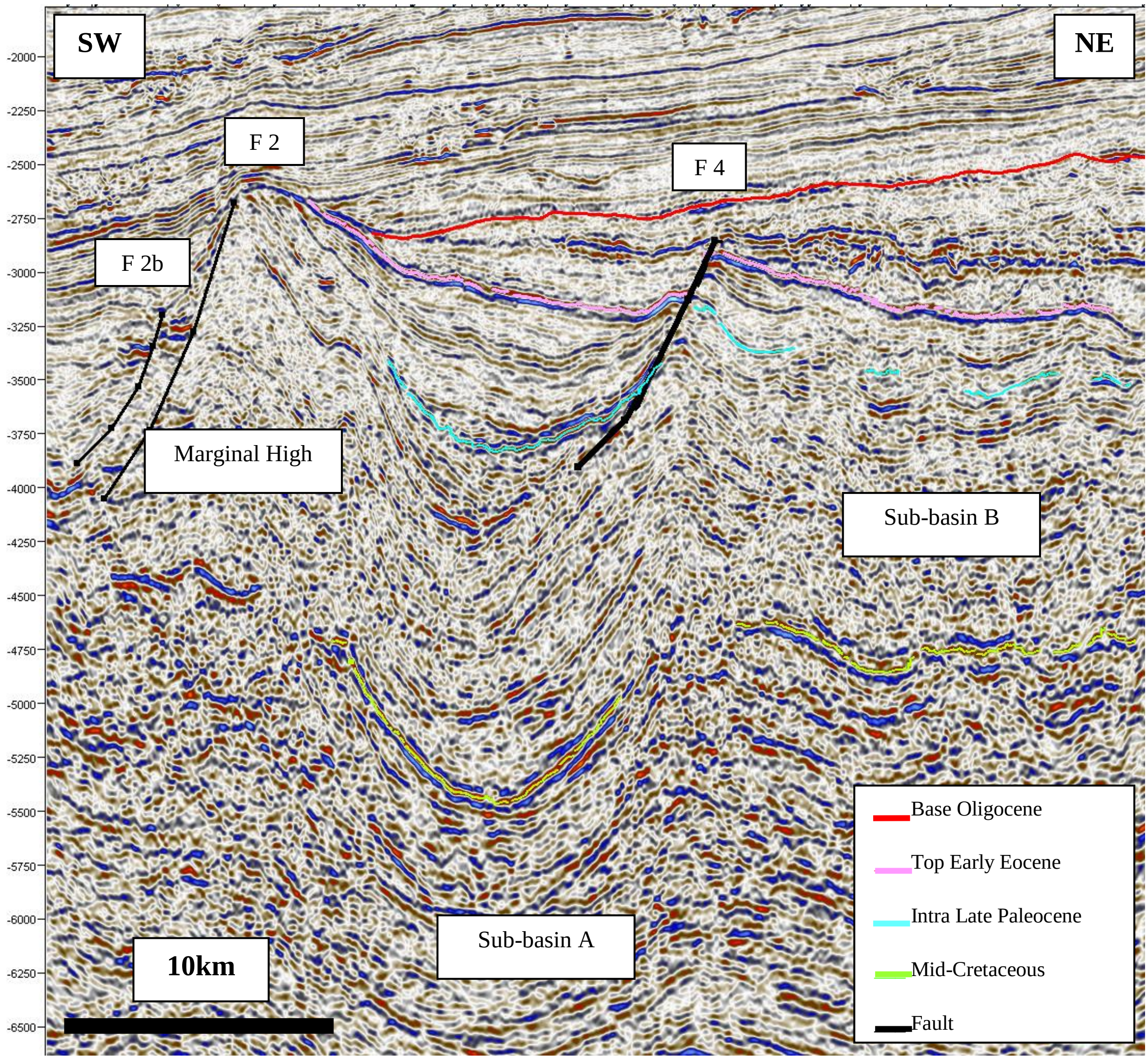

Figure 4.16. Crossline 3850 seismic interpretation. See figure 4.10 for line location

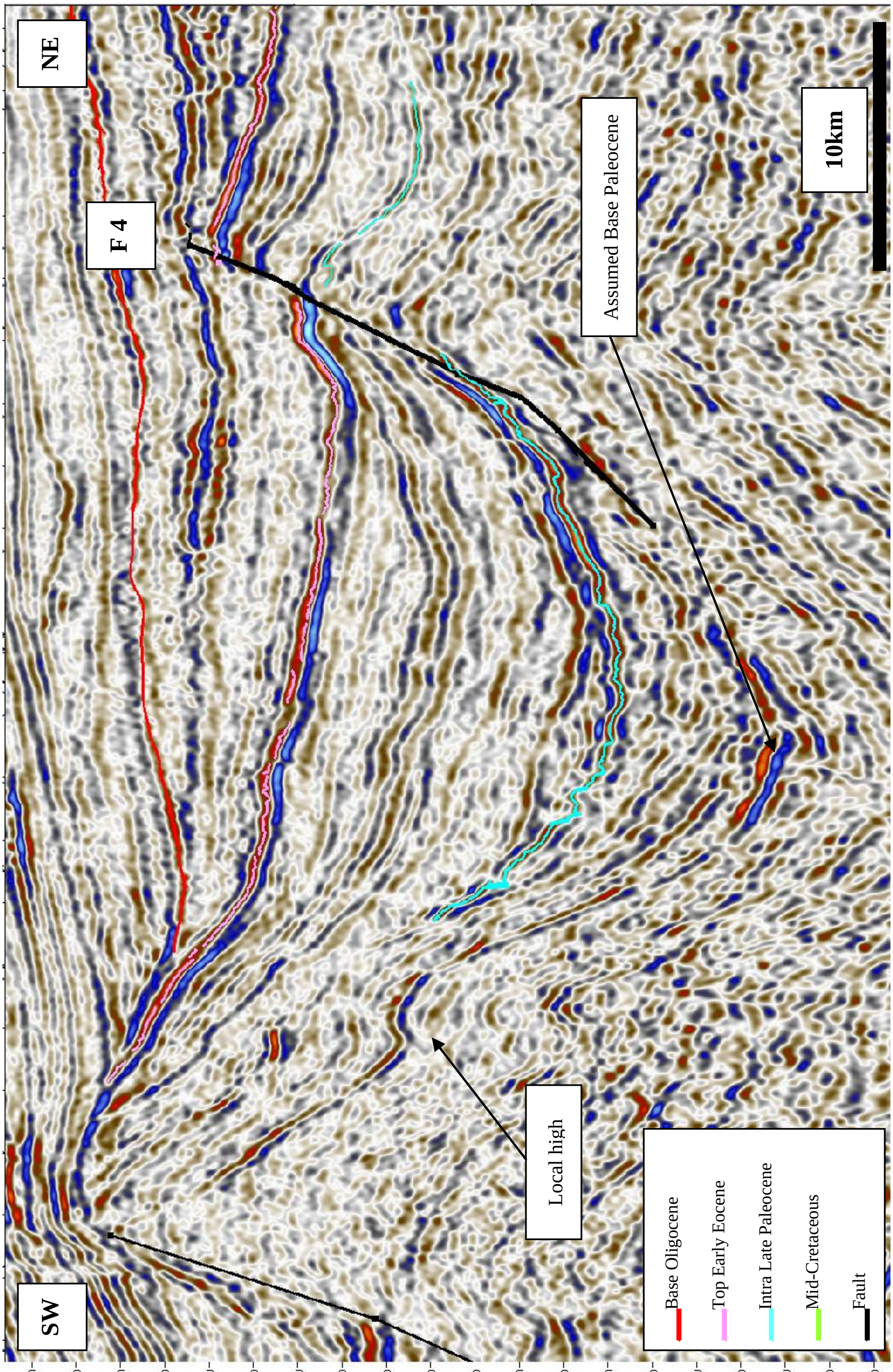

Figure 4.17. Crossline 3850 seismic interpretation (close-up from figure 4.16).

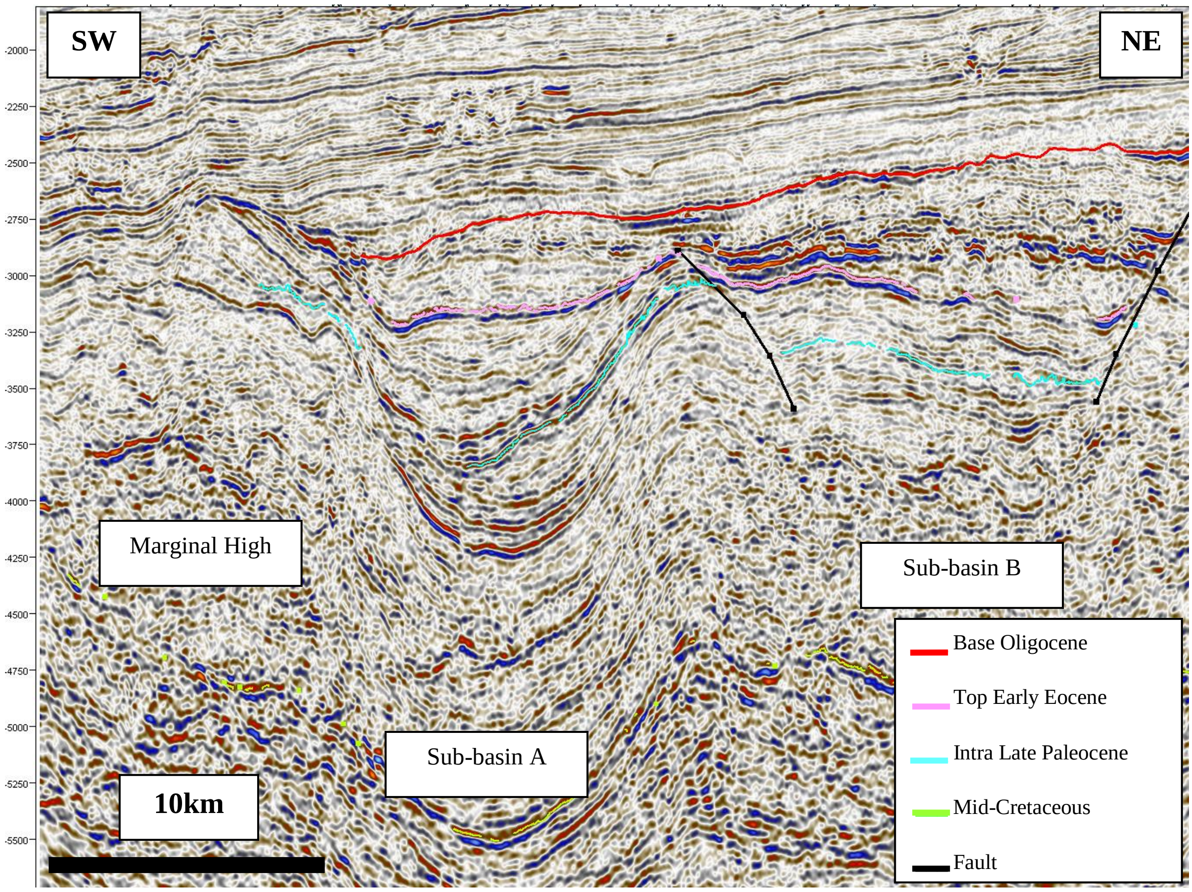

Figure 4.18. Crossline 4000 seismic interpretation. See figure 4.10 for line location

Top Early Eocene reflection on this section is strong and continuous towards the marginal high. The sequence between Top Early Eocene and Base Oligocene has a lens shape in Sub-basin A. Its maximum thickness (figure 4.18) is a little bit to the southwestern part of Sub-basin A while the Base Oligocene reflection has an anticlinal shape. In addition to that, the transparent layers normally found within this sequence still exist both in Sub-basin A and Sub-basin B.

Focusing on Sub-basin A, onlap reflections can clearly be seen (figure 4.19). Two reflections above the assumed Base Paleocene, onlap not too far from the basin axis towards the southwestern part. However, their onlap towards NE appear to be a little bit farther from the basin axis. This may indicate how those two reflections were eventually folded.

Crossline 4600

Crossline 4600 has slightly different pattern from the previous crossline sections. This crossline is located in the southeasternmost part of the seismic data among the crosslines selected

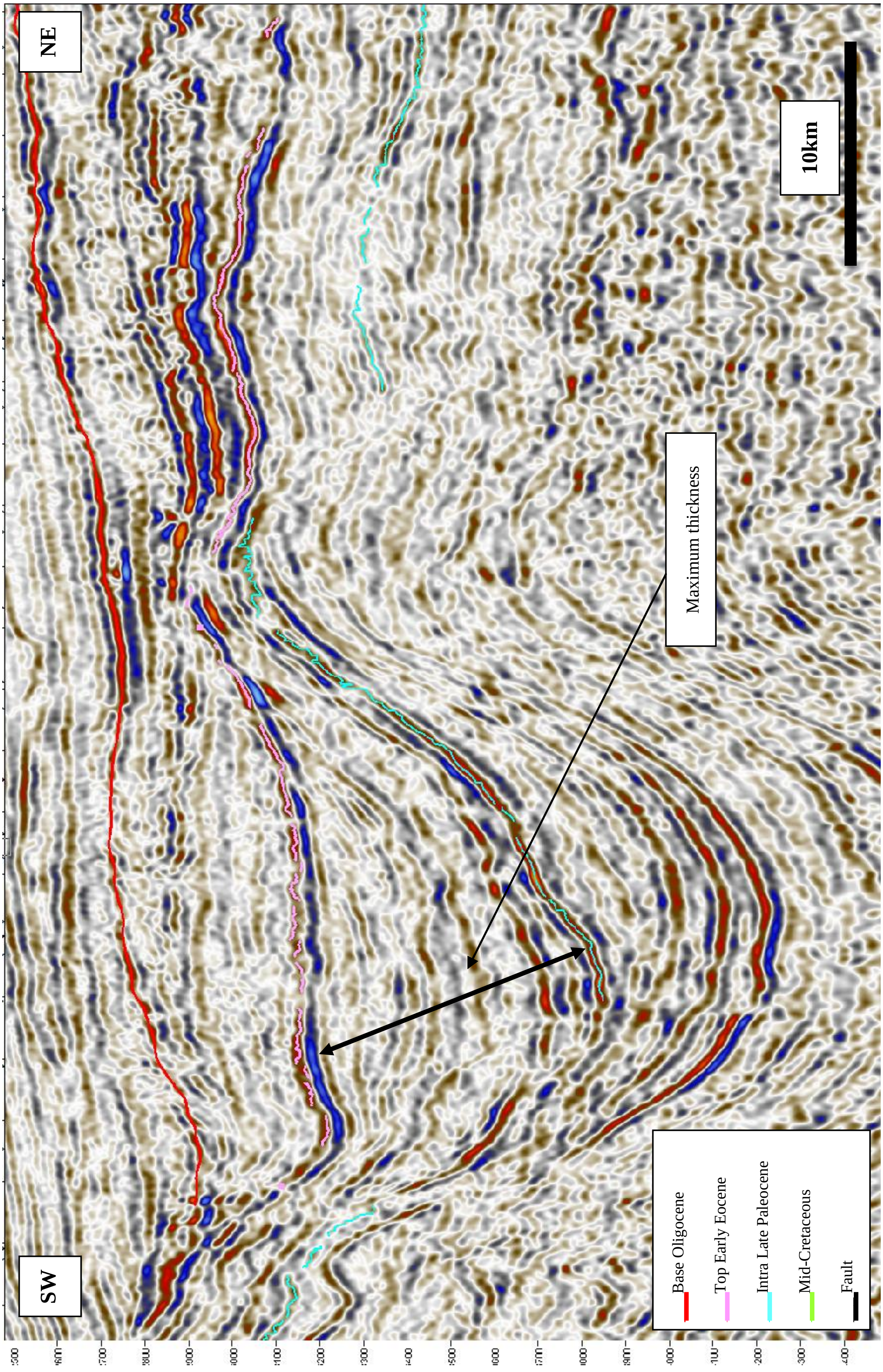

Figure 4.19. Crossline 4000 seismic interpretation (close-up from figure 4.18).

to be described in this study (figure 4.10). This section clearly shows clearer reflections which are more conformable (figure 4.20). However, the uplift still definitely affects the reflections and creates a local high (figure 4.18) in the southwestern part and followed by a syncline (Sub-basin A).

Clearer, stronger, and more continuous reflections below the Mid-Cretaceous reflection are shown (figure 4.20). Marginal high is beyond the seismic coverage on this section. These reflections just basically follow the fold pattern and which is also similar to the folded Mid-Cretaceous reflection. However, the uplift does not create a symmetric syncline in the Mid-Cretaceous reflection. The local high is not uplifted very dramatically compared to the previous sections.

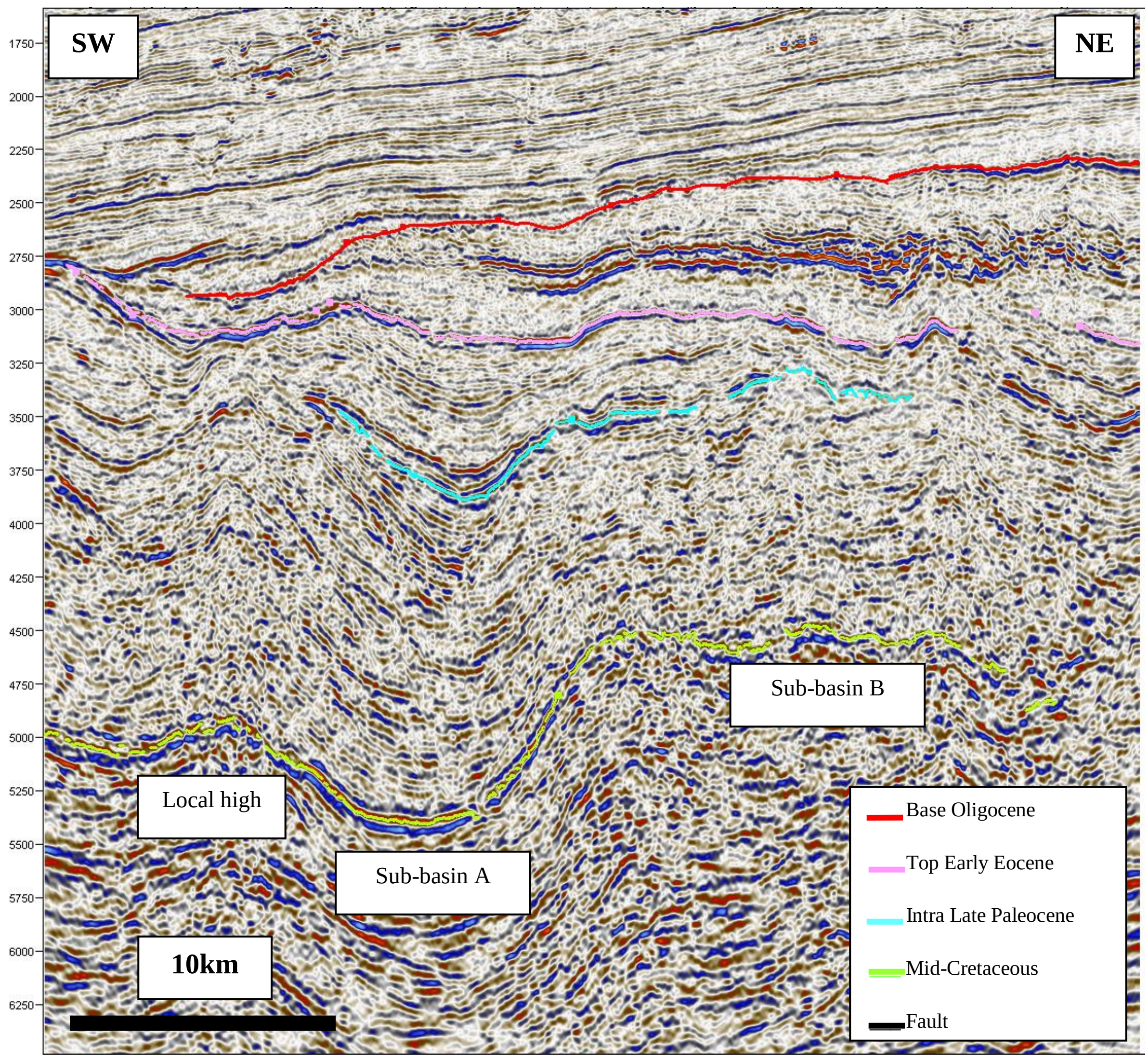

Figure 4.20. Crossline 4600 seismic interpretation.

The Paleocene succession on this section is difficult to be interpreted since the reflections are not as strong as on the previous reflections (figure 4.20). On this section, it is clearly shown that the local high is deeper than Sub-basin B which was not shown in the previous sections. Intra Late Paleocene reflection is clearly interpreted to onlap to a local high.

The sequence between Top Early Eocene and Base Oligocene wedges towards the marginal high. In addition to that, it is a little bit hard to see any fault within this level. However, the transparent unit and the strong reflections above it do exist on this section without being faulted.

4.6. Time-structure maps

Base Oligocene, Top Early Eocene, Intra Late Paleocene, and Mid-Cretaceous have been used to build 4 time-structure maps. These maps provide a base for regional interpretation of the basin development and the deposition pattern that characterized the Sørvestsnaget Basin.

Base Oligocene time-structure map

Base Oligocene reflection can be tracked in the entire seismic coverage since this reflection is very continuous, has strong amplitude, and has minor structural effect. However, several areas had to be interpreted carefully such as the one onlapping towards the NE and an uplift in the SW (figure 4.21) since they might have led the interpretation to some deviation. It is situated between 1900 ms to 3000 ms.

Generally, this surface tells about its dips which has direction NEE. In the northwestern part of the area, this reflection onlaps to the Base Oligocene. Furthermore, the high in figure 4.21 is due to the effect of the salt diapir appearing in the southeastern part of the study area. Structurally, there is no major effect from any structural event affecting this area. It actually has very minor impact from the structural events below it. Fold and faults are not found both on the structural map or surface attribute (figure 4.25).

Top Early Eocene time-structure map

The unit of depth within time from 2300 to 3600 ms (figure 4.22). It also covers almost the entire area of the 3D data since it is relatively easy to interpret. This time-structure map does not explicitly give a lot of information about the dipping relief compared to Base Oligocene time-structure map. There are some lows and highs identified. Beside that, some fold or fault appears as well in this figure.

Number 1 points to where the lows are located on this time-structure map (figure 4.22). These lows are actually located on the central part of the map. They have elongated shape with trend NE-SW which is similar to the extensional fault trend. However, the southernmost low shows deeper basin towards the south. Number 2 shows folds and rotated fault blocks.

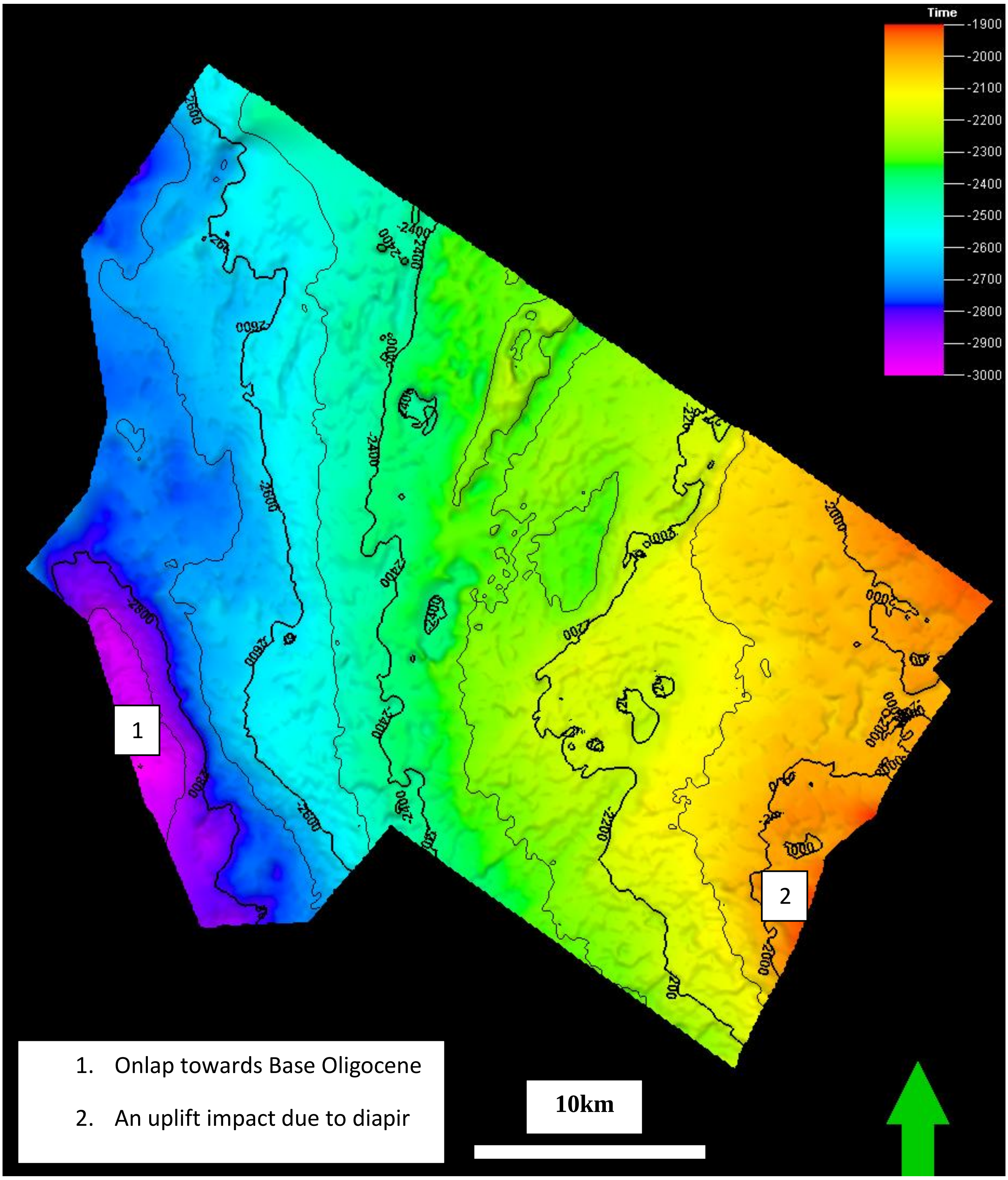

Figure 4.21. Base Oligocene time structure-map.

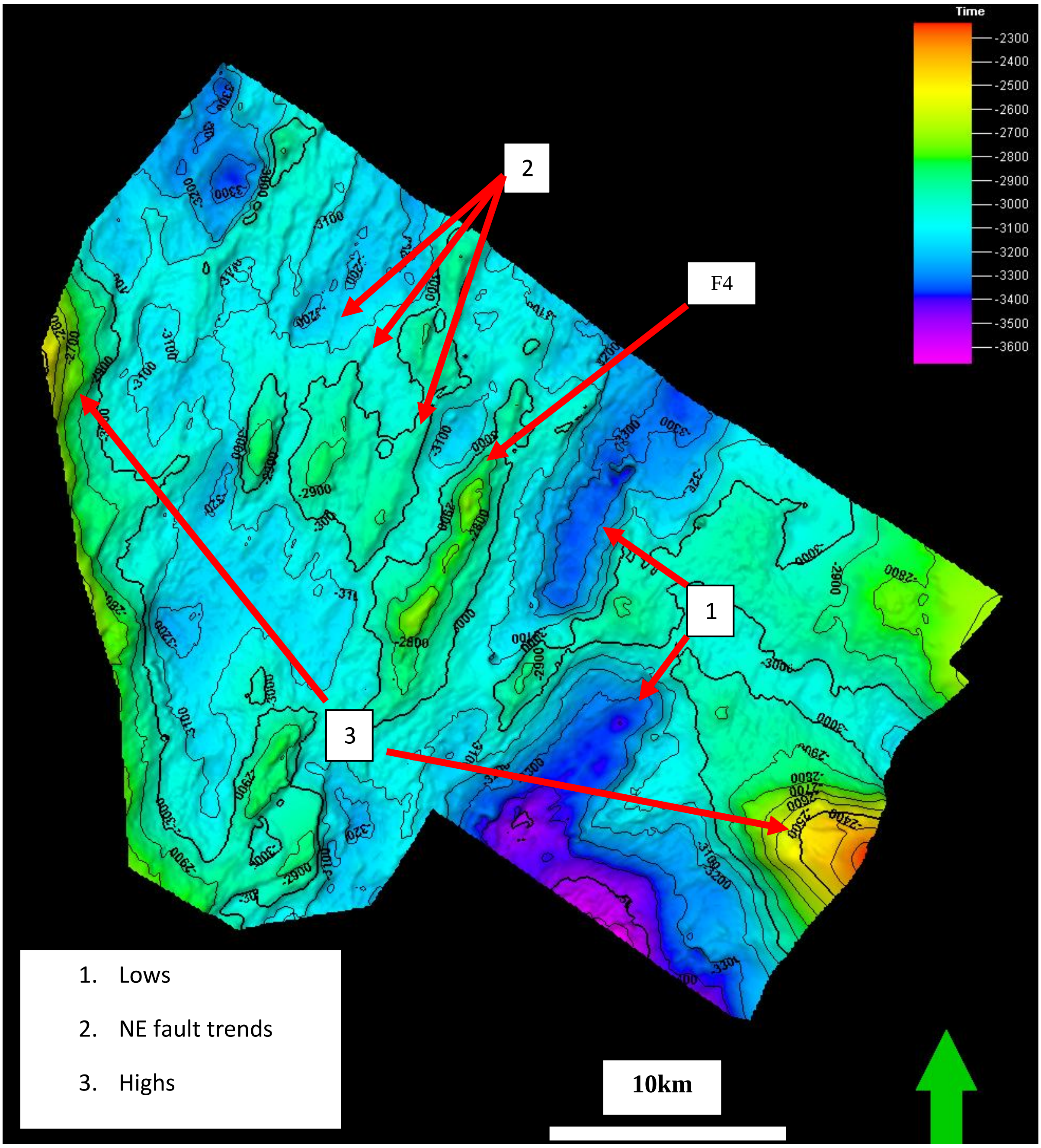

Figure 4.22. Top Early Eocene time-structure map.

These folds and faults trend NE-SW. They can be tracked to maximum 20 kilometers (for Fault 4) (figure 4.22). Number 3 shows where the highs are. Two bright colored features in the northwestern and southeastern most of this map show highs. The southeastern most high is correlated to the salt while the northwestern most part high might be correlated to the uplift (marginal high).

Intra Late Paleocene time-structure map

The time-structure map of Intra Late Paleocene is situated from 3000 to 4000 ms TWT (figure 4.23). This time-structure map does not cover the entire area of the 3D data since it is interpreted to onlap to a reflection below it which is now show in the southwestern part of the map (number 1) . This figure does not give a lot of information about the relief compared to Base Oligocene time-structure map. There are some lows (number 2) and highs (number 3) identified.

Almost all crossline sections show that the interpretation on Intra Late Paleocene reflection onlap to a high. This reflection in figure 4.17 stops and onlaps to the southwestern due to a local uplift. The interpretations of inlines result in some rotated fault blocks due to extensional faults. They also create displacements and thickness differences between hanging walls and the footwalls, even among the rotated fault blocks. Those interpretations can be projected to a map and they can give some explanations to number 2 and number 3.

When it comes to the direction of the trends, it is a good figure to be observed. The trends of the faults and possible rotated fault blocks are similar to the above reflection which is Top Early Eocene. They just shift a little bit to NE-SW. The most interesting part is the elongated low feature in the southwestern part of the map. The low generally elongates NW-SE. However, this low still may partly be faulted by small faults which have the same trends as the large faults NE-SW. To see how and why there is an elongated low, an observation of Mid-Cretaceous is necessary.

Mid-Cretaceous time-structure map

Figure 4.24 displays the time-structure map of Mid-Cretaceous reflection. The unit of depth within time from 3600 to 5400 ms. This time-structure map does not cover the entire area of the 3D data since it is extremely difficult to follow its interpretation to the southeastern part of the seismic data. The reflections look very chaotic towards both NE and marginal high.

This time-structure map looks significantly different from the previous ones. There is a low which obviously elongates to the NW (number 1). The northeastern part of the basin is relatively flat. The difference between this basin and the Intra Late Paleocene basin is that it does not have any influence from extensional fault system. If there is, a more technically careful observation might have to be performed such as running the seismic attribute for structural geology. In addition to that, another basin is also pointed by number 1. In figure 4.24, this basin is elongated towards the same direction as the more prominent one. However, the seismic data does not cover more space in the southern part. Therefore, the interpretation needs to stop at the maximum interpretable seismic data.

Number 2 shows a high which is actually the marginal high. The interpretation of Mid-Cretaceous reflection is not continued towards exactly where the marginal high is located. There is also limitation of seismic data coverage.

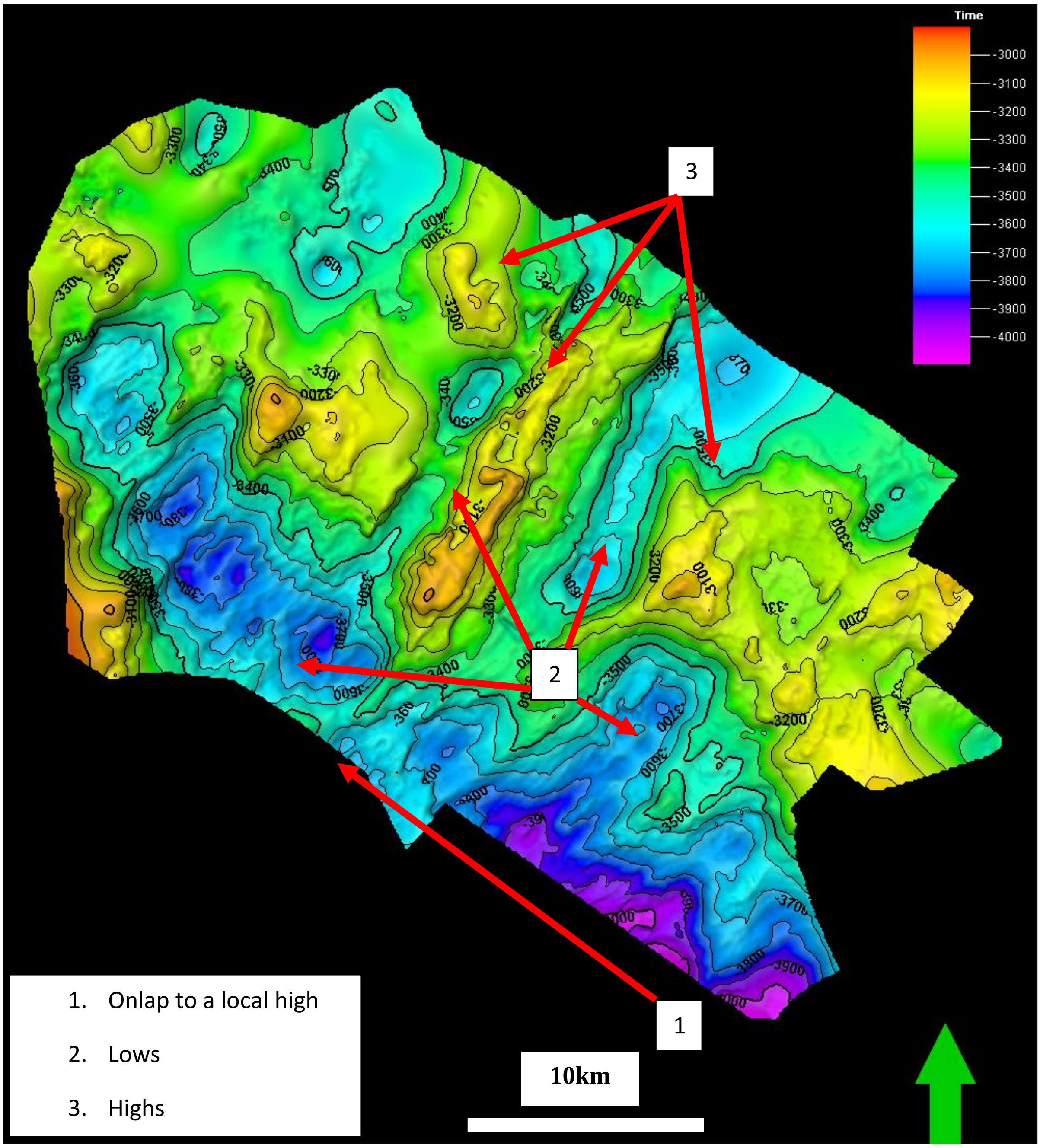

Figure 4.23. Intra Late Paleocene time structure-map.

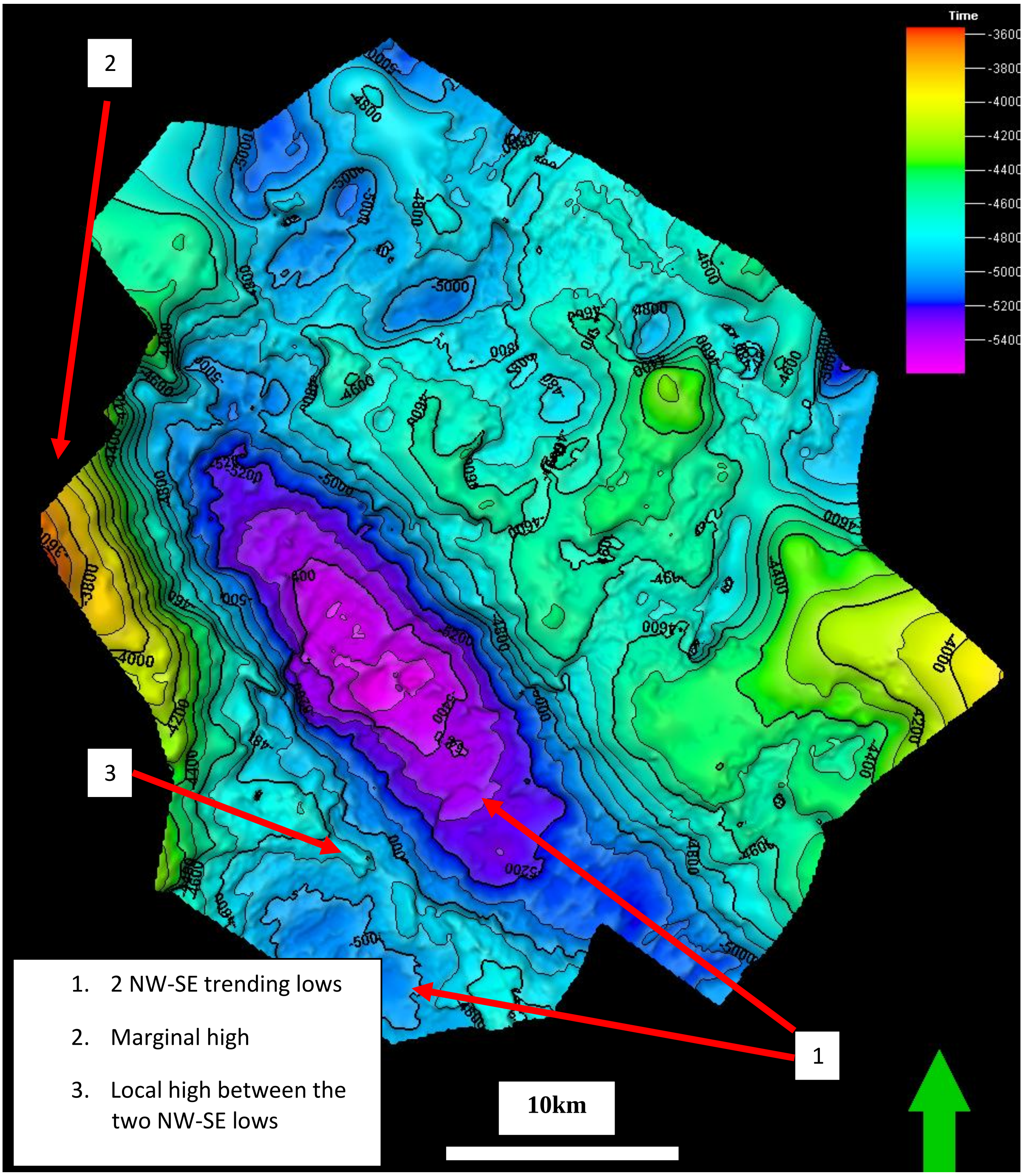

Figure 4.24. Mid-Cretaceous surface time structure-map.

Moreover, these two lows are separated by a slight high which is pointed by number 3. This might explain the fold in the Mid-Cretaceous reflection in the southwestern part of the seismic data. It is also different in terms of fault system since the rotated fault blocks just cannot be observed on this map.

Seismic Attributes

A seismic attribute for structural geology was created as well. The name of the seismic attribute is Dip Angle. It basically calculates the dip of any folds or high structures and shows them in a nice color map. Base Oligocene does not have significant highs (figure 4.25.a). A series of high angle features with NE trend are shown in figure 4.25 b. However, the features in the southeastern part have different direction from the highs located in the more northwestern part which rotate slightly to the west (anticlockwise).

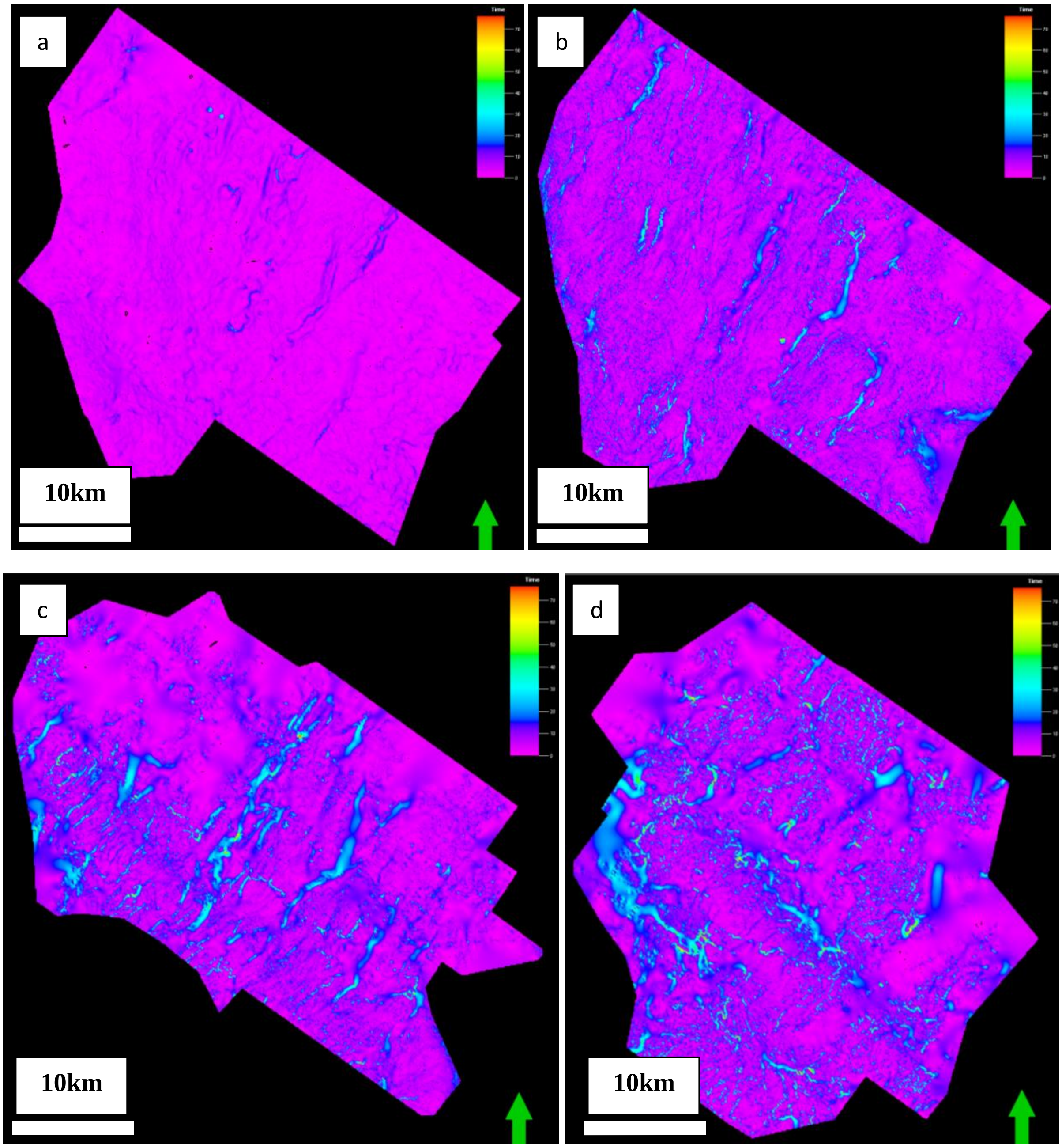

Figure 4.25. Dip angle seismic attribute on each surface. a, b, c, d are Base Oligocene, Top Early Eocene, Intra Late Paleocene, and Mid-Cretaceous respectively.

Figure 4.25.c shows bolder displays of the dipping features. There is a similarity between figure 4.25b and 4.25c. Figure 4.25b has a curved NE-SW fault/fold trend in the middle part of the attribute map. This curved feature is also shown in figure 4.25c. Moreover, in figure 4.25c, there are more very subtle faults that apparently occur in the elongated basin in the southwestern part. They are very consistent and occur along the elongated basin. Eventually, figure 4.25d shows completely different pattern compared to the other seismic attributes. Its basin flank is clearly shown by the light blue color that makes an elongate looking feature. However, in the NE part of the mapview, it can barely be observed although there might be some subtle faults in that area.

Time-Thickness Maps

Time-Thickness Map of Mid-Cretaceous – Intra Late Paleocene

In figure 4.26, the time-thickness of the Mid-Cretaceous to Intra Late Paleocene sequence ranges between 800 to 2000 ms TWT. The thickness in the southwestern part of the map can be correlated with elongated basin in Mid-Cretaceous due to the similar pattern. The lows on the northeastern part of the map correlate with the rotated fault blocks. The highs are correlated with extensional fault. The extensional faults can create basins in the hanging walls that might have a difference thickness during or after the deposition of the basin.

A NW-SE trending thickness (figure 4.26) is shown in the southwestern part of the map. It is also the location where the NW-SE trending Sub-basin A located. In addition to that, the thin features in this time-thickness map are associated with the growth fault (figure 4.11 and 4.12). They trend similarly to the fault trends.

Thickness Map of Intra Late Paleocene –Top Early Eocene

This thickness map which is displayed in figure 4.27 is to show thickness difference between rotated fault blocks. The thickness differences are shown by pairs of a-b, and c-d. The footwall which is represented by b & d is thinner compared to the hanging wall which is represented by a & c.. The southwestern part of this map shows a much thicker sequence between Intra Late Paleocene and Top Early Eocene. Generally, this time-thickness map shows that the maximum thickness of Intra Late Paleocene to Top Early Eocene sequence reaches 700 ms TWT.

Time-Thickness Map of Top Early Eocene sequence – Base Oligocene

This time thickness has two different thickness trends (figure 4.28). The northwestern part of this map comprises thickness variation trending NE and is generally thinner then the southeastern part of the map. The lows (figure 4.28a) show relatively thicker trends towards NE. Different trend of thicker part of the map is shown in the southeastern part that reaches 1300 ms thick. Whereas the high (figure 4.28c) is located close to where the salt diapir is situated.

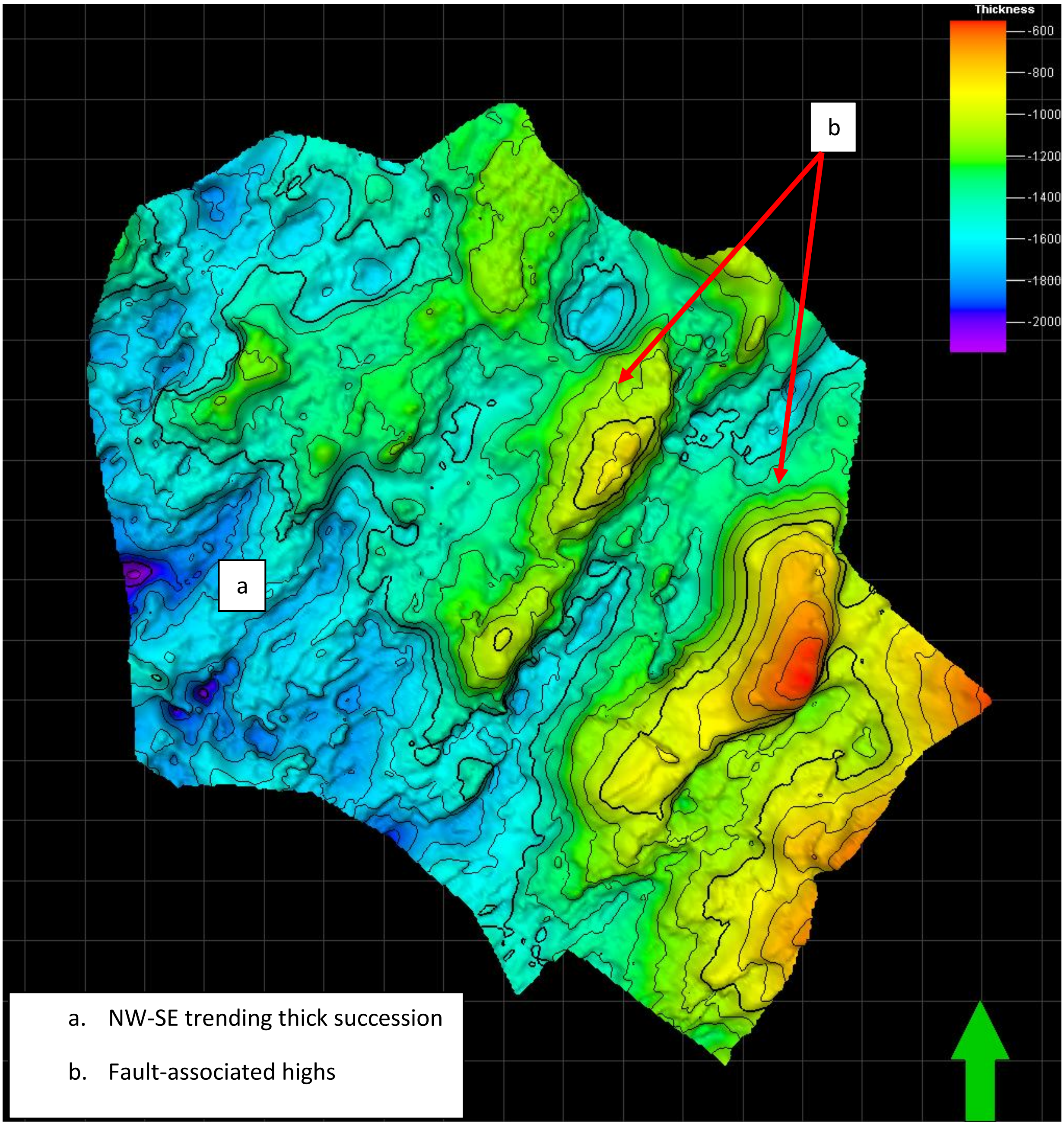

Figure 4.26. Time-thickness map Mid-Cretaceous to Intra Late Paleocene sequence.

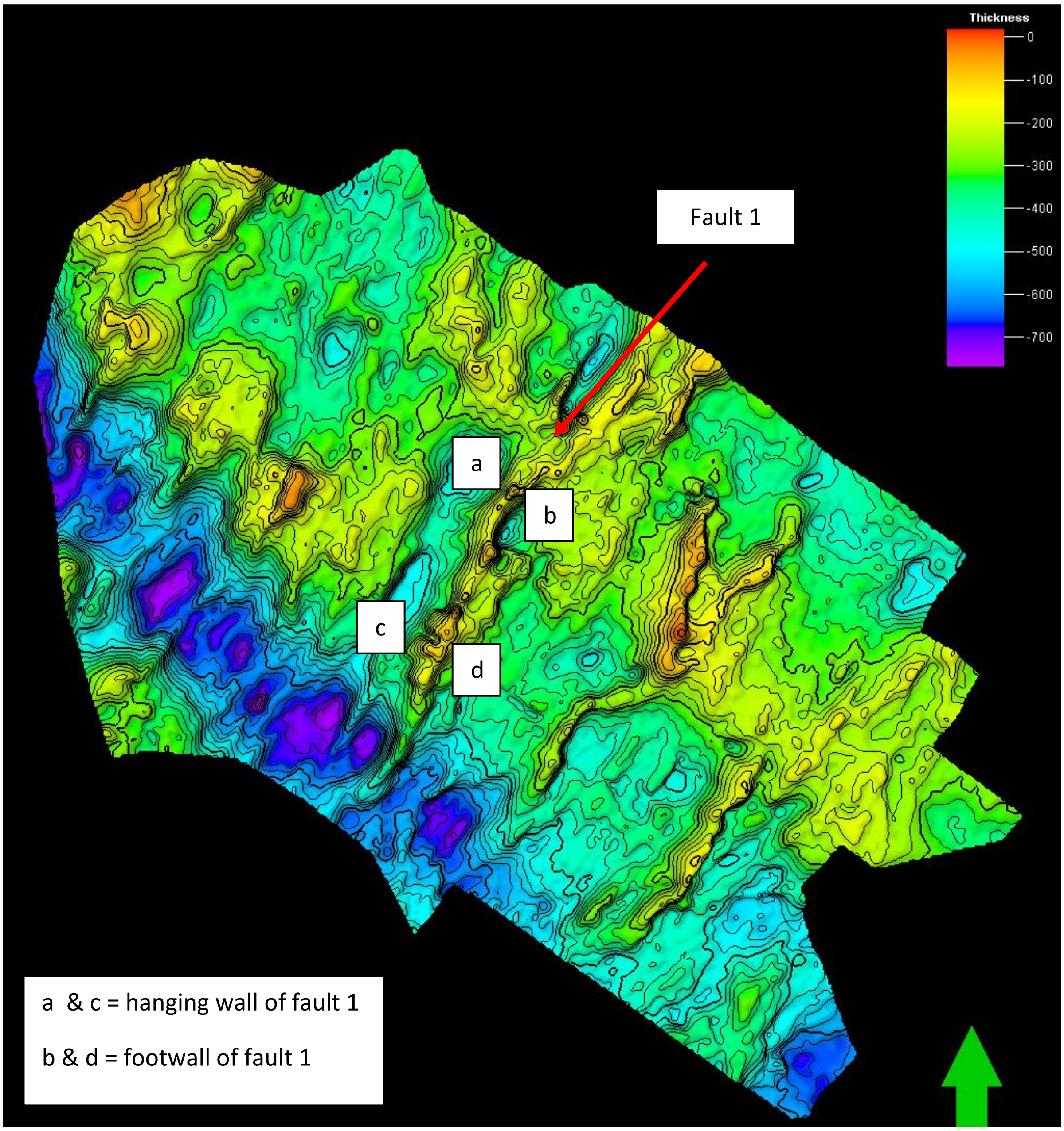

Figure 4.27. Time-thickness map of Intra Late Paleocene to Top Early Eocene sequence.

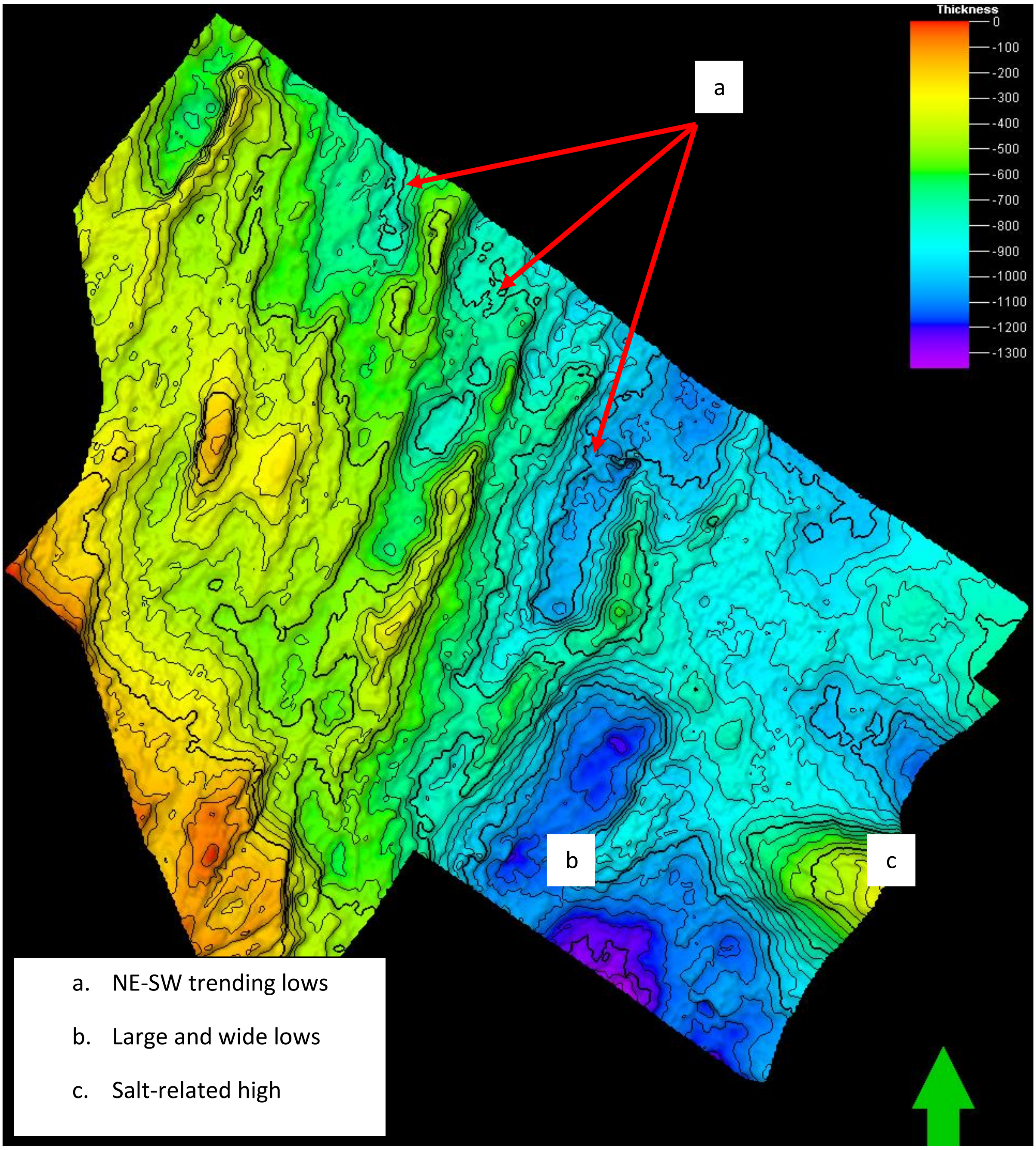

Figure 4.28. Time-thickness map of Top Early Eocene to Base Oligocene sequence.

Chapter 5

Discussion

In the following discussion, the points below will particularly be emphasized:

- Sequence and style of tectonic events
- Plate tectonic setting

In this analysis, the identification and delineation of the main tectonic and depositional events are crucial. To accomplish this, several principal geometries and observations related to different tectonic regimes have been stressed (figure 5.1).

5.1. Characteristics of Tectonic Regimes

Extensional regime

Nøttvedt et al. (1995) illustrated the scheme of the tectonostratigrapic stages in rift basin evolution (figure 5.1). These stages are proto-rift stage, rift stage, and post-rift stage. The phase of rifting immediately before active stretching is sometimes referred to as the pre-rift stage. Nøttvedt et al. (1995) preferred the term proto-rift to emphasize that it refers to a stage that is genetically related to and preceding active stretching. Furthermore, the proto-rift stage is sometimes characterized by deposition in a wide, slowly subsiding basin with only minor fault activity.

The rift stage following proto-rift stage describes the phase of active stretching and fault block rotation (Nøttvedt et al., 1995). Rift initiation is when the fault blocks are still compartmentalized and undergo weak tilting. Prosser et al. (1993) described the rift initiation on a seismic section as perfect wedge shapes to reflector packages, minor onlap onto the hanging wall, discontinuous hummocky internally (figure 5.2). Furthermore, during the the rift climax the basin experiences strong tilting and focusing on rift structure (figure 5.1). On seismic, this rift climax can be identified to have chaotic zone close to the footwall scarp, aggradation and downlap if resolution is good enough. There is minor onlap at top of hanging wall (Prosser et al., 1993). Deposition and erosion during rifting may be dominantly sourced from the footwall where

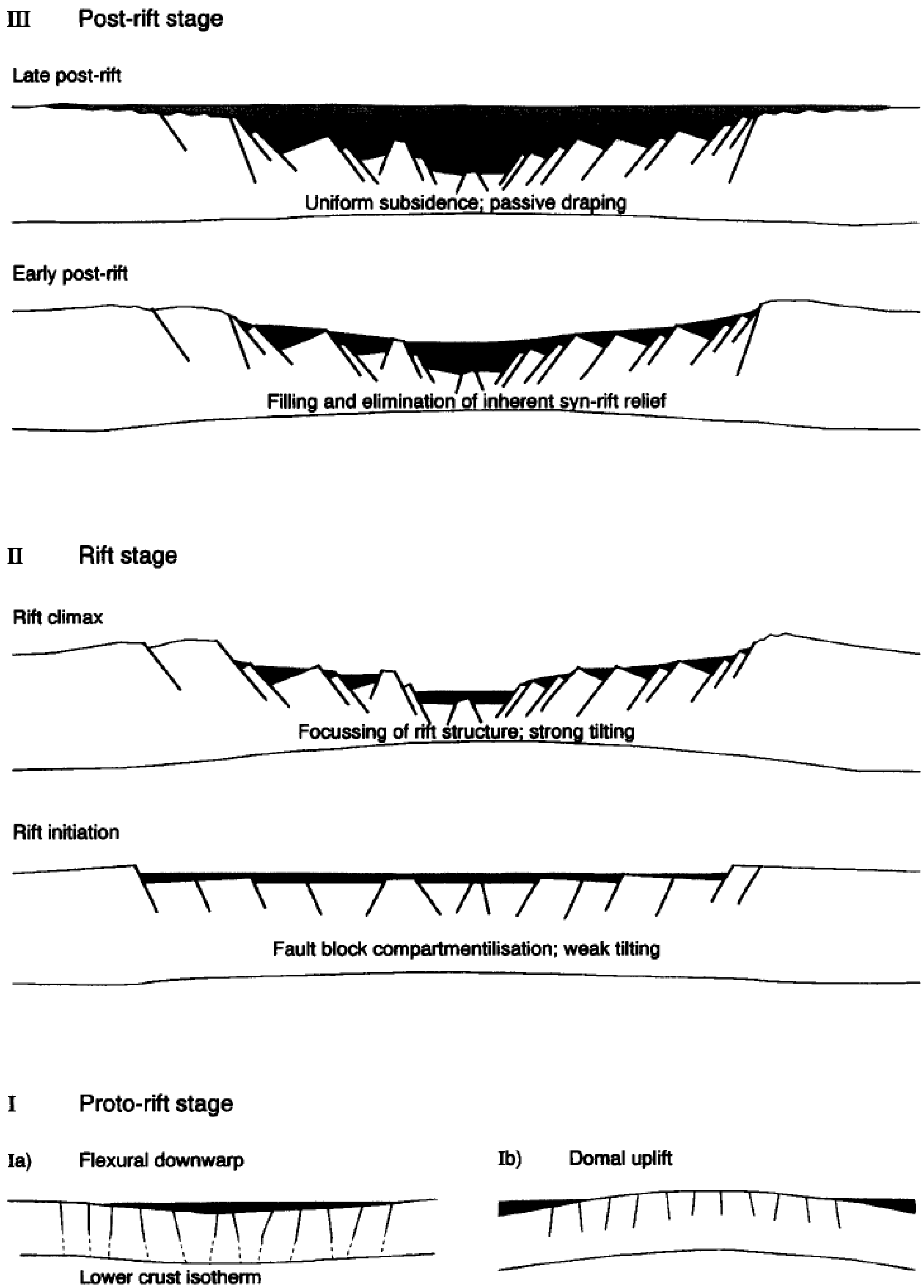

Figure 5.1. Schematic illustration of the tectonostratigraphic stages in rift basin evolution (Nøttvedt et al., 1995)

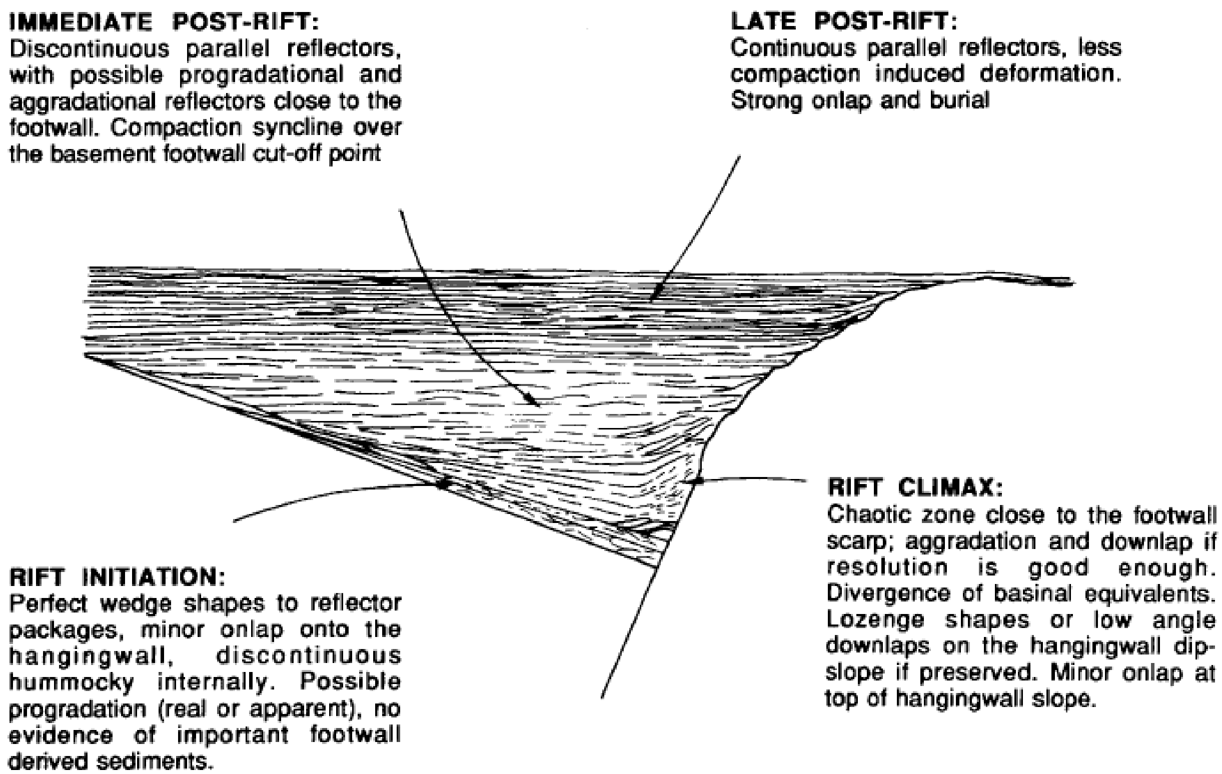

Figure 5.2. An idealized section of a line drawing of a seismic section through an ideal basin, where each tectonic systems tract can be identified. The characteristic seismic expression of each is summarized in the annotation. This will not always be possible (Prosser et al., 1993)

the fault scarp contributes the most (figure 5.3). Gabrielsen et al. (1995) explained the fault pattern which gives the possibility of accumulation of a considerable thickness of sediment, and with potentially good strike-continuity in the hanging wall fault blocks of the master fault (figure 5.3). However, the hanging wall has more extensive surface erosion. Onlaps towards both hanging wall and footwall are to fill the basin.

In the post-rift stage, the basin evolution is dominated by deposition. In the early/immediate post-rift, it concentrates in filling the inherent syn-rift relief. It is described on seismic as discontinuous parallel reflections, with possible progradational and aggradational reflections close to the footwall. This is a period when the direction (rotation) of sedimentation is reverse compared to the rotation of the fault blocks. Moreover, during the late post-rift, the subsidence tends to be more uniform. It can also be described as continuous parallel reflections, less compaction induced deformation.

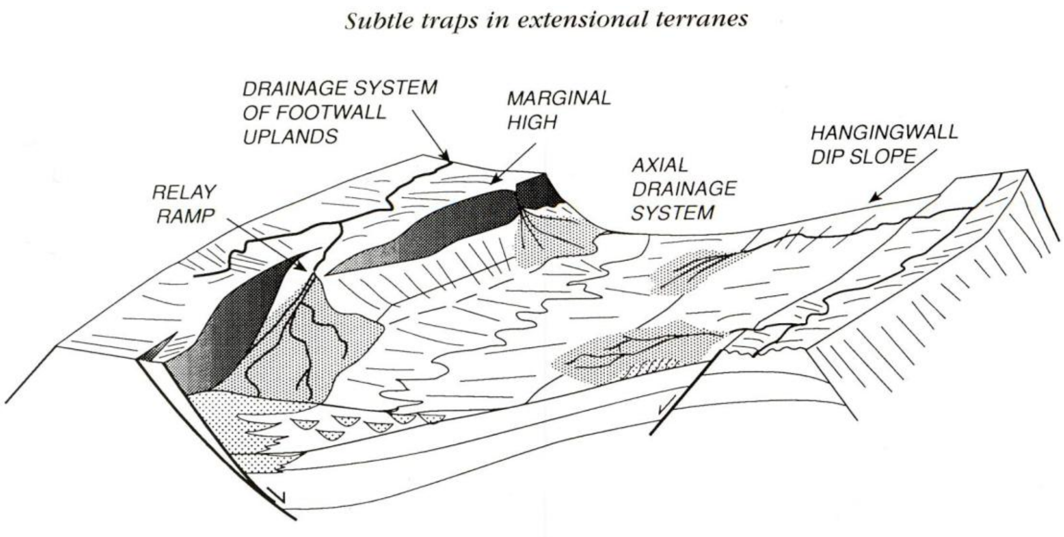

Figure 5.3. Schematic representation of interaction between depositional patterns of erosional products from footwall uplands to hanging wall dip-slope of rotated fault blocks, and axial transport systems along the fault scarp (Gabrielsen et al., 1995)

Compressional regime

In this regime, a layer faulted by a contractional fault will be shortened (figure 5.4). Contractional faults result in repetition of section if it is measured along a line that crosses the fault. A fold is normally formed in contractional system. A reconstruction of an inverted growth fault system is shown in figure 5.5.

Strike-slip regime

This regime relates to transtension and transpression (figure 5.6). A bend a long a strike-slip fault at which transtension occurs is a releasing bend, and a discrete bend at which transpression occurs is a restraining bend (Pluijm and Marshak, 1997). At restraining bends, pieces of crust on opposite sides of of the fault push together, causing crustal shortening. If the shortening is substantial enough, a fold and- thrust belt forms at the bend and a mountain range is uplifted. At releasing bends, and followed by stepovers, pieces of crust on opposite sides of the fault are pulling apart, normal faults develop, and a basin form. Basins formed in this manner are called pull-apart basin (figure 5.6). The amount of subsidence in pull-apart basins depends on the size of the basin and on the amount of extension. Formation of small basins probably only involves brittle faulting in the upper crust. In contrast, formation of large basins probably involves thinning of the entire lithosphere, with the result of that after extension has ceased, the floor of the basin thermally subsides, leading to development of a larger sedimentary basin. In some cases transtension or transpression occurs along the entire length of a fault zone because the zone is oblique to the vectors describing relative movement of blocks across the fault (Pluijm and Marshak, 1997).

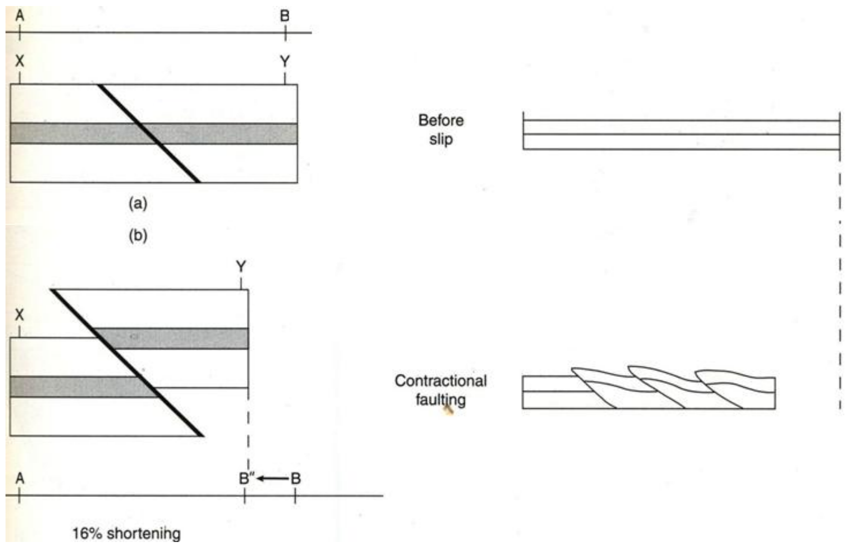

Figure 5.4. Concept of contactional faulting (a) Starting condition (b) Contraction (modified from Pluijm and Marshak, 1997)

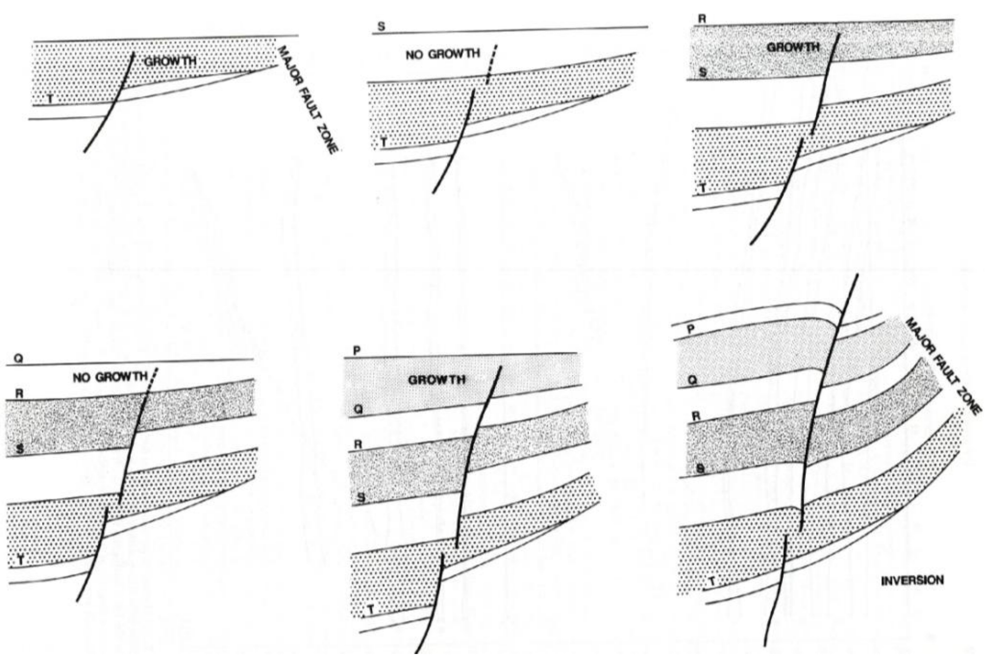

Figure 5.5. Sequential restoration produced by successively flattening the older horizon (Chapman and Meneilly., 1990)

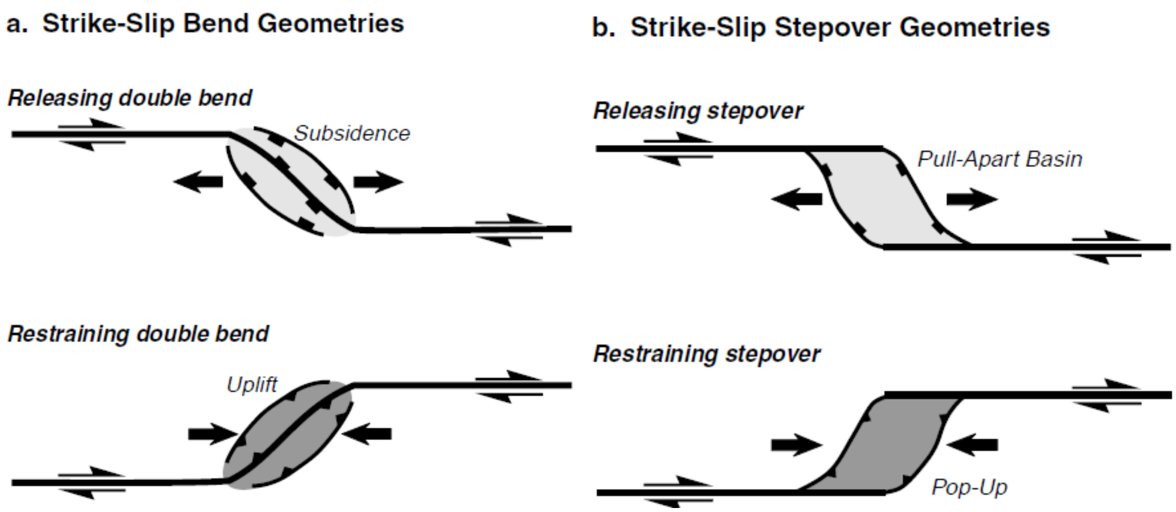

Figure 5.6. Figure 1. General characteristics of strike-slip fault systems in plain view. (a) Bends in the fault surface produce localized zones of extension and subsidence, whereas restraining bends produce localized zones of contraction and uplift. (b) Stepovers between two offset fault systems produce either pull-apart basins for releasing stepovers or pop-ups and uplifts for restraining stopovers (McClay and Bonora, 2001).

5.2. Sequence and style of tectonic events

Identification of tectonosedimentary events that correspond to distinct principal stress configurations observed will be displayed and discussed in this sub-chapter (e.g. figure 5.7 and figure 5.8). The Sørvestsnaget Basin was formed by down faulting at basin-bounding faults that separates the basin from Veslemøy High and Senja Ridge (figure 2.1). This rifting phase is distinguished by a very thick layer of Upper Cretaceous strata in the Sørvestsnaget Basin whereas Upper Cretaceous strata rarely occurs in Veslemøy High (figure 2.1) and Senja Ridge. The principal extensional geometries shown in figures 5.1 – 5.3 match this system.

The thickness of Late Cretaceous succession in Sørvestsnaget Basin is uniform. Conformable reflections also occur in this succession (figure 4.16 and 4.20). This means that the Late Cretaceous succession underwent a relatively uniform deposition in a rapidly subsiding Sørvestsnaget Basin. There might be a local subsidence that occurred during this time that created reflections in Late Cretaceous succession that appear to onlap to the Mid-Cretaceous reflection (figure 4.15). Furthermore, line 234 and its 3D arbitrary line (figure 4.8 and 4.9) show that there is a local fold that is shown together in the

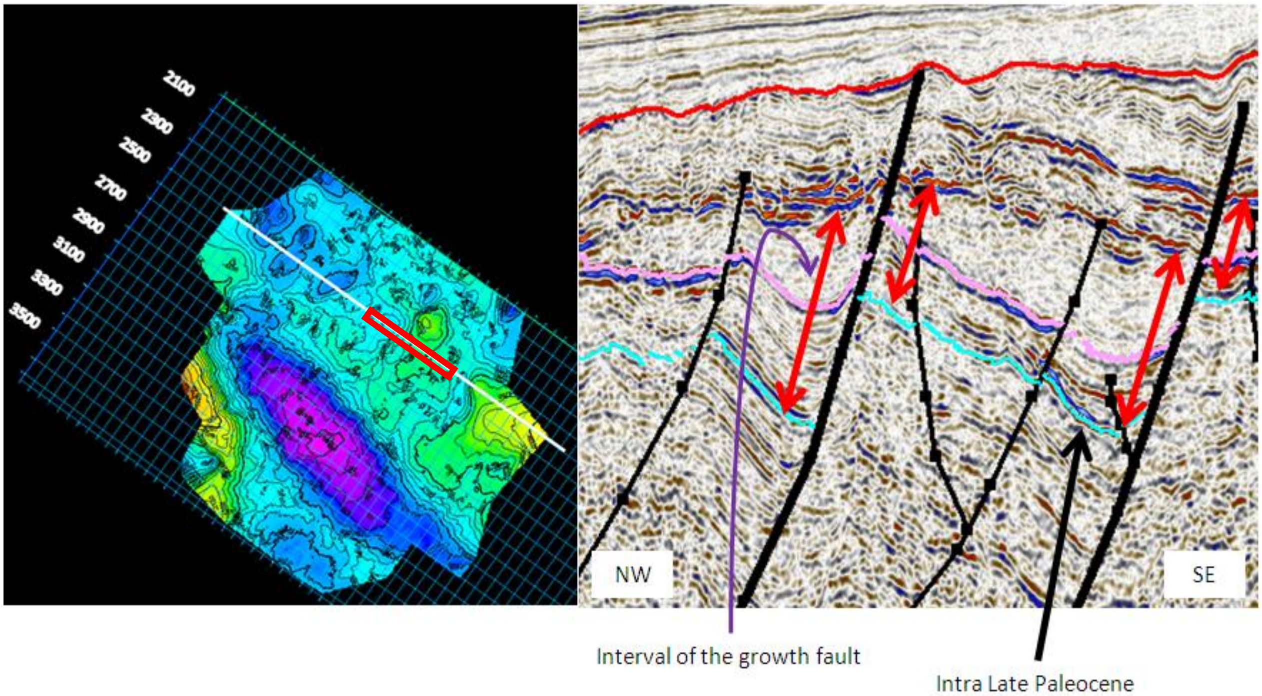

Figure 5.7. A growth fault that was active during (at least) Intra Paleocene through Eocene shown in inline 2500. Colours indicating interpreted horizons, scale of time-structure map, and north direction refer to figure 4.11 and 4.24.

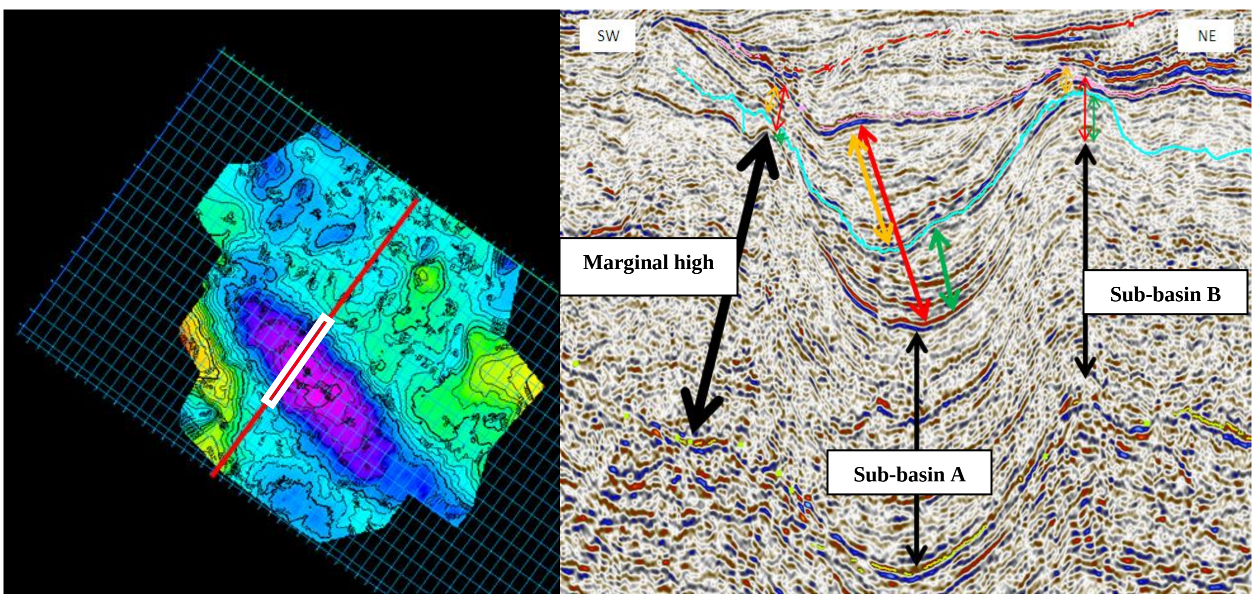

Figure 5.8. Indication of a growth fault that was active during Paleocene through Early Eocene shown in crossline 4000 by a thickness difference in the particular interval in the area of Sub-basin A and Sub-basin B. Thickness differences were also found in the particular interval in the area of Sub-basin A and marginal high with more complexities.

similar-thickness of Late Cretaceous succession. This even more strongly indicates that the fold was not formed before the end of Late Cretaceous.

The Early- Middle Paleocene succession is bounded by the assumed Base Paleocene (figure 4.15) and Intra Late Paleocene. A thickness difference within this sequence was observed in crossline 4000 (figure 5.8) in Sub-basin A and Sub-basin B. It is clearly seen that the assumed Base Paleocene to Intra Late Paleocene sequence wedges towards the Sub-basin B and towards the marginal high (figure 5.8). The same wedging also occurred in the unit above between Intra Late Paleocene and Top Early Eocene. Moreover, Late Eocene succession was also affected by extension/transtension during Late Eocene deposition shown by a thickness difference (figure 5.9). Therefore, this fault system was active during the deposition of Paleocene and Eocene successions. This system matches the principal extensional geometries shown in figures 5.1– 5.3.

Moreover, folds (figure 4.20, 5.9, 5.10), exaggerated narrow basin (figure 5.7), lens shaped basin (figure 4.14), parasitic folds (4.14), and NW-SE trending Sub-basin A (figure 4.24 and 5.8) involves a different tectonic regimes than extensional/transtensional system. Those features fit contractional/transpressional concepts (figures 5.4 – 5.6). Rapid deposition and extensional/transtensional regime occurring during Paleocene – Eocene times was followed by a contractional/transpressional system in Sørvestsnaget Basin then followed to occur in Late Eocene time. The contractional/transpressional features mentioned in this paragraph affected the entire Early Cenozoic succession (Paleocene – Eocene). Therefore, a contractional/transpressional system in Sørvestsnaget Basin is suggested to occur in Late Eocene.

However, there are more complexities in the marginal high area. Marginal high might have been uplifted giving rise to an even thinner Paleocene – Top Early Eocene sequence than in Sub-basins A and B (figure 5.8) by another contractional system. This contractional system also created a fold or a local high (figures 4.8, 4.9, 4.20, 4.24). It might be related to the heat coming from sea floor spreading in the Lofoten Basin to the west uplift part of Sørvestsnaget Basin. This heat might have had impact only at the marginal high as the contraction resulting from it should not affect Sub-basins A and B in the Sørvestsnaget Basin. Sometime between magnetic anomaly 18 and 13 is the most possible time when the heat affected the study area in central part of the Sørvestnaget Basin(figures 5.11 and 5.11d). These magnetic anomalies were the times when the sea floor spreading occurred.

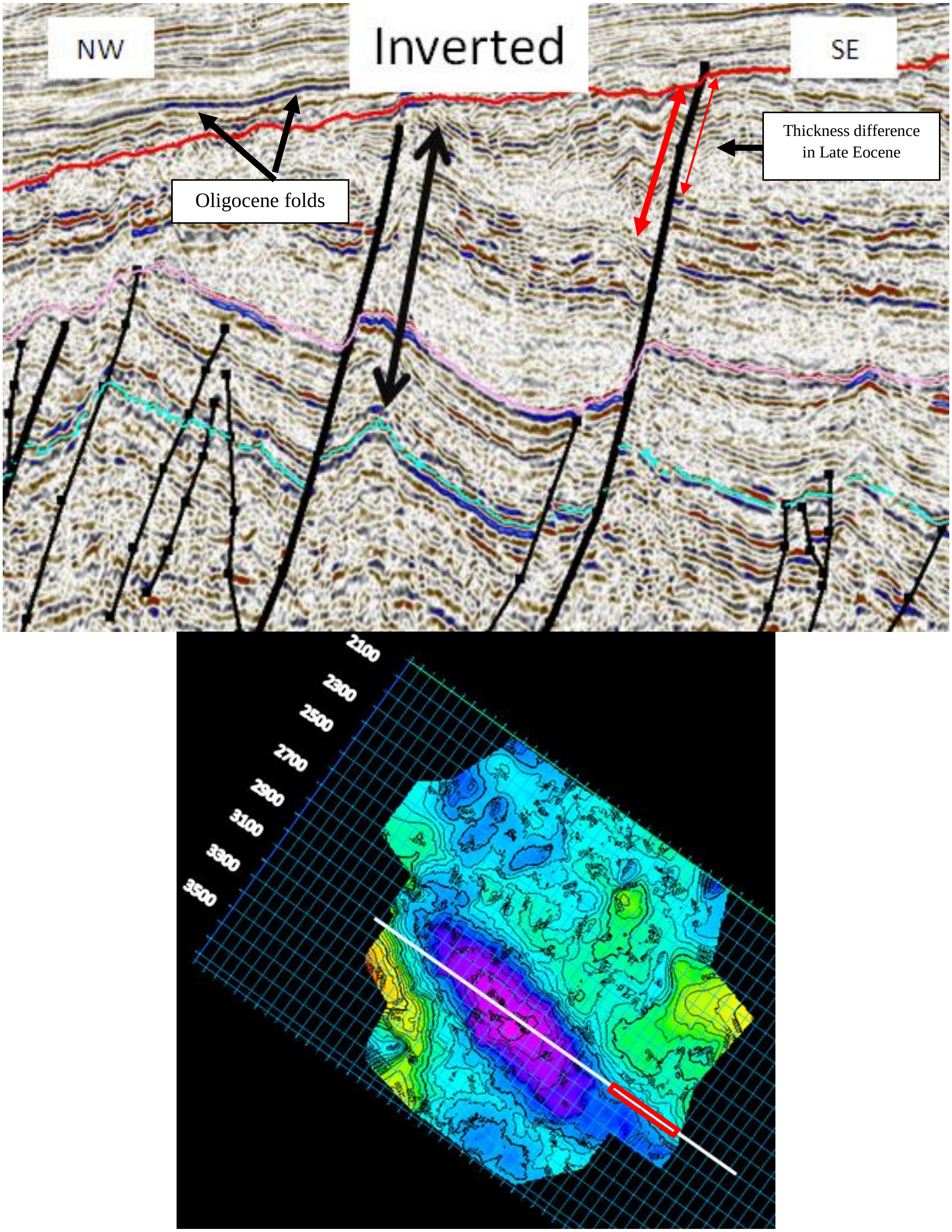

Figure 5.9. Inversion happened to almost the entire section shown by a series of folded reflections clearly shown from Intra Late Paleocene Base Oligocene shown in inline 3100. Colours indicating interpreted horizons, scale of time-structure map, and north direction refer to figure 4.13 and 4.24.

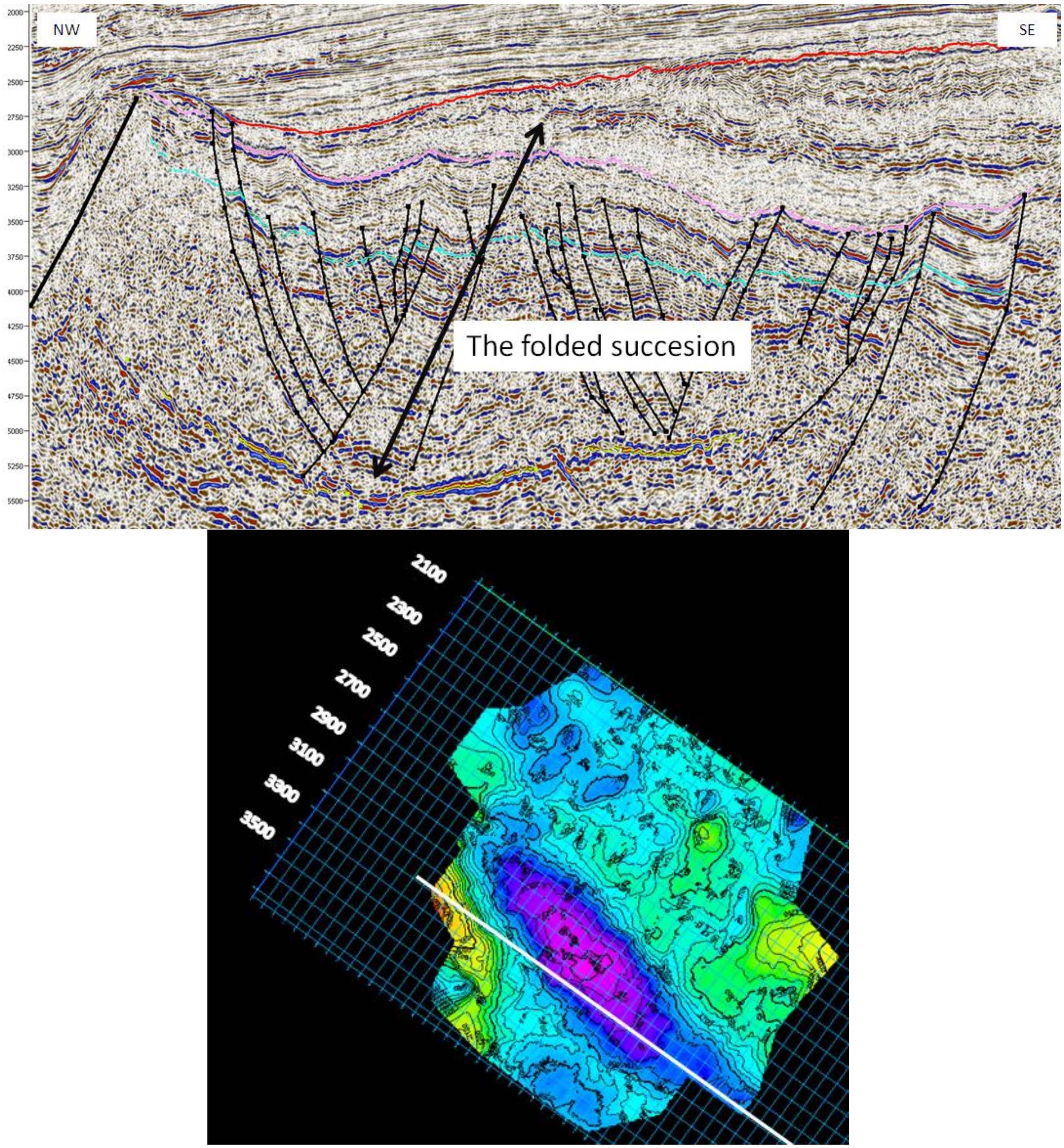

Figure 5.10. A large fold affecting Late Cretaceous through Mid Eocene strata. This is fold is followed by parasitic folds. Colours indicating interpreted horizons, scale of time-structure map, and north direction refer to figure 4.14 and 4.24.

Finally, a synthesis of the geological evolution of the Sørvestnaget Basin is described in table 5.1. The study area within central parts of Sørvestnaget Basin is divided into three main areas which are Sub-basin A with the NW-SE trend, Sub-basin B, and marginal high. These three areas have different structural geometries and also underwent different tectonic impact. Sub-basin A might have experienced transpressional deformation to create a NW-SE trending basin. Sub-basin B might have had more impact of transtensional because more deeply penetrating extensional/transtensional fault occurred and wedge towards Sub-basin A. Marginal high was possibly affected as well by Eocene seafloor spreading in the Lofoten Basin of the Norwegian-Greenland Sea (figure 5.11).

Furthermore, Oligocene – recent deposition has been mostly tectonically calm. Some subtle folds observed in figure 4.14 and 5.9 might show the plate tectonic relaxation after Iceland emerged which was probably in Miocene. Therefore, there is a subtle tectonic activity after Oligocene.

Age	Marginal High	Sub-basin A	Sub-basin B
Early Oligocene – Recent (33.9 – 0 Ma)	Subsidence (post heat contraction)	Subsidence & Fold in Oligocene (tectonic relaxation)	Subsidence & Fold in Oligocene (tectonic relaxation)
Middle – Late Eocene (48.6 – 33.9)	Uplift produced by the heat →← transpression in Late Eocene →←	NW-SE Transtension ←→ transpression in Late Eocene →←	NW-SE Transtension ←→ transpression in Late Eocene →←
Early Paleocene – Early Eocene (65.5 - 48.6)	NW-SE Transtension/Extension ←→	NW-SE Transtension/Extension ←→	NW-SE Transtension/Extension ←→
Late Cretaceous (99.6 – 65.5)	Thick Late Cretaceous Basin formation ←→	Thick Late Cretaceous Basin formation ←→	Thick Late Cretaceous Basin formation ←→

Table 5.1. Synthesis of tectonic evolution in Sørvestsnaget Basin

5.3. Late Cretaceous – Early Cenozoic evolution

A model of transform margin is shown in figure 5.12. In this system, shearing stage initially occurs (figure 5.12; stage 1). It is then continued by the break up (figure 5.12; stages 2,3,4) which creates a thin continental crust and also an oceanic ridge. The shearing zone locates where the transtension and transpression take place. The shear system eventually ends when the ocean is formed and replace the continent-continent transform system.

Sørvestsnaget Basin evolution was initiated by rifting phase, subsidence, and followed by transform margin system. During rifting phase in Late Cretaceous, Sørvestsnaget Basin was formed with and separated from Veslemøy High and Senja Ridge by a basin bounding fault system (figure 2.1). This gave rise massive deposition in Late Cretaceous succession in Sørvestsnaget Basin compared to its deposition in Veslemøy High and also Senja Ridge.

Massive deposition in Early Paleocene still existed. However, there might have been transtension system occurring as well during this time. This might be related to releasing bends in this area accommodated by more displacement in the existing faults. It was proven by more growth faults towards Sub-basin B compared to the growth towards Sub-basin A. In Sub-basin A, the transtensional/extensional faults did not create any thickness differences.

The position of Sørvestsnaget Basin right before the break up which occurred in Ypressian or Early Eocene is shown in figure 5.11a. It also shows the shear and transform zone within the Sørvestsnaget Basin. At this time, Sørvestsnaget Basin was still having sediment infill from Senja Ridge and Veslemøy Highl. Eventually the break-up occurred and it affected the Sørvestsnaget Basin to experience more transtension.

A thermal exchange between cold continental and hot oceanic lithosphere might have occurred and affected Sørvestsnaget Basin sometime between Bartonian and Rupellian in the Eocene or Magnetic anomaly 18 and 13 respectively (figure 5.11c, d and figure 5.12c). The seismic interpretation performed in this study suggests that there also might have been a transpression system occurring in Late Eocene (Priabonian) that created a NW-SE trending Sub-basin A. Eventually, the last stage is the passive subsidence stage where the thermal subsidence occurred (figure 5.11e, f and figure 5.12d). However, due to the emerging Iceland, there was a plate tectonic relaxation in Miocene and this was compensated by some contraction at many NE Atlantic margins, including the Sørvestsnaget Basin at this southwest Barents Sea margin.

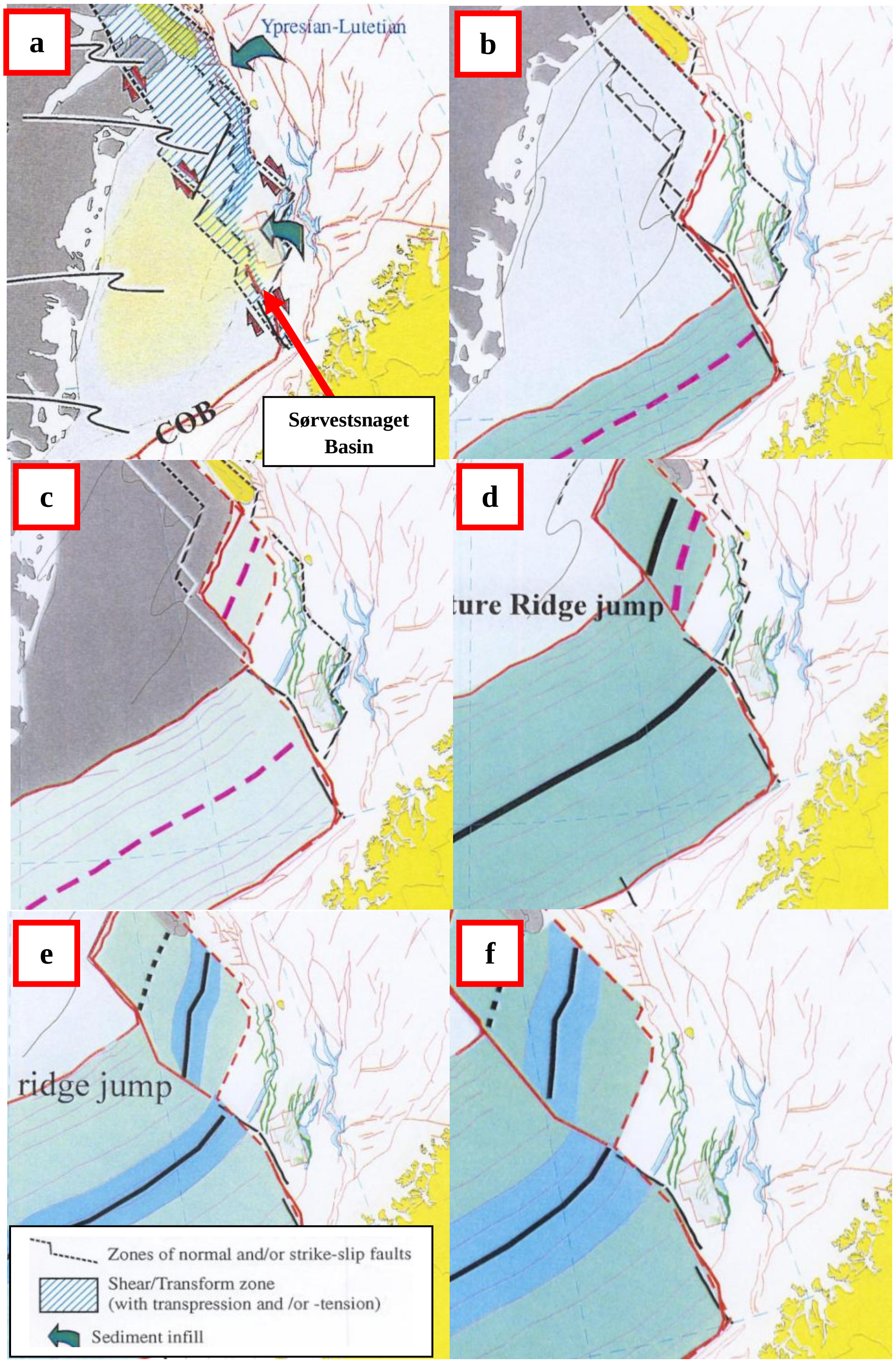

Figure 5.11. Cenozoic plate tectonic evolution of the Norwegian-Greenland Sea; a. Anomaly 24 (E. Ypressian); b. Anomaly 21 (E. Lutetian); c. Anomaly 18 (Bartonian); d. Anomaly 13 (Rupellian); e. Anomaly 7 (Chattian); f. Anomaly 6 (Burdigalian) (modified from Mosar 2001). For present-day configuration see figure 1.1

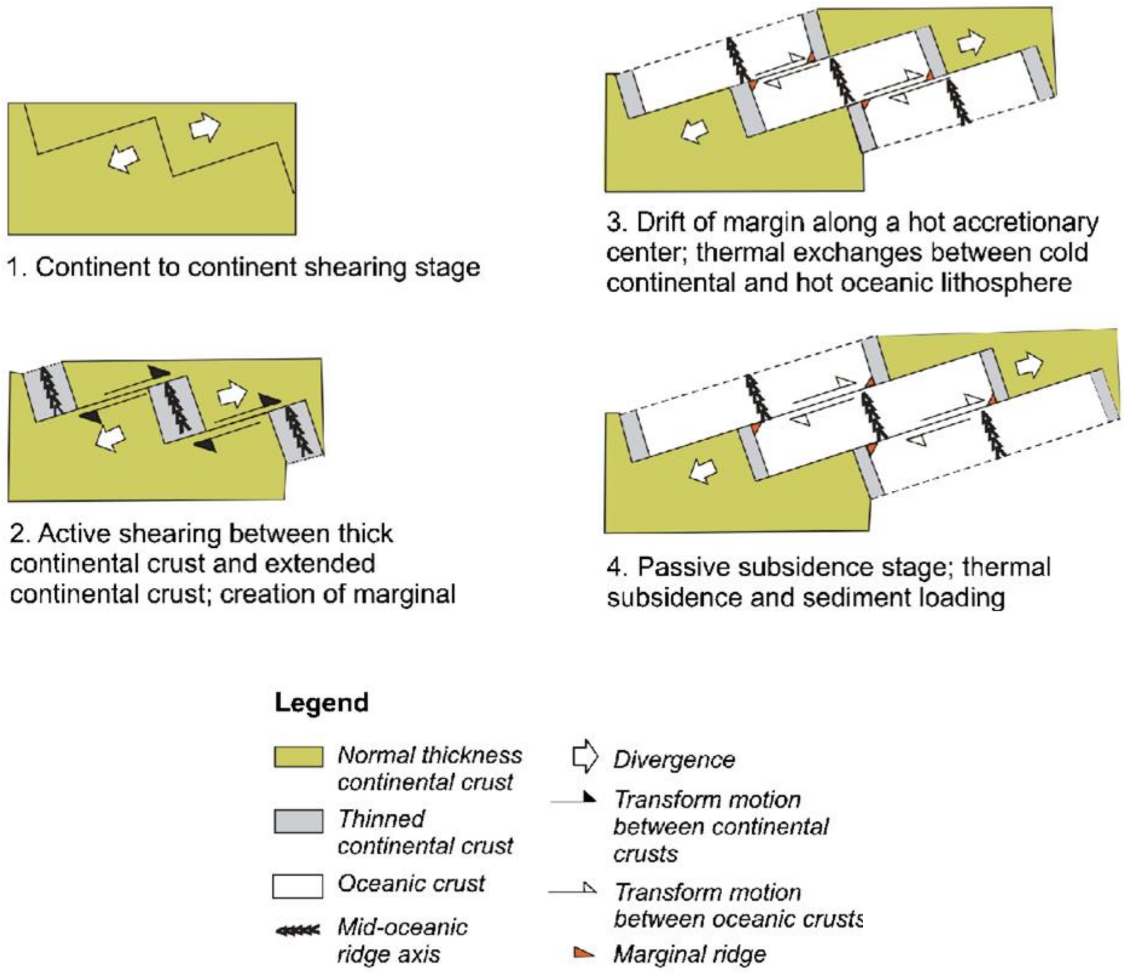

Figure 5.12. A simplified model showing the evolution of a transform margin (Antobreh et al., 2009)

Chapter 6

Conclusions

This study focused on the structure and Late Cretaceous – Early Cenozoic tectonic evolution of central part of the Sørvestsnaget Basin. Its location in the southwestern Barents Sea which is close to the Senja Fracture Zone makes this basin affected by the plate tectonic evolution.

The evolution of the Sørvestsnaget Basin is divided into 5 stages during Late Cretaceous – Cenozoic times:

1. Late Cretaceous down-faulting of the Sørvestsnaget Basin
2. Late Paleocene – Early Eocene extensional / transtensional faulting associated with break up in the Norwegian – Greenland Sea
3. Middle – Late Eocene uplift of the marginal high in response to shear along and heat transfer across the continent-ocean boundary as the spreading ridge migrated along the Senja Fracture Zone.

   Narrowing / deepening of Sub-basin A and inversion of its NE flank also occurred in Late Eocene time and may be related tp uplift of the marginal high.
4. In Oligocene – Early (?) Miocene, there was no major faulting but mild compression giving rise to minor folds. These could be similar to compressional structures observed widespread on continental margins surrounding the NE Atlantic.
5. Late Pliocene – Pleistocene glaciations uplift / erosion of the Barents Shelf and subsidence / deposition of glacial fans along the western Barents Sea margin.

References

Antobreh, A.A., Faleide, J.I., Tsikalas, F., Planke, S., 2009: Rift-shear architecture and tectonic development of the Ghana margin deduced from multichannel seismic reflection and potential field data. Marine and Petroleum Geology 26, pp. 345-368

Brekke, H. and Riis, F. 1987: Tectonics and basin evolution of the Norwegian shelf between 62° and 72°N. Norsk Geologisk Tidskrift 67, 295 - 321.

Breivik, A.J., Faleide, J.I. and Gudlaugsson, S.T. 1998: Southwestern Barents Sea margin: late Mesozoic sedimentary basins and crustal extension. Tectonophysics 293, 21 - 44.

Bergh, S.G. and Grogan, P., 2003: Tertiary structure of the Sorkapp-Hornsund region, south Spitsbergen, and implications for the offshore southern extension of the fold-thrust belt: Norsk Geologisk Tidsskrift, v. 83, pp. 43–60.

Bryn, P., Berg, K., Forsberg, C.F., Solheim, A. and Kvalstad, T.J., 2005: Explaining the Storegga Slide: Marine and Petroleum Geology, v. 22, pp. 11–19.

Cavanagh, A.J., Primio, R.D., Scheck-Wenderoth, M., and Horsfield, B. 2006: Severity and timing of Cenozoic exhumation in the southwestern Barents Sea. Journal of the Geological Society 163, 761-774.

Chapman, T.J., and Meneilly.A.W., 1991: The geometry of Normal Faults, Geological Society Special Publication No. 56, pp. 183-191

Corcoran, D.V. and Dore´, A.G. 2002: Depressurization of hydrocarbon-bearing reservoirs in exhumed basin settings: evidence from Atlantic margin and borderland basins. In: Dore´, A.G., Cartwright, J.A., Stoker, M.S., Turner, J.P. and White, N.J. (eds) Exhumation of the North Atlantic Margin: Timing, Mechanisms and Implications for Petroleum Exploration. Geological Society, London, Special Publications, 196, 457–483.

Dahlgren, K.I.T., Vorren, T.O., Stoker, M.S., Nielsen, T., Nygård, A., and Sejrup, H.P., 2005: Late Cenozoic prograding wedges on the NW European continental margin: their formation and relationship to tectonics and climate: Marine and Petroleum Geology, v. 22, pp. 1089–1110.

Dalland, A., Worsley, D. & Ofstad, K. 1988: A lithostratigraphic scheme for the Mesozoic and Cenozoic succession offshore midand northern Norway. Norwegian Petroleum Directorate Bulletin 4, 1-65.

Dimakis, P., Braathen, B.I., Faleide, J.I., Elverhøi, A., and Gudlaugsson, S.T., 1998: Cenozoic erosion and the preglacial uplift of the Svalbard-Barents Sea Region: Tectonophysics, v. 300, pp. 311–327.

Doré, A.G., 1991: The structural foundation and evolution of Mesozoic seaways between Europe and the Arctic. Palaeogeograhy, Palaeoclimatology, Palaeoecology, v. 87, pp. 441–492.

Doré, A.G. and Lundin, E.R., 1996, Cenozoic compressional structures on the NE Atlantic margin: nature, origin and potential significance for hydrocarbon exploration: Petroleum Geoscience, v. 2, pp. 299–311.

Eidvin, T., Bugge, T., and Smelror, M., 2007: The Molo Formation, deposited by coastal progradation on the inner Mid-Norwegian continental shelf, coeval with the Kai

Formation to the west and the Utsira Formation in the North Sea: Norwegian Journal of Geology, v. 87, pp. 75–142.

Eldholm, O. and Ewing, J., 1971: Marine geophysical survey in the southwestern Barents Sea. Journal of Geophysics. Research 76, 3832-3841

Eldholm, O., Faleide, J.I. and Myhre, A.M. 1987: Continent-ocean transition at the western Barents Sea/Svalbard continental margin. Geology 15, 1118 - 1122.

Evans, D., Harrison, Z., Shannon, P.M., Laberg, J.S., Nielsen, T., Ayers, S., Holmes, R., Hoult, R.J., Lindberg, B., Haflidason, H., Long, D., Kuijpers, A., Andersen, E.S., and Bryn, P., 2005, Palaeoslides and other mass failures of Pliocene to Pleistocene age along the Atlantic continental margin of NW Europe: Marine and Petroleum Geology, v. 22, pp. 1131–1148.

Faleide, J.I., Myhre, A.M. and Eldholm, O. 1988: Early Tertiary volcanism at the western Barents Sea margin. In: A.C. Morton and L.M. Parsons (eds), Early Tertiary Volcanism and the Opening of the North Atlantic. Geological Society, London, Special Publications 39, 135 - 146.

Faleide, J.I., Gudlaugsson, S.T., Eldholm, O., Myhre, A.M. and Jackson, H.R. 1991: Deep seismic transect across the sheared western Barents Sea - Svalbard continental margin. Tectonophysics 189, 73 - 89.

Faleide, J.I., Vågnes, E. and Gudlaugsson, S.T. 1993a: Late Mesozoic - Cenozoic evolution of the southwestern Barents Sea in a regional rift-shear tectonic setting. Marine and Petroleum Geology 10, 186 - 214.

Faleide J.I., Vågnes, E. and Gudlaugsson, S.T. 1993b: Late Mesozoic - Cenozoic evolution of the south-western Barents Sea. In: J.R. Parker (ed), Petroleum Geology of North West Europe: Pro-ceedings of the Fourth Conference. Geological Society, London, 933 - 950.

Faleide, J.I., Solheim, A., Fiedler, A., Hjelmestuen, B.O., Andersen, E.S. and Vanneste, K. 1996: Late Cenozoic evolution of the western Barent Sea - Svalbard continental margin. Global Planetary Change 12, 53-74.

Faleide, J.I., Tsikalas, F., Breivik, A.J., Mjelde, R., Ritzmann, O., Engen, Ø., Wilson, J., Eldholm, O., 2008: Structure and evolution of the continental margin off Norway and Barents Sea. Episodes. v. l.31, No 1.

Færseth, R.B. and Lien, T., 2002: Cretaceous evolution in the Norwegian Sea—a period characterized by tectonic quiescence: Marine and Petroleum Geology, v. 19, pp. 1005–1027.

Gabrielsen, R.H., Færseth, R.B., Jensen, L.N., Kalheim, J.E. and Riis, F. 1990: Structural elements of the Norwegian continental shelf. Part I: The Barents Sea region. Norwegian Petroleum Directorate Bulletin 6, 1-33.

Gabrielsen, R. H., Steel, R.J., and Nøttvedt, A., 1995: Subtle traps in extensional terranes: a model with reference to the North Sea. Petroleum Geoscience, v. 1, pp. 223-235.

Gernigon, L., Ringenbach, J.C., Planke, S., Le Gall, B., and Jonquet-Kolstø, H., 2003: Extension, crustal structure and magmatism at the outer Vøring Basin, Norwegian margin: Journal of the Geological Society, London, v. 160, pp. 197–208.

Gradstein, F.M., Kaminski, M.A., and Agterberg, F.P., 1999: Biostratigraphy and paleoceanography of the Cretaceous seaway between Norway and Greenland. Earth Science Reviews, v. 46, pp. 27–98.

Grogan, P., Østvedt-Ghazi, A.M., Larssen, G.B., Fotland, B., Nyberg, K., Dahlgren, S., and Eidvin, T., 1999: Structural elements and petroleum geology of the Norwegian sector of the northern Barents Sea, in Fleet, A.J. and Boldy, S.A.R., eds. Petroleum geology of Northwest Europe; proceedings of the 5th conference: Geological Society London, pp. 247–259.

Hinz, K. and Weber, J., 1975: Zum geologischen Aufbau des Norwegischen Kontinentalrandes und der Barents-See nach reflexionsseismische Messungen. Compendium 75/75, Erganzungsband der Zeitschrift "Erdol und Kohle, Ergas, Petrochemie", 3-29.

Håkansson, E. and Pedersen, S.A.S., 2001: The Wandel Hav strike-slip mobile belt; a Mesozoic plate boundary in north Greenland. Bulletin of the Geological Society of Denmark, v. 48, pp. 149–158.

Hjelstuen, B.O., Eldholm, O., and Faleide, J.I., 2007: Recurrent Pleistocene mega-failures on the SW Barents Sea margin: Earth and Planetary Science Letters, v. 258, pp. 605–618.

Jebsen, C. and Faleide, J.I., 1998: Tertiary rifting and magmatism at the western Barents Sea margin (Vestbakken volcanic province): III international conference on Arctic margins, ICAM III; abstracts; plenary lectures, talks and posters, pp. 92.

Knutsen, S.-M. and Larsen, K.I. 1997: The Late Meosozoic and Cenozoic evolution of the Sørvests-naget Basin: a tectonostratigraphic mirror for regional events along the southwestern Barents Sea margin. Marine and Petroleum Geology 14, 27-54.

Knutsen, S.-M., Augustson, J.H. and Haremo, P. 2000: Exploring the Norwegian part of the Barents Sea - Norsk Hydro's lessons from nearly 20 years of experience. In: K. Ofstad, J.E. Kittilsen and P. Alexander- Marrack (eds), Improving the Exploration Process by Learning from the Past, Norwegian Petroleum Society Special Publications 9, 99-112. Elsevier, Amsterdam.

Laberg, J.S., Stoker, M.S., Dahlgren, K.I.T., de Haas, H., Haflidason, H., Hjelstuen, B.O., Nielsen, T., Shannon, P.M., Vorren, T.O., van Weering, T.C.E., and Ceramicol, S., 2005: Cenozoic alongslope processes and sedimentation on the NW European Atlantic margin: Marine and Petroleum Geology, v. 22, pp. 1069–1088.

Lundin, E.R. and Doré, A.G., 2002: Mid-Cenozoic post-breakup deformation in the "passive" margins bordering the Norwegian-Greenland Sea: Marine and Petroleum Geology, v. 19, pp. 79–93.

Løseth, H. and Henriksen, S., 2005: A mid to Late Miocene compression phase along the Norwegian passive margin, *in* Doré, A.G. and Vining, B.A., eds., Petroleum Geology: North-West Europe and Global Perspectives—Proceedings of the 6th Petroleum Geology Conference: Geological Society, London, pp. 845–859.

Maher, H.D. Jr., 2001: Manifestations of Cretaceous High Arctic large igneous province in Svalbard. Journal of Geology, v. 109, pp. 91–104.

Mclay, K., and Bonora, M., 2001: Analog models of restraining stopovers in strike-slip. AAPG Bulletin, v. 85, No. 2, pp 233-260.

Mjelde, R., Breivik, A.J., Elstad, H., Ryseth, A.E., Skilbrei, J.R., Opsal, J.G., Shimamura, H., Mu-rai, Y. and Nishimura, Y. 2002: Geological development of the Sørvestsnaget Basin, SW Barents Sea, from ocean bottom seismic, surface seismic and potential field data. Norsk Geologisk Tidskrift 82, 183 - 202.

Mosar, J., 2001: Structural and plate tectonic evolution of the SW Barents Sea: A perspective from Area A; Sørvestsnaget Basin. Scientific report, Geological survey of Norway (NGU), Report number 2001.058

Myhre, A. M. and Eldholm. 1988: The western Svalbard margin (74'-80"N) Marine and Petroleum Geology, v. 5, 134-156.

Myhre, A.M., Eldholm, O. & Sundvor, E. 1982: The margin between Senja and Spitsbergen fracture zones: Implications from plate tectonics. Tectonophysics 89, 33 - 50.

Mørk, M.B.E. and Duncan, R.A. 1993: Late Pliocene basaltic volcanism on the Western Barents Shelf margin: implications from petrology and 40Ar - 39Ar dating of volcaniclastic debris from a shallow drill core. Norsk Geologisk Tidskrift 73, 209 - 225.

Norsk Polarinstitutt, 1985: Western Barents Sea Gravity. 4 map sheets, scale 1:1500000. Norsk Polarinstitutt skrifter., 173c.

Nygård, A., Sejrup, H.P., Haflidason, H. and Bryn, P., 2005, The glacial North Sea Fan, southern Norwegian Margin: architecture and evolution from the upper continental slope to the deep-sea basin: Marine and Petroleum Geology, v. 22, pp. 71–84.

Nøttvedt, A., Berglund, L.T., Rasmussen, E. and Steel, R. 1988: Some aspects of Tertiary tectonics and sedimentation along the western Barents Shelf. In: A.C.Morton and L.M. Parsons (eds), Early Tertiary Volcanism and the Opening of the North Atlantic. Geological Society, London, Special Publications 39, 421 - 425.

Nøttvedt, A., Cecchi, M., Gjelberg, J., Kristensen, S.E., Lønøy, A., Rasmussen, A., Rasmussen, E., Skott, P.H. and van Veen, P. 1992: Svalbard - Barents Sea correlation: a short review. In: Vorren, T.O., Bergsager, E., Dahl-Stamnes, Ø.A., Holter, E., Johnsen, B., Lie, E. and Lund, T.B., (eds.), Arctic Geology and Petroleum Potential, Norwegian Petroleum Society Special Publication 2, 363-375. Elsevier, Amsterdam.

Nøttvedt, A., Gabrielsen, R.H., and Steel, R. J., 1995: Tectonostratigraphy and sedimentary architecture of rift basins, with reference to the northern North Sea. Marine and Petroleum Geology, v. 12, No. 8, pp. 881-901.

Pluijm, B.A.V.D., and Marshak, S., 1997: Earth structure: An introduction to structural geology and tectonics. WBC/McGraw-Hill, pp. 388-403

Prosser, Sarah., 1993: Rift-related linked depositional systems and their seismic expression. Tectonics and Seismic Sequence Stratigraphy. Geological Society Special Publication No. 71, 35-66

Rasmussen, E., Skott, P.H. and Larsen, K-B. 1995: Hydrocarbon potential of the Bjørnøya West Province, western Barents Sea Margin. In: Hanslien, S. (ed), Petroleum Exploration and Exploitation in Norway. Norwegian Petroleum Society Special Publication 4, 277 - 286. Elsevier, Amsterdam.

Ren, S., Faleide, J.I., Eldholm, O., Skogseid, J. and Gradstein, F., 2003: Late Cretaceous-Paleocene tectonic development of the NW Vøring Basin: Marine and Petroleum Geology, v. 20, pp. 177–206.

Renard, V. and Malod, J., 1974. Structure of the Barents Sea from seismic refraction. Earth and Planetary Science. Letters 24, 33-47.

Riis, F., Vollset, J. and Sand, M. 1986: Tectonic development of the western margin of the Barents Sea and adjacent area. In: Hallbouty, M.T. (Ed), Future Petroleum

Provinces of the world. American Association of Petroleum Provinces of the World Memoir, 40, 661-676.

Rise, L., Ottesen, D., Berg, K. and Lundin, E., 2005: Large-scale development of the mid-Norwegian margin during the last 3 million years: Marine and Petroleum Geology, v. 22, pp. 33–44.

Ryseth, A., Augustson, J.H., Charnock, M., Haugerud, O., Knutsen, S.-M.,Midbøe, P.S., Opsal, J.G. and Sundsbø, G. 2003: Cenozoic stratigraphy and evolution of the Sørvestsnaget Basin, southwestern Barents Sea. Norwegian Journal of Geology, v. 83, pp. 107-130

Rønnevik, H.C., Bergsaker, E.I., Moe, A., Øvrebrø, O., Navrestad, T. and Stagenes, J. 1975: Petroleum and the continental shelf of North-west Europe, Vol.1, Geology Institute of Petroleum, Great Britain, 117-129.

Skogseid, J., Pedersen, T., Eldholm, O. and Larsen, B.T. 1992: Tectonism and magmatism during NE Atlantic continental break-up: the Vøring Margin. In: B.C.Storey, T. Alabaster and R.J. Pankhurst (eds), Magmatism and the Causes of Continental Break-up. Geological Society, London, Special Publication 68, 305 - 320.

Skogseid, J., Planke. S., Faleide, J.I., Pedersen, T., Eldholm, O. and Neverdal, F. 2000: NE Atlantic continental rifting and volcanic margin formation. In: A. Nøttvedt, (ed), Dynamics of the Norwegian Margin.Geological Society, London, Special Publication 167, 295 - 326.

Solheim, A., Berg, K., Forsberg, C.F., and Bryn, P., 2005: The Storegga Slide complex: repetitive large scale sliding with similar cause and development: Marine and Petroleum Geology, v. 22, pp. 97–107.

Spencer, A.M., Home, P.C. and Berglund, L.T., 1984: Tertiary structural development of the western Barents Shelf: Troms to Svalbard. In A.M. Spencer (Editor), Petroleum Geology of the North European Margin. Norwegian Petroleum Society., Graham and Trotman, London, pp. 199-209.

Stoker, M.S., Hoult, R.J., Nielsen, T., Hjelstuen, B.O., Laberg, J.S, Shannon, P.M., Praeg, D., Mathiesen, A., van Weering, T.C.E., and McDonnell, A., 2005a: Sedimentary and oceanographic responses to early Neogene compression on the NW European margin: Marine and Petroleum Geology, v. 22, pp. 1031–1044.

Syrstad, E., Bergseth, S., Navrestad, T. 1976: Gravity modeling offshore Troms, Northern Norway. In: Exploration Geology and Geophysics. Offshore North Sea Conference, Article T-1=4, Norwegian Petroleum Society, 24 pp.

Sættem, J., Bugge, T., Fanavoll, S., Goll., R.M., Mørk, A., Mørk, M.B.E., Smelror, M.and Verdenius, J.G. 1994: Cenozoic margin development and erosion of the Barents Sea: core evidence from southwest of Bjørnøya. Marine Geology 118, 257 - 281.

Sundvor, E., 1974: Seismic refraction and reflection measurements in the southern Barents Sea. Marine Geology 16, 255-273

Talwani, M. and Eldholm, O. 1977: Evolution of the Norwegian – Greenland Sea. Geological Society of America Bulletin 88, 969 - 999.

Tsikalas, F., Eldholm, O., and Faleide, J.I., 2002: Early Eocene sea floor spreading and continent-ocean boundary between Jan Mayen and Senja fracture zones in the Norwegian-Greenland Sea: Marine Geophysical Researches, v. 23, pp. 247–270.

Tsikalas, F., Faleide, J.I., and Eldholm, O., 2001: Lateral variations in tectono-magmatic style along the Lofoten-Vesterålen volcanic margin off Norway. Marine and Petroleum Geology, v. 18, pp. 807–832.

Vorren, T.O., Richardsen, G., Knutsen, S.M. and Henriksen, E. 1991: Cenozoic erosion and sedimentation in the western Barents Sea. Marine and Petroleum Geology 8, 317 - 340.

Vågnes, E. 1997: Uplift at thermo-mechanically coupled ocean-continent transforms: Modeled at the Senja Fracture Zone, southwestern Barents Sea. Geo-Marine Letters 17, 100 - 109.

Vågnes, E., Gabrielsen, R.H., and Haremo, P., 1998: Late Cretaceous-Cenozoic intraplate contractional deformation at the Norwegian continental shelf: timing, magnitude and regional implications: Tectonophysics, v. 300, pp. 29–46.

Whitham, A.G., Price, S.P., Koraini, A.M., and Kelly, S.R.A., 1999: Cretaceous (post-Valanginian) sedimentation and rift events in NE Greenland (71–77 degrees N), in Fleet, A.J. and Boldy, S.A.R., eds., Petroleum Geology of Northwest Europe: Proceedings of the 5th Conference. Geological Society, London, pp. 325–336.